



Electronic Communications Committee (ECC)
within the European Conference of Postal and Telecommunications Administrations (CEPT)

**COMPATIBILITY OF WIND PROFILER RADARS IN THE RADIOLOCATION
SERVICE (RLS) WITH THE RADIONAVIGATION SATELLITE SERVICE (RNSS)
IN THE BAND 1270-1295MHZ**

Lübeck, September 2006

0 EXECUTIVE SUMMARY

This ECC report considers the potential impact of Radionavigation satellite service (RNSS) systems in the band 1260-1300 MHz on Wind Profiler Radars (WPR) that operate in the Radiolocation Service (RLS).

The signal interface of the European Galileo system is taken to define RNSS system characteristics that are considered representative for all RNSS-systems intending to share the band 1240-1300 MHz which is allocated on a primary basis to the Radiolocation service. Resolution 217 urges administration to implement wind profiler radar in the band 1270 – 1295 MHz. WPR require about 5 MHz bandwidth to cope with all operational requirements. Centre frequencies can vary within the allocation to allow for flexibility in the national allotment of centre frequencies.

Present and planned use by WPR in all CEPT countries was surveyed in detail with a questionnaire issued by the ECC Working Group Spectrum Engineering. Approximately 25 WPRs operate presently in the band 1270-1295MHz in many CEPT countries. Two types of WPR, named in this report as WPR-A and WPR-B, were identified as representative for a generic investigation of radio compatibility with RNSS. Other types may be available but were not tested.

The weather services use WPRs for routine meteorological weather observations as well as for scientific research. Further use is reported in the monitoring of wind conditions in the vicinity of airports and critical industries with potentially hazardous emissions such as chemical and nuclear power plants. Administrations that responded to the survey plan to continue using these systems in the allocated band.

The issue of band sharing is mainly relevant for Region 1. In Region 2 WPR are operated in the band 904 – 928 MHz is. In Region 3 frequencies above 1300 MHz are used.

Comprehensive simulations and compatibility test were performed to investigate the conditions for electromagnetic compatibility between the Galileo E6-signal and WPR which occupies the entire band 1260-1300 MHz.

The simulations conclude that for five-beam WPR, both, the WPR-A and the WPR-B type, show minor performance degradation imposed by the Galileo E6-signal only. Degradation can be slightly more significant with a three-beam WPR (WPR-A and WPR-B three-beam radars).

Compatibility tests were therefore performed in addition using simulated Galileo signals fed into the antenna of WPR-A and WPR-B. Tests have shown that the formal protection limit of $I/N = -6\text{dB}$ as recommended in Rec ITU-R M.1461, is too severe in this case taking other operational and statistical improvements into consideration.

Galileo signal power level used in the UK study were about 2dB higher than the values that will actually be transmitted by the satellites. Although these measurements give a good idea of the WPR behaviour when facing a RNSS-like type of interference, only limited conclusions about the real impact of Galileo can be derived from these measurements because the E6-signal was modified by the European Union after the measurements had been performed (see section 5.2).

UK and German measurements also included investigations about WPR operated in spectral nulls of the Galileo E6-signal. These tests showed that with an appropriate shift of the WPR frequency the compatibility with the Galileo E6-signal can be ensured. In this case, even WPR operation for scientific purposes would be possible provided that the research systems have comparable performance parameters as the ones considered in this report.

The German compatibility tests investigated the impact of the new baseline Galileo E6-signal in terms of operationally perceivable degradations taking radar consensus processing as well as skills and experience of the radar operator into account.

In conclusion,

- (1) Representative measurements with reproducible signal conditions for the Galileo E6-signal as well as the WPR signal returns show that there are minor degradations of the radar performance occurring at times of full exposure to a satellite signal, i.e. in times, when a satellite is in full boresight view of the WPR-antenna beam. .
- (2) There are no coherent effects, i.e. the E6-signal under worst case conditions does not create false alarms.

- (3) Residual incoherent noise-like interference imposed by the E6-signal in the worst can slightly degrade the instantaneous height performance of the radar, depending on the atmospheric backscattering conditions. However, even in these cases, the times of visibility of each satellite of the constellation is accurately predictable.
- (4) However, in cases of scientific measurements additional mitigation options were investigated, one of these by shifting frequency of the WPR into a Null of the E6-signal.

Further mitigation techniques are also described that could be applied in cases of three-beam WPR-systems to minimise the impact of the Galileo E6-signal on WPR operations. It should be noted that some of those mitigation techniques are GALILEO system dependent. Some of these mitigation techniques might not be possible for future RNSS systems.

Table of contents

0	EXECUTIVE SUMMARY.....	2
1	INTRODUCTION.....	7
2	WIND PROFILER RADARS.....	7
2.1	USAGE PATTERNS.....	7
2.2	EUROPEAN WPR USAGE.....	8
2.3	OVERVIEW OF WIND PROFILER RADAR.....	9
2.3.1	<i>Operational characteristics of WPR.....</i>	9
2.3.2	<i>Wind Profiler Altitude Performance.....</i>	10
2.3.3	<i>Scattering physics.....</i>	12
2.3.4	<i>Radar hardware.....</i>	15
2.4	AN EXAMPLE OF MEASUREMENT SEQUENCE FOR ONE WPR TYPE.....	25
2.4.1	<i>WPR operating modes.....</i>	25
2.4.2	<i>Transmission duty cycle and signal processing characteristics.....</i>	26
2.5	WIND PROFILER DATA PRESENTATIONS.....	27
2.6	OPERATING TECHNIQUES.....	29
2.7	INTERFERENCE TO WPR.....	29
2.8	INTERFERENCE CRITERIA.....	30
3	RADIONAVIGATION SATELLITE SERVICE AND THE EUROPEAN GALILEO SYSTEM.....	31
3.1	THE GALILEO RNSS SYSTEM.....	31
3.2	CONSTELLATION INFORMATION.....	31
3.3	GALILEO SIGNAL CHARACTERISTICS.....	31
3.4	GALILEO E6-SIGNAL SPECTRUM.....	32
3.5	GALILEO E6 SATELLITE PFD VERSUS ELEVATION.....	33
4	SIMULATION STUDIES.....	34
4.1	SIMULATION OBJECTIVES.....	34
4.2	GALILEO SYSTEM PARAMETERS.....	34
4.3	WPR CHARACTERISTICS.....	35
4.4	SIMULATION RESULTS.....	36
4.4.1	<i>Assumptions.....</i>	36
4.4.2	<i>Simulation of WPR-A availabilities over location latitude.....</i>	36
4.4.3	<i>Simulation of WPR-B Wind Profiler Radar availabilities over location latitude.....</i>	39
4.5	SIMULATION CONCLUSIONS.....	42
5	COMPATIBILITY TESTS.....	42
5.1	INTRODUCTION.....	42
5.2	UK MEASUREMENT CAMPAIGN.....	42
5.2.1	<i>Campaign objectives and performance.....</i>	42
5.2.2	<i>WPR-B Test Conclusions.....</i>	42
5.2.3	<i>UK WPR Test Conclusions.....</i>	43
5.3	GERMAN MEASUREMENT CAMPAIGN.....	43
5.3.1	<i>Campaign objectives and performance.....</i>	43
5.3.2	<i>German WPR Test Conclusions.....</i>	45
6	INTERFERENCE MITIGATION - OPTIONS TO IMPROVE THE WPR-RNSS COMPATIBILITY.....	46
6.1	INTERFERENCE ANALYSIS SUMMARY AND OPTIONS FOR INTERFERENCE MITIGATION.....	46
6.2	POSSIBLE MITIGATION TECHNIQUES.....	46
6.2.1	<i>Introduction.....</i>	46
6.2.2	<i>Antenna Pointing.....</i>	47
6.2.3	<i>Additional WPR Beam positions.....</i>	50
6.2.4	<i>Antenna beam polarisation.....</i>	50

6.2.5	<i>Cancellation</i>	50
6.2.6	<i>WPR central frequency Shift within the 1270-1295 MHz</i>	51
6.2.7	<i>Spectral parasitic elimination</i>	52
6.2.8	<i>Use of pulse compression coding</i>	52
6.2.9	<i>Combination of different modes</i>	52
6.3	MITIGATION TECHNIQUES SUMMARY	53
7	CONCLUSIONS AND RECOMMENDATIONS	54
7.1	GENERAL CONCLUSIONS RELATED TO RNSS IN THE 1270-1295 MHZ BAND	54
7.2	SPECIFIC CONCLUSIONS RELATED TO GALILEO AND CURRENT EUROPEAN WPR IN THE 1270-1295 MHZ BAND	54
8	GLOSSARY AND LIST OF ACRONYMS	56
9	REFERENCES	56
ANNEX A:	WMO DATA QUALITY REQUIREMENTS	60
ANNEX B:	WIND PROFILER RADAR SITES IN CEPT COUNTRIES	61
ANNEX C:	TEST CAMPAIGN UK (SUMMARY)	69
1	TEST OUTLINE	69
2	DEGREANE WPR	70
2.1	THE DEGREANE 1300 WPR	70
2.2	INTERPRETING THE WPR OUTPUTS	71
2.3	THE SIMULATED GALILEO SIGNAL	71
2.4	MEASUREMENT RESULTS	71
2.4.1	<i>Presentations</i>	71
2.4.2	<i>WPR at Null E</i>	72
2.4.3	<i>Degreane WPR Test Conclusions</i>	73
3	VAISALA WPR	73
3.1	THE VAISALA LAP3000 WPR.....	73
3.2	INTERPRETING THE WPR OUTPUTS	74
3.3	MEASUREMENT RESULTS	74
3.3.1	<i>Nominal conditions</i>	74
3.3.2	<i>WPR at Null E</i>	75
3.3.3	<i>WPR at Null G</i>	77
3.3.4	<i>WPR at Null H</i>	78
3.3.5	<i>Tests with Other Pulse Lengths at Nominal Frequencies</i>	78
3.4	VAISALA WPR TEST CONCLUSIONS.....	78
4	SUMMARY	78
ANNEX D:	TEST CAMPAIGN GERMANY (SUMMARY)	80
1	OBJECTIVES OF THE GERMAN COMPATIBILITY TESTS	80
2	TEST SET-UP	80
2.1	TEST SYSTEM ARCHITECTURE AND LEVEL DIAGRAM	80
2.2	THE NEW BASELINE GALILEO E6-SIGNAL.....	81
2.3	E6-SIGNAL GENERATOR.....	82
3	TEST RESULTS	82
3.1	TEST SCHEDULE	82
3.2	TESTS PERFORMED	83
3.2.1	<i>Overview</i>	83

3.2.2	<i>Test A: Verification of test set-up</i>	83
3.2.3	<i>Test B: Impact of coherent noise interference onto radar</i>	84
3.2.4	<i>Test C: Impact of incoherent noise interference (coloured noise)</i>	88
3.2.5	<i>Test D: Variation of radar parameters</i>	90
3.2.6	<i>Test E: Options for interference mitigation.....</i>	94
4	CONCLUSIONS.....	97

Compatibility of wind profiler radars in the radiolocation service (RLS) with the radionavigation satellite service (RNSS) in the band 1270-1295 MHz

1 INTRODUCTION

Wind profiler radars (WPR) play an important part in our understanding of the atmosphere. WPR measurements are fed directly into atmospheric models, which are essential tools for weather forecasting. WPR also play a part in making air travel safer.

They are used for nowcasting, where for example an aviation meteorologist gives real time wind information for approaching air traffic. In addition data are used for weather forecasting

The Radionavigation satellite service (RNSS) is also important, with a myriad of new applications emerging daily; these also make our lives safer or more convenient.

In future both WPR and RNSS systems will operate in the band 1270-1295MHz and simple geometry suggests a potential for interference. With almost global coverage, a Medium Earth orbit RNSS system with space-to-Earth transmissions will be visible to upward facing WPR antenna.

This report studies the impact of RNSS emissions on WPR's performance in the 1270-1295MHz band, and investigates techniques that could minimize this impact.

2 WIND PROFILER RADARS

2.1 Usage Patterns

Wind Profiler Radars (WPR) are used for meteorological, scientific and aircraft safety purposes.

WPRs operating in the 1290 MHz band provide automatically continuous updates of wind data for meteorological awareness typically at 10 to 30 minutes intervals. In addition to the wind data, the returned signal power offers together with other measurements a tool for nowcasting, e.g. weather front passage, fog dissipation nowcasting, freezing level altitude, and cloud tops. A wind profile composes wind speed and direction in the respect of altitude from near surface up to about 3000 meters depending on the weather situation.

Typically, operations are automated, with WPRs sending data to collection centres for integration into atmospheric models. This is done continuously with the only interruptions being for maintenance purposes.

Scientific operations are carried into atmospheric chemistry, in particular ozone reactions and pollution measurement. Research work involves using the radars over their full range of capabilities and for arbitrary periods and times. When not in use for scientific experiments, WPRs are used for wind profiling in operational meteorological networks.

Wind Profiler Radars (WPR) are part of the general family of Doppler Radar Profilers (DRP) that are also essential for basic research in atmospheric dynamics which is needed to enhance our understanding of weather and climate in general. In particular, the instruments are used in the following fields of meteorology:

- Atmospheric Boundary Layer research
- Turbulence research
- Investigation of atmospheric waves
- Cloud and precipitation physics
- Air quality investigations

Resolution 217 (WRC-97) urges administrations to (only) implement wind profiler radars as radiolocation service systems in particular bands, including the band 1270-1295MHz in which the radiolocation service has primary status. Many WPR systems now operate in the recommended bands. WRC-2000 allocated the band 1260-1300MHz to the Radionavigation satellite service on a primary basis. The band 1215-1260MHz was already allocated to the RNSS and therefore the band 1215-1300MHz is now one contiguous primary RNSS allocation.

Currently RNSS systems utilise only the 1215-1260MHz portion, but at least one system, Galileo, plans to use the 1260-1300MHz portion that overlaps with the WPR band.

Both WPR and RNSS will operate co-primary in the band 1270-1295MHz.

2.2 European WPR usage

The WPR is a developing new service for meteorology. Their use will grow in the future when local area weather models develop to provide improved temporal and spatial short term forecasts. The following table provides the present distribution of European WPR systems as a function of the operating frequency band.

Operating Frequency band	45-65 MHz	482 MHz	915 MHz	1235-1300 MHz	TOTAL
Number	9	4	2	24	38

Figure 1 provides the location of most of these WPR, which are reporting data to the CWINDE processing hub based at the Met Office, Exeter (UK).



Figure 1: Wind Profiler Radar sites in Europe

There are further WPR systems not provided on this map but also contributing to the processing:

- Denmark : Faroe Islands
- France : three Mobile systems
- Germany : two Mobile systems
- Spain : Bilbao
- UK : one Mobile systems

Table 1 provides, for the above WPR operating in the 1260-1300 MHz band, information about the radar beams (i.e. number of beams used, number of possible beams, beam elevation) and latitude.

No.	WPR location	Centre Frequency (MHz)	Latitude North (°)	Possible beam pos	Beam pos used	Beam elevation (°)
1	Vienna (Austria)	1280	48.1	3, 4 or 5	3, 4 or 5	74.5
2	Innsbruck (Austria)	1280	47.2	3, 4 or 5	3, 4 or 5	74.5
3	Salzburg (Austria)	1280	47.5	3, 4 or 5	3, 4 or 5	74.5
4	Faroe Island (Denmark)	1290	62	3	3	73
5	Marignane (France)	1274	43	3, 4 or 5	5	73
6	Nice, (France)	1274 (during 06)	43.5	3, 4 or 5	5	73
7	Toulouse (France)	1274	Mobile system	3, 4 or 5	3, 4 or 5	73
8 & 9	Meteo-France	1274	Mobile systems	3, 4 or 5	3, 4 or 5	73
10	Lindenberg (Germany)	1290	52.2	3, 4 or 5	5	74.5
11 & 12	Germany	1290	Mobile systems	3, 4 or 5	3, 4 or 5	84
13	Budapest (Hungary)	1290	47.7	3	3	73
14	Szeged (Hungary)	1290	46.4	3, 4 or 5	3, 4 or 5	74.5
15	L'Aquila (Italy)	1290	42.5	3, 4 or 5	3, 4 or 5	74.5
16	Torino (Italy)	1290	45.5	3, 4 or 5	3, 4 or 5	74.5
17	Cabauw (Netherlands)	1290	51.9	3, 4 or 5	3	74.5
18	Bilbao (Spain)	1290	43.4	3, 4 or 5	5	74.5
19	Payerne (Switzerland)	1290	46.8	3, 4 or 5	3 or 4	74.5
20	Meteo Swiss (Switzerland)	1290	Mobile system	3, 4 or 5	3	74.5
21	Dunkeswell (UK)	1290	50.9	3, 4 or 5	4	74.5
22	Wattisham (UK)	1290	52.1	3, 4 or 5	4	74.5
23	Aberystwyth (UK)	1290	52.5	3	3	73
24	Helsinki (Finland)	1290	60.1	5	5	74.5

Table 1: Details on European WPR installations

2.3 Overview of Wind Profiler Radar

2.3.1 Operational characteristics of WPR

To derive criteria to assess the impact of RNSS emissions on WPRs it is useful to introduce briefly the operational characteristics of profiler radars. Radar wind profiling has to deal with the following four tasks:

1. Generation and transmission of a directed electromagnetic wave (EMW) into the atmosphere
2. Interaction of the EMW and the atmosphere, generation of scattered EMW's containing atmospheric information
3. Reception of the scattered waves and transformation to a measurable function (Receiver voltage)
4. Extraction of the desired atmospheric information using mathematical signal processing

The following is a high-level overview considered important to understand the specific operational criteria of these radars and the statistical nature of potential interference conditions when sharing the spectrum between RNSS and this service.

Atmospheric physics, reflectivity of the atmosphere, radar use in meteorology, and especially WPR are widely described and discussed in literature (see section 9).

2.3.2 Wind Profiler Altitude Performance

The equation that binds the returned power, system characteristics, altitude (distance of the target) and atmospheric reflectivity concerning Wind Profilers is given by

$$P_r = ((sys\ para) \cdot t \cdot A \cdot P_t) \cdot \frac{n}{r^2} \quad (1)$$

where

P_r returned power

P_t transmitted power

sys para contains constants and system related design factors, which are fixed

t pulse width / pulse length

A Antenna aperture

n reflectivity of the atmosphere

r range

The range effect is only range raised to the second power because of the volume target. But the real important factor is the, n , reflectivity of the atmosphere that is studied both theoretically and experimentally by various authors. The, in the Wind Profiler context, generally accepted model is given by [8], page 452.

$$n = 0.38 * Cn2 * (-\lambda / 3) \quad (2)$$

where

$Cn2$ is called refractive index structure parameter

λ wave length of the radar

The approximate equation (2) is valid in the inertial subrange for wave lengths less than about 20cm. Inertial subrange is the lower part of the atmosphere, where turbulence energy is transformed to kinetic energy. This happens typically in lower altitudes. Even if the factor λ (-1/3) suggests that higher frequency Wind Profilers would have better altitude performance, this is not the case because the scattering mechanism on the other hand requires that the target, "turbulent eddy", has the size matching half of the wave length of the transmitted signal (Bragg scatter condition).

The 1290 MHz Wind Profilers are typically lower atmospheric profilers intended to perform measurements in the Convective Boundary Layer (CBL), where locally important weather conditions may vary quickly. In the CBL the use of higher frequency is justified because of the existence right size of turbulent eddies.

For the altitude dependency of the refractive index structure parameter, $Cn2$, competent authors give an estimation [8] page 454

$$Cn2 = 3.9 \cdot k \cdot 10^{\frac{-H(km)}{2}} \quad (3)$$

The formula (3) finally tells that reflectivity, n , is the function of altitude (H) and a factor " k ", which depends on the weather condition, and varies by experience widely within CBL. Usually it is given that the nominal value is given $k = 10^{-15}$ whereas the variation may have the range: $10^{-17} < k < 10^{-13}$. The $Cn2$ depends on the combined factor of the moisture and temperature. The best conditions are when air is moist and warm, whereas poor conditions for wind profiling prevails when the atmosphere is cold and dry.

In the Figure 2 the solid line depicts assumed nominal conditions, and the gray area usual variation depending on the weather conditions.

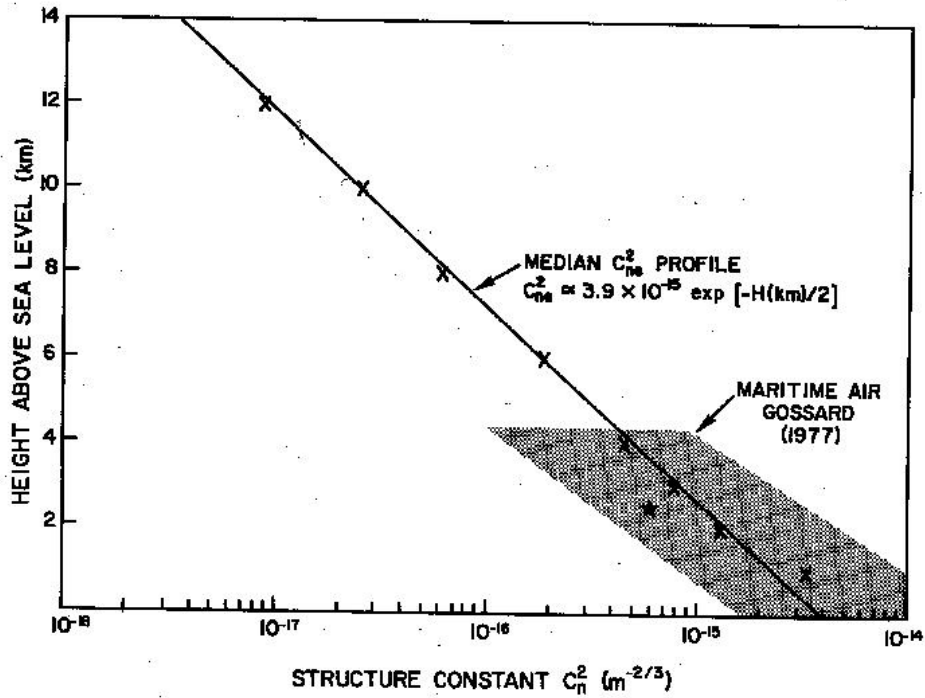


Figure 2: C_n^2 dependency of the altitude (by Doviak and Zrinick) [8]

A good example of quick change in the atmospheric conditions is given in the Figure 3. Site is Helsinki (60° N, 24° E) and time is from evening October 19th to morning October 20th. The gap in data at 1530 hours UTC was an intended break. The change of the weather pattern brought dry air into the site, consequently the maximum altitude decreases from about 4 km down to 3 km.

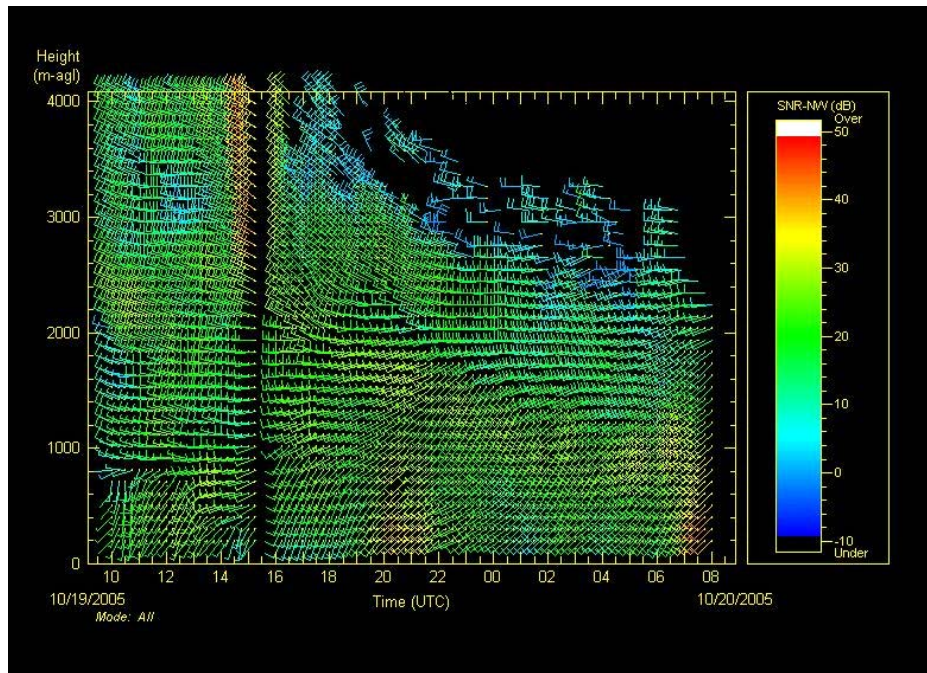


Figure 3: Example from changing weather conditions

Figure 4 depicts the situation when there are "gaps" in the air. From lower atmosphere the returns are good enough to be detected; the factor r^2 in the denominator has not yet taken the effect. Higher the combined factor of squared distance and low C_n^2 is causing too low SNR for the signals to be detected. In the altitude the approaching front carries moist air and consequently the C_n^2 dominates over the range factor: $C_n^2(\text{dry})/r^2 \lll C_n^2(\text{moist})/r^2$ even if $r^2 > r^2$.

For example, one can perceive the situation calculating that the range factor from 2 km to 3 km increases the factor r^2 from 4 to 9 equaling a performance decrease by a factor of - 3.5 dB. In addition the factor $\exp(-H(\text{km})/2)$ in the C_n^2 has an effect of about -2.2 dB. At the same time the factor "k" may increase by 10dB...15dB due to the moisture, and consequently there returned power increases.

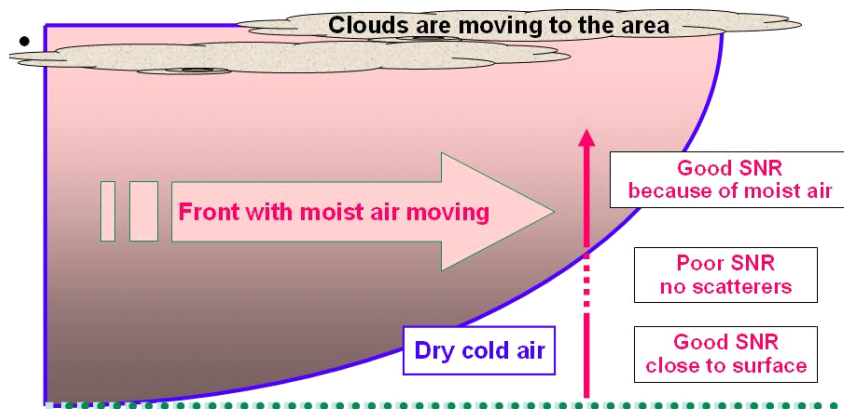


Figure 4: Frontal passage

2.3.3 Scattering physics

Every natural medium has a very complicated space and time dependence and can therefore only be described by means of statistics. The propagation of the waves on the other hand is a topic of Electrodynamics. The connection of both is the mainstay of the understanding of the WPR backscattering problem. The first synthesis of Maxwell's electromagnetic theory and statistical fluid mechanics was pioneered by [60]. It still is an area of active research, see [41].

The major scattering processes for WPR are scattering at small particles and scattering at inhomogeneities of the refractive index. As in every special area of physics, there exists a considerable amount of literature on that topic, including textbooks (e.g. [27, 21, 8]).

In the following, the problem of clear-air scattering is briefly summarized as this is the weaker scattering process (and thus more susceptible to interference) for 1290MHz WPRs. Details can be found in [26]. For a random continuous medium with fluctuating permittivity $\epsilon(\vec{r},t)=1+\epsilon'(\vec{r},t)$, Maxwell's equations can be combined to the following wave equation describing the scattering phenomenon:

$$\Delta \vec{E}_s(\vec{r}) + \epsilon_0 \mu_0 \omega^2 \vec{E}_s(\vec{r}) = \epsilon_0 \mu_0 \omega^2 \epsilon'(\vec{r}) \vec{E}_0(\vec{r}) - \vec{\nabla} [\vec{E}_0(\vec{r}) \cdot \vec{\nabla} \ln \epsilon'(\vec{r})] \quad (1)$$

This is an inhomogeneous vector Helmholtz equation with a known right hand side. \vec{E}_0 denotes the incident electric field vector, whereas \vec{E}_s is the scattered field. The scattering geometry is shown in Figure 5.

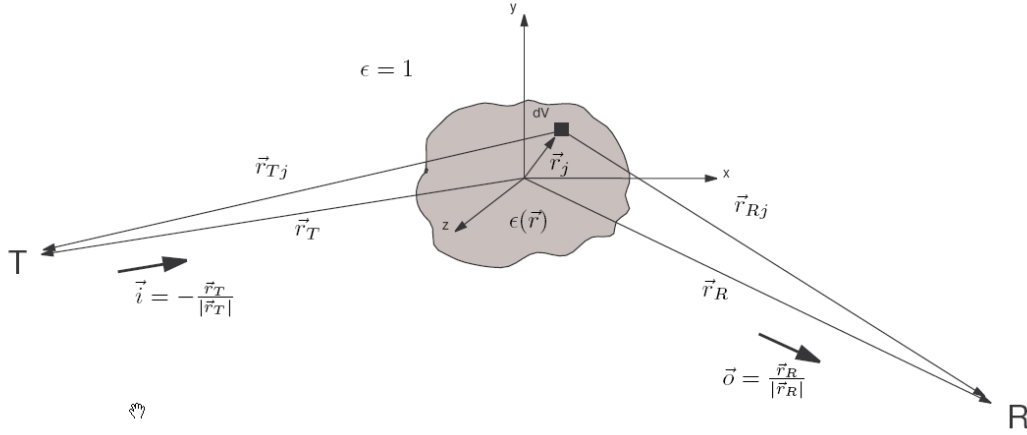


Figure 5: Scattering geometry

Assuming, the scattering region is illuminated by a monochromatic plane wave, that is linearly polarized with normalized (unity) amplitude, i.e. we have for the incident wave:

$$\vec{E}(\vec{r}, t) = \vec{e}_i e^{i(k\vec{i}\cdot\vec{r} - \omega t)}, \quad k = \omega \sqrt{\mu_0 \epsilon_0} \quad (2)$$

In a sufficiently large distance R from the scattering area (the receiver must be in the far field) and neglecting the harmonic time dependence, the scattered wave can formally be written as:

$$\vec{E}_s(\vec{r}, t) = \vec{f}(\vec{o}, \vec{i}) \frac{e^{ikR}}{R} \quad (3)$$

Here, we have introduced the *scattering amplitude*, $\vec{f}(\vec{o}, \vec{i})$, which is generally used in the theory of scattering processes (e.g. [27, 44]). It describes amplitude, phase and polarization of the scattered wave in the far field.

The energy transfer of the wave is described by the Poynting vector $\vec{S} = \vec{E} \times \vec{H}^*$. For an electromagnetic wave progressing in unit direction \vec{n} , we have a known relation between the electric and the magnetic field in the wave zone, thus the Poynting vector can be expressed as

$$\vec{S} = \frac{|\vec{E}|^2}{\sqrt{\eta}} \vec{n} \quad (4)$$

where $\eta = \sqrt{\frac{\mu_0}{\epsilon \epsilon_0}}$ is the wave impedance.

The scattering cross section σ is usually defined as:

$$\sigma(\vec{o}, \vec{i}) = \lim_{R \rightarrow \infty} \frac{4\pi R^2 S_s(\vec{o}, R)}{S_i(\vec{i})} = 4\pi |\vec{f}(\vec{o}, \vec{i})|^2 \quad (5)$$

Radar meteorology has generally to deal with distributed (or volume) targets, therefore it is customary to define a volume reflectivity η as the radar cross section per unit volume:

$$\eta = \frac{d\sigma}{dV} \quad (6)$$

In the case of backscattering, that is $\vec{o} = -\vec{i}$, we get the following (monochromatic) solution of equation 1 using the Fraunhofer approximation (small-volume scatter approach):

$$\vec{E}_s(\vec{r}) = \vec{E}_o \frac{k^2}{4\pi r} e^{ikr} \iiint_V \varepsilon'(\vec{r}') e^{-i2k\vec{r}' \cdot \vec{i}} d^3\vec{r}' \quad (7)$$

Here, $k = \omega\sqrt{\mu_o\varepsilon_o}$ is the wave number. For the scattering amplitude \vec{f} , one gets:

$$\vec{f}(-\vec{i}, \vec{i}) = \frac{k^2}{4\pi} \iiint_V e^{-i2k\vec{i} \cdot \vec{r}'} \varepsilon'(\vec{r}') d^3\vec{r}' \quad (8)$$

We need to consider, that the field of fluctuations of the dielectric number ε' is a random function, because only its statistical properties are known (at best). Therefore, also the scattering amplitude is a random function [27, 8]. Thus, we get

$$\sigma_b = \frac{k^4}{4\pi} \iiint_V \iiint_V \langle \varepsilon'(\vec{r}'_1) \varepsilon'(\vec{r}'_2) \rangle e^{i2k\vec{i} \cdot (\vec{r}'_1 - \vec{r}'_2)} d^3\vec{r}'_1 d^3\vec{r}'_2 \quad (9)$$

The function $B_\varepsilon = \langle \varepsilon'(\vec{r}_1) \varepsilon'(\vec{r}_2) \rangle$ is the correlation function for the dielectric fluctuations. At this point, it is useful to introduce new coordinates:

$$\vec{\sigma} = \frac{1}{2}(\vec{r}_1 + \vec{r}_2) \quad \vec{\delta} = (\vec{r}_1 - \vec{r}_2) \quad (10)$$

This allows us to write

$$\sigma_b = \frac{k^4}{4\pi} \iiint_V \iiint_V B_\varepsilon(\vec{\sigma}, \vec{\delta}) e^{i2k\vec{i} \cdot \vec{\delta}} d^3\vec{\delta} d^3\vec{\sigma} \quad (11)$$

The last integral can be interpreted as a Fourier-transformation of B_ε with respect to $\vec{\delta}$. As it is known from statistical turbulence theory, this gives the variance spectrum Φ of ε [17]. We can therefore write

$$\sigma_b = 2\pi^2 k^4 \iiint_V \Phi_\varepsilon(\vec{\sigma}, 2k\vec{i}) d^3\vec{\sigma} \quad (12)$$

For the volume reflectivity $\eta = d\sigma_b / dV$ get thus

$$\eta_b = 2\pi^2 k^4 \Phi_\varepsilon(\vec{\sigma}, 2k\vec{i}) = 8\pi^2 k^4 \Phi_n(\vec{\sigma}, 2k\vec{i}) \quad (13)$$

It can be seen that the volume reflectivity (and therefore the echo power received by an atmospheric radar from fluctuations in the refractive index) is directly proportional to the 3-D variance spectrum of refractivity for a wave number corresponding to the half radar wavelength. The sampling of Φ at only one wave number is the Bragg condition, which is a condition for constructive interference. Note that the variance spectrum is sampled at wave vector $2k\vec{i}$, so there might be a dependence of the volume reflectivity on the direction of the incident wave in case of an anisotropic variance spectrum. However, at UHF one can assume the easier case of locally isotropic fluctuations that is found in the inertial-sub range of turbulence.

There exist several models for the variance spectrum of the refractive index [27]. The most important one is justified by the statistical theory of Kolmogorov [17]: In case of fully developed, local homogeneous and isotropic turbulence, there exists an inertial sub range, where the three-dimensional variance spectrum has a typical wave number dependence of $k^{-\frac{11}{3}}$ can be written as

$$\Phi_n(\bar{\sigma}, k) = 0.0330 c_n^2(\bar{\sigma}) k^{\frac{11}{3}} \quad (14)$$

where c_n^2 is the structure parameter for the refractive index [17]. After insertion, one finally arrives at the following classical result of radar meteorology for the volume reflectivity caused by fluctuations of the refractive index; see e.g. [40] and references cited therein:

$$\eta_b = 0.3787 c_n^2(\bar{\sigma}) \lambda^{\frac{1}{3}} \quad (15)$$

Again, this expression is only valid if the Bragg scale of the radar ($\lambda/2$) is well within an existing inertial sub range of turbulence $l_o \leq \lambda/2 \leq L_o$, where l_o denotes the inner scale and L_o the outer scale of turbulence. For scales smaller than l_o , the viscous dissipation of kinetic energy dominates and the spectrum is extremely small or zero [27]. This is essential in the understanding of why there are constraints in the selection of operating (carrier) frequencies for WPR's.

2.3.4 Radar hardware

2.3.4.1 Doppler radar profiler systems (WPR)

Wind Profiler Radars¹ can be classified into three main groups [42]. Their hardware architecture can vary substantially:

1. Single signal systems
2. Two signal systems
3. Multi-signal systems

Single signal systems are the classical form of Doppler radar profiler. They are monostatic² pulse radars using one single carrier frequency with the hardware architecture resembling that of a typical Doppler radar system, as described in [51]. Examples of this type of profiler system are described in [34, 57, 11, 3, 10, 58]. The term *single signal* refers to the characteristics of the instruments sampling function, which is an equation that maps a field describing the physical properties of the atmosphere relevant for the actual scattering process to the received radar (voltage) signal. For clear-air scattering, this is the scalar field of the refractive index (or permittivity) irregularities.

Two signal systems are extensions of the single signal architecture, where two different sampling functions are realized to improve the retrieval of atmospheric properties of interest. Two techniques that have been used most often are the frequency-domain interferometry (FDI) using a mono-static radar with two different carrier frequencies [30, 4, 35] and the spaced-antenna technique using one carrier frequency and multiple receiving antennas [32, 9].

Recently, *multi-signal systems* have been developed. Similarly, they either use a bi-static combination of a single transmit and a multitude of receiving antennas to perform digital beam forming [37, 47, 24] or they transmit several carrier frequencies to achieve so-called range imaging (RIM) with a single (mono-static) antenna [45, 52, 5, 6].

It is obvious, that it is beyond the scope of this note to discuss potential interference effects for all existing and envisaged Doppler radar profilers. It is nevertheless necessary to highlight the importance of frequency bands for this type of environmental research. Especially RIM has already been implemented at higher UHF (915 MHz) in the United States and similar instruments in Europe would critically depend on the availability of an uncontaminated L-band at 1290 MHz, if no other band can be found.

¹ also addressed as Doppler Radar Profiler (DRP)

² the same antenna is used for transmitting and receiving.

2.3.4.2 A 1290 MHz Doppler beam swinging radar wind profiler

In the following, the discussion will be restricted to existing single signal systems, in particular to the 1290 MHz system at Lindenberg [11]. It is important to note that the considered profiler is a typical instrument for Boundary Layer measurements; it is mostly used to measure the mean horizontal wind components. However, it can also be used for other investigations like the determination of mixing height, high-resolution measurements of the vertical wind, cloud and precipitation studies.

Although this type is in wide-spread use, one needs to have in mind that these radars are not standardized. In other words, the transmitted signals and the used sampling and processing of the received signals are not harmonized with other devices. This is in contrast to systems used in communication. That means that one needs to be careful in terms of the general applicability of the measurement results, in particular when significant compatibility improvements seem to be feasible through the use of sophisticated (and perhaps proprietary) digital signal processing methods.

The general hardware architecture is shown in the block diagram. The central unit is the radar controller, which uses a highly stable oscillator (coherent oscillator or COHO) as the single reference for all signals and is activated by the radar processor. The signal to be transmitted is generated by a waveform generator, which can be looked at as an amplitude and phase modulator. After up-conversion and amplification (power amplifier) the transmit signal is delivered to the antenna. A duplexer allows the use of a single antenna for transmitting and receiving. It is comprised of a solid-state ferrite circulator and additional receiver protecting devices.

The antenna is an electronically steered phased array, comprised of microstrip printed circuit boards. A relay-switched true-time delay phase shifting unit is used to generate the necessary phasing of the individual elements required to generate five fixed beam directions.

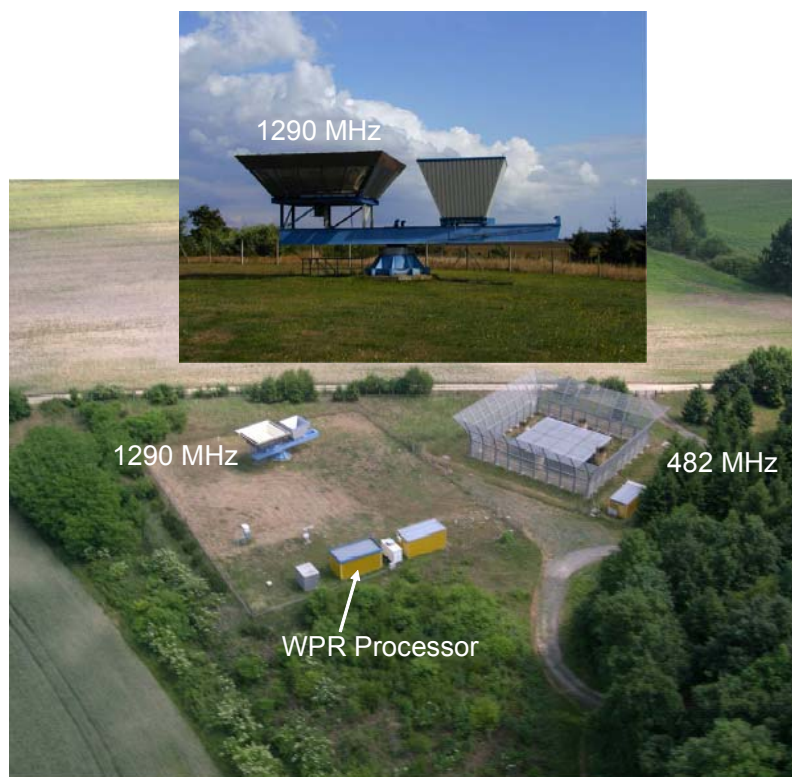


Figure 6: Photograph of 1290 MHz Doppler radar profiler at MOL, Lindenberg, Germany

The receiver is of the classical superheterodyne type. A broadband low-noise amplifier with an excellent noise-figure is necessary to raise the signal level of the weak atmospheric return for further processing. After down-conversion to an intermediate frequency (IF), the signal is bandpass-filtered (actually matched filtering to maximize the per-pulse SNR), demodulated and A/D converted for further digital processing in the radar processor. The actual technical implementations differ, for example the received signal can be digitized either at

IF (so called digital IF receivers) or at base-band, after further analogue down-conversion by a quadrature detector (analogue receiver).

The radar shown in Figure 6 has a rather unique configuration; it is mounted on a turntable that can be rotated by 360°. This system can therefore be used for special investigations on the influence of the exact position of the RASS source on measurements of the virtual temperature and others.

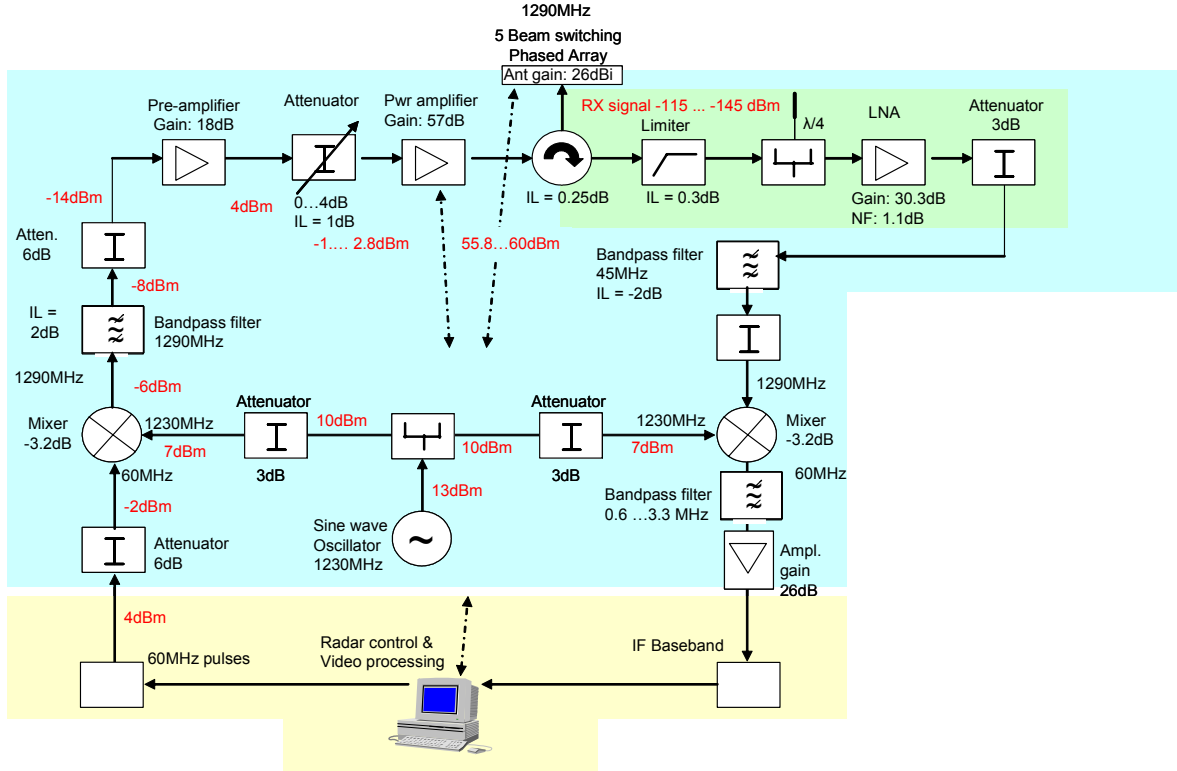


Figure 7: Block diagram of a typical DBS radar wind profiler (WPR-A)

2.3.4.3 Wind measurement using the Doppler beam swinging method

Most current-day wind profilers use the method of Doppler beam swinging to determine the wind vector. At least three linear independent beam directions and assumptions concerning the wind field are required to transform the measured 'line-of-sight' radial velocities into the wind vector. This principle will be briefly discussed for a typical five beam system as depicted in Figure 8.

Assuming that the wind field \vec{v} with components (u, v, w) in a Cartesian coordinate system in the vicinity of the radar can be written as a linear Taylor series expansion in the horizontal coordinates

$$\vec{v}(x, y, z) = \vec{v}(x_o, y_o, z) + \nabla_h \vec{v}(x, y, z) \Big|_{x_o, y_o} \cdot \vec{\Delta r} \tag{16}$$

For simplicity without loss of generality, it is further assumed that the antenna beam directions are aligned in parallel to the Cartesian coordinate axis (i.e. x East, y North). If the radial velocity measured in the 'line-of-sight' of a radar beam described by unit directional vector \vec{n} is written as

$$v_r = \vec{v} \cdot \vec{n} \tag{17}$$

we get with $\delta x = \delta y = z \tan(\alpha_o) \cos(\alpha_o)$ for the differences of the radial winds of the four oblique beams at height z.

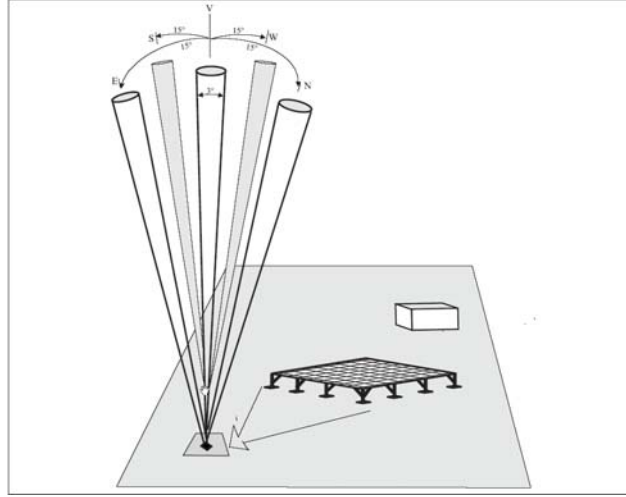


Figure 8: Beam configuration of a typical DBS radar wind profiler

$$[v_{rE} - v_{rW}](z) = 2u_o(z) \sin(\alpha_o) + 2 \frac{\partial w}{\partial x}(z) \delta x(z) \quad (18)$$

$$[v_{rN} - v_{rS}](z) = 2v_o(z) \sin(\alpha_o) + 2 \frac{\partial w}{\partial y}(z) \delta y(z) \quad (19)$$

Here, α_o is the zenith distance of the oblique beams, z is the height above ground and the subscripts denote East, West, North and South, respectively. It is immediately clear that one assumption is required to determine the (horizontal) wind components u_o, v_o , namely:

$$\frac{\partial w}{\partial x} = \frac{\partial w}{\partial y} = 0$$

In meteorological terminology, the horizontal shear of the vertical wind must vanish to retrieve the horizontal wind without errors. This condition is not always given; however, it is usually correct over a longer time interval (on average).

2.3.5 Signal processing

The main parameters of the signal generated by the backscattered electromagnetic wave are: power, mean Doppler velocity, and velocity variance (e.g. the first three moments of the Doppler spectrum). Signal processing ends with the estimation of the moments of the Doppler spectrum and further data processing is then performed to finally determine the wind and other meteorological parameters using measurements from all radar beams.

This distinction, which goes originally back to [29], has become more and more blurred, because modern algorithms are trying to select the moments of the Doppler spectrum with the help of continuity and other information [7, 65, 39]. However, here we will refer to the usually applied and well-established "classical" signal processing, as described by [62, 49], among others.

The mean Doppler shift of the received signal is used to determine the velocity component of "the atmosphere" projected onto the beam direction. As the bandwidth B of a transmitted electromagnetic pulse of duration τ is much larger ($B \propto 1/\tau \approx 100 \dots 1000 \text{ kHz}$) than the Doppler shift ($f_d \approx 10 \dots 500 \text{ Hz}$), the frequency shift can not

be determined from the processing of a single pulse. Instead, the return of many pulses is evaluated to compute the Doppler frequency from the slowly changing phase of the received signals [2] over a long dwell time³.

2.3.5.1 Demodulation

The backscattered electromagnetic signal is received by the antenna with radiation pattern $\vec{g}_A(\vec{\rho})$ and converted into a voltage signal:

$$V_{rx}(\vec{r}_o, t) = \iint_F \vec{E}_s(\vec{r}_o + \vec{\rho}, t) \vec{g}_A(\vec{\rho}) d^2 \vec{\rho} \quad (20)$$

This voltage signal is a measured physical quantity and as such necessarily real. Moreover, it is a narrow-band signal and can be written as

$$V_{rx}(t) = A(t) \cos[\omega_c t + \Phi(t)] \quad (21)$$

The atmospheric information is contained in the instantaneous amplitude $A(t)$ and the instantaneous phase $\Phi(t)$ and need to be extracted by the demodulation process. However, in the equation above the definition of instantaneous amplitude and phase is not unique. To avoid this ambiguity, the received signal is "complexified" by analytic extension through the Hilbert transform H .

$$V^+(t) = V(t) + iH[V(t)] = \tilde{V}(t)e^{i\omega_c t} \quad (22)$$

Here, the complex envelope $\tilde{V}(t)$ was defined, which can now easily be determined by just multiplying the analytic signal with a complex exponential. This is the actual demodulation step.

$$\tilde{V}(t) = V^+(t)e^{-i\omega_c t} = I(t) + iQ(t) \quad (23)$$

The Hilbert transform is difficult to implement in real systems. Instead, the real "in-phase" $I(t)$ and the imaginary "quadrature phase" $Q(t)$ part of the complex envelope are determined using a quadrature demodulator. As already mentioned, there are two different receiver implementations used for WPRs. Both are build upon the super-heterodyne architecture, but their back-ends differ considerably.

The classical analogue system uses a hardware (mixer)-based quadrature detector to down-convert the signal to baseband and to determine the complex envelope by determining the in-phase and quadrature-phase components, the so-called complex video signal. Matched filtering is also performed in hardware before the complex signal is sampled and digitized by two A/D converters.

The modern digital system starts by first digitizing the signal at IF. Usually, the Nyquist criterion would require quite a high sampling rate to unambiguously represent the signal. However, if certain conditions (mainly signal bandwidth limitations) are fulfilled, a specified sub sampling can be used to both down-convert the signal and to determine the quadrature components digitally at the same time (quadrature sampling). In this approach, matched filtering is performed digitally.

³ The dwell time is the measurement time for generating the Doppler spectrum.

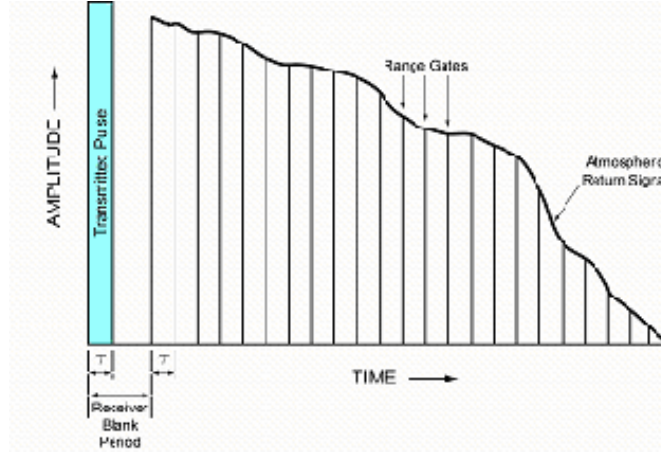


Figure 9: Range gates

Range gating is usually done in the A/D process using sample and hold circuitry. The sample strobe for range gating z_j is provided by the radar controller. That is, for each range gate a discrete complex time series $\{V_k(z_j)\}$ of the complex envelope is generated:

$$\tilde{V}_j[t_k] = I_j[t_k] + iQ_j[t_k] \quad (24)$$

The discrete time increment ΔT between the samples in each of the N_h (number of range gates) time series is given by the pulse repetition time (the so-called Inter-Pulse Period). For a typical wind profiler it is of the order of 10^{-4} s. In the following, we will only consider one range gate j and suppress the index.

2.3.5.2 Digital filtering

For historical reasons, most existing wind profiler systems employ a simple digital filtering method that is called coherent integration. As the sample rate ΔT was beyond hardware capabilities of the first wind profilers, hardware adder circuits were used to reduce the data rate. This allows a reduction of the data rate at the expense of the analyzable Nyquist interval. Coherent integration can be written as

$$V^{ci}[t_m] = \frac{1}{N_{ci}} \sum_{k=0}^{N_{ci}-1} V[t_m + k \cdot \Delta T] \quad (25)$$

This method poses normally no problems, if the number of coherent samples N_{ci} is chosen not too large. However, one has to keep in mind that the above process can be seen as a digital boxcar filter operation, followed by sub-sampling [12]. This gives rise to frequency response characteristics that are sometimes referred to as comb-filtering [50]. The filter amplitude transfer characteristics is given by

$$|H(f_o)| = \frac{\sin(N_{ci}\pi f_o \Delta T)}{N_{ci} \sin(\pi f_o \Delta T)} = D_{N_{ci}}(f_o \Delta T) \quad (26)$$

where $D_{N_{ci}}$ is the Dirichlet kernel. A plot of this function around baseband is shown in Figure 10. Note that the function is periodic and only plotted over a finite interval.

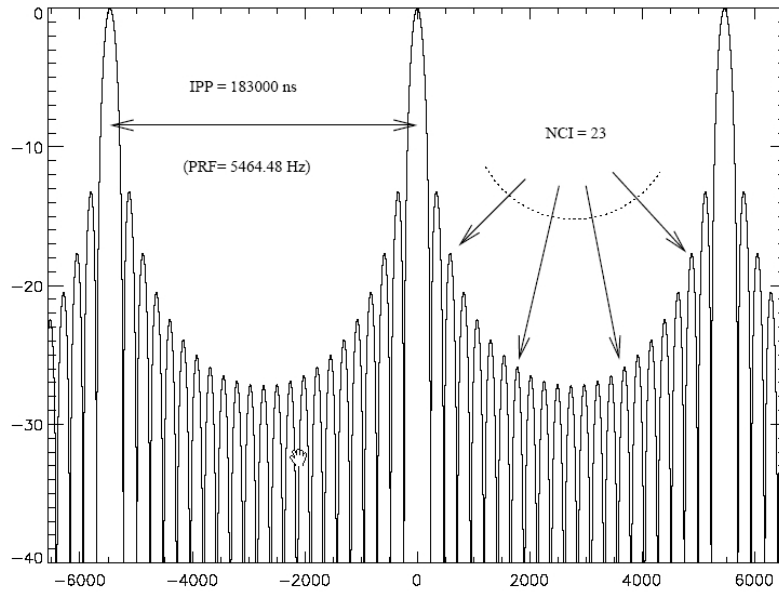


Figure 10: Coherent filter response (dB) characteristics for IPP=183 μs and Nci=23. The unit on the abscissa is Hz

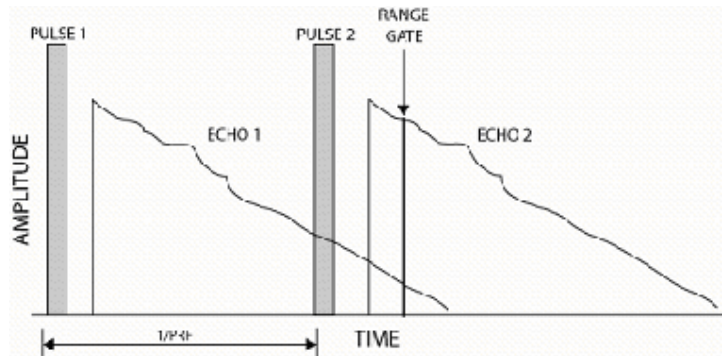


Figure 11: Impact of the pulse repetition frequency

2.3.5.3 Estimation Power spectrum

The coherently integrated time series $V^{ci}[t_m]$ for atmospheric returns can be modelled as a Gaussian random process. Therefore, it suffices to consider the auto-covariance function or, equivalently, the power spectrum for this process without a loss of information. The latter is usually referred to as the Doppler spectrum. In wind profiler radars, a classical nonparametric estimator of the power spectrum is used - the Periodogram [28]. This method uses no further a-priori information and produces reasonable results for a large class of processes.

The Periodogram estimator with window4 coefficients h_n is given by

$$P_k = \frac{1}{N} \left| \sum_{n=0}^{N-1} h_n \bar{V}_n^{ci} e^{-i \frac{2\pi k n}{N}} \right|^2 \quad (27)$$

⁴ For ease of implementation a Hanning (von Hann) window is used frequently.

The Periodogram viewed as statistical estimator has quite bad variance properties. Additional smoothing is thus required, which is done by the method of incoherent averaging (Welch method).

$$\bar{P}_k = \frac{1}{N_{sp}} \sum_{n=k}^{k+N_{sp}} P_n \quad (28)$$

This produces decent estimates of the power spectrum, provided the above mentioned assumptions hold. It is known that these assumptions are violated in the case of intermittent clutter contributions [42], but this discussion is irrelevant in this context.

The Doppler spectrum is usually given as a function of velocity instead of frequency. The conversion between frequency f and radial velocity v_r uses the well-known relation $f = 2v_r/\lambda$, where λ denotes the radar wavelength.

2.3.5.4 Signal detection and classification

An example of a typical Doppler spectrum is shown in Figure 12.

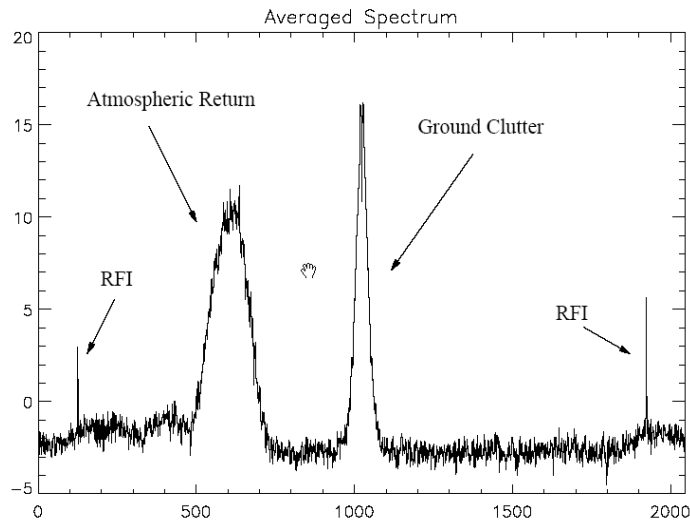


Figure 12: A typical averaged Doppler spectrum, estimated by a 2048 point Periodogram

It can be seen, that various spectral maxima are present that reside on white noise. To discriminate between noise and signals, an objective noise level is estimated using the method put forward by [25]. This method works well, if white noise occupies a sufficient part of the spectrum. In the next step it is necessary, to select the signal peak caused by the atmospheric return. For single peak spectra, there exists a well-established method, which is called the first moment algorithm [58, 36].

For multiple peak spectra (as shown in the example, other peaks may be generated by various clutter contributions to the signal) a variety of methods has been proposed. Among them are simple methods as the one proposed by [48], which is in widespread use. Also other, more complex algorithms [22, 7, 64, 39] are occasionally in use.

2.3.5.5 Parameter estimation

Very often, the power spectrum of the atmospheric signal is also assumed to have a Gaussian form though this can be violated for *certain radar returns* [66]. However, the assumption of Gaussian spectral shape has the advantage that only three parameters (Power, mean frequency and frequency spread) are sufficient for a complete description of the signal, which simplifies processing a great deal [67]. Even if this assumption of the

form of the power spectrum is violated, these parameters are well defined. If $S(\omega)$ denotes the power spectrum associated with the random process signal then the fundamental base parameters are:

$$P = \int S(\omega)d\omega \quad \text{Power} \quad (29)$$

$$\Omega = \frac{1}{P} \int \omega S(\omega)d\omega \quad \text{Mean Doppler shift} \quad (30)$$

$$W^2 = \frac{1}{P} \int (\omega - \Omega)^2 S(\omega)d\omega \quad \text{Spectral Width} \quad (31)$$

2.3.5.6 Nonlinear consensus-filtering

Because of the weak scattering at refractive index fluctuations, wind profilers usually operate in regions of very small SNR values. This is generally true at least at the uppermost range gates. Consequently, one has to make a compromise in setting the detection threshold.

Unlike classical radars, profilers operate with low detection thresholds that lead to the fact, that *for weak signals the probability of false alarm may be as high as the probability of detection* [13]. Of course, one has to live then with an inevitably high number of bad estimates [15]. The same problem occurs with other remote sensing systems, for instance with LIDAR [53].

The probability density function (PDF) of a maximum energy based estimate \hat{V} for the true mean Doppler velocity v in case of white noise (SNR parameterized by $0 \leq b \leq 1$) is [15]:

$$p(\hat{v}) = \frac{b}{2v_N} + \frac{1-b}{\sqrt{2\pi} g} e^{-\frac{(\hat{v}-v)^2}{2\sigma^2}} \quad (32)$$

This is a Gaussian resting on white noise. The simplified model assumes that the atmosphere behaves quasi-stationary over sufficiently short periods. "Sufficiently" in this context means less than one hour.

The Gaussian is more pronounced for a higher SNR (within a smaller bandwidth B) or less pronounced for a low SNR (for a larger bandwidth B). In other words, a low SNR increases the chance that the estimated Doppler velocity estimate is drawn from the white noise part of the PDF. To avoid a selection of these noise-caused estimates, nonlinear digital filtering is performed by means of the so-called consensus average [14, 58].

The consensus has the following two purposes:

1. It acts as a decision statistics to discriminate between (false) Doppler estimates caused by random noise peaks and (correct) estimates, which are due to stationary atmospheric returns.
2. It is a homogeneous, nonlinear estimator for the Doppler velocity that includes outlier suppression

Other nonlinear filters are possible as well (for instance the Median), but consensus has proven its robustness and accuracy [58]. The principle is best illustrated graphically as shown in Figure 13.

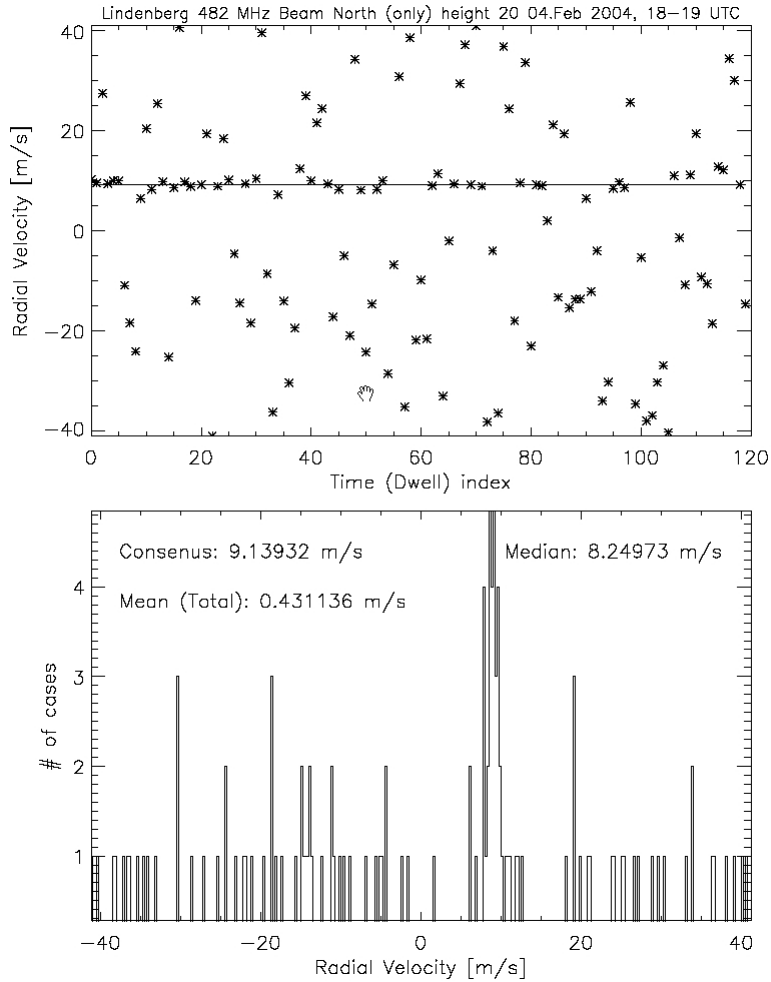


Figure 13: The consensus principle

The upper part in Figure 13 shows the distribution of 120 individual estimates for the Doppler velocity at one range gate of a UHF wind profiler measured over one hour. The line shows the consensus estimate. The lower part shows the histogram (distribution) of the individual estimates. Note that this resembles the pdf discussed above. A distinct maximum of Doppler estimates can be seen near 9 m/s - this is in agreement with the value estimated by the CNS. Median values and arithmetic mean are shown for comparison reasons.

2.3.5.7 *Pulse compression*

WPRs generally aim at very high resolutions. Recent approaches like the RIM systems have been mentioned before. A good radial (along the beam) resolution is a goal for classical wind profilers performance. High resolution obviously implies a high bandwidth of the transmitted signal. For a simple pulse, this means that the pulse length needs to be short as the range resolution is given by $c\tau/2$.

On the other hand, one is also interested in high transmitted power to maximize the detectability in case of weak scattering. This poses a problem, however, because pulse peak power is technically limited.

One way to overcome this difficulty is the method of pulse compression. Pulse compression uses the fact, that a long pulse can have the same spectral bandwidth as a short pulse, provided that the long pulse has an additional modulation (in frequency or phase) [51]. When receiving such a return signal, one has then to make sure that this long pulse is appropriately "compressed" to a short pulse by the matched filter of the radar receiver (analogue or digitally).

Wind profiler systems very often use the method of (mostly binary) phase modulation (coding) where a long pulse is divided into N sub-pulses, each having the length to yield the desired range resolution. This means, that the transmitted signal

$$\tilde{s}_{tx}(t) = \sum_{p=0}^{N-1} c_{p+1} \Pi\left(\frac{t - (p+1/2)\tau}{\tau}\right) e^{i\omega_p t} \quad (33)$$

with the gate function $\Pi(t)$ is defined by

$$\Pi(t) = \begin{cases} 1; & \text{for } -1/2 \leq t \leq 1/2, \\ 0; & \text{elsewhere} \end{cases} \quad (34)$$

Here, c_k is a complex vector determining the phase of the individual sub-pulses ($c_k = e^{i\Phi_k} = \cos\Phi_k + i\sin\Phi_k$).

Most current wind profiler employ only binary phase coding that is either $\Phi = 0^\circ$ or 180° .

Complementary codes are used, in which the sidelobes of the autocorrelation function of a first code sequence A are the negative image of the second sequence B.

On receive, the decoding (compression) process comprises three steps:

1. Sampling of V_k for each range gate and separate coherent integration for pulses with code sequence A and B.
2. Correlation of V_k for both data streams with the bit-pattern of either code sequence A or B.
3. Addition of both series A and B.

Note that due to the complementary nature of the sequences A and B, the compression takes place at step 3.

Pulse compression achieves both, positive and negative effects:

Among the positive effects are a de-sensitization of the radar against some RFI signals [55]. Negative effects are the appearance of range sidelobes, sometimes called self-clutter, and problems in getting signals from the lowest range gates. These problems are described in detail by [50, 59, 63, 19].

The last problem is especially significant for radar wind profilers: Using a code sequence length of N , one has problems with the decoding of the lowest $N-1$ range gates. Here, a procedure called partial-decoding can be employed [18, 55], but one has to live with a decrease of the SNR and with a worse situation in respect of range-sidelobes in case of radial reflectivity gradients. Optimization is possible [54, 56], but not implemented in every system.

2.4 An example of measurement sequence for one WPR type

2.4.1 WPR operating modes

Wind profiling requires either two oblique orthogonal and one vertical measurement, or four orthogonal oblique measurements. Two oblique measurements in opposite directions (e.g. East-West) can solve the vertical component.

Because wind profilers have only one transmitter and one receiver, the required measurements are done in close sequence, usually a few ten seconds in each one direction. This is first done with short pulse for low altitude high resolution profiling followed by long pulse profiling for higher altitudes though compromising the vertical resolution.

The result of one complete sequence, with short and long pulses, is called a "raw wind vector" profile. This is usually produced in about three minutes consisting of about half minute of each three beams and two pulses. In some applications these "raw wind vectors" are used as data products for the application, but for some other purposes a number of "raw wind vectors" are processed using a statistical method of consensus averaging to provide the data product, e.g. ten samples of "raw wind vectors" making half an hour average wind. The

consensus average cannot be produced reliably if more than a specified number of the "raw wind vector" profiles are suspect in quality.

The WPR system investigated can work with three or five beam directions and engage up to five operating modes on the acquisition level of which only two can be use for wind profiles production (two wind profiles).

The five possible operating modes are given in Table 2.

Mode	Emission Power P_e (Watts)	Pulse width τ (μ s)	Pulse figure	Repetition period T_R (μ s)		
1	3500	0,5	Gaussian	25		
2	3500	1	Gaussian	35		
3	3500	2,5	Trapezoidal	60/65		
4	270	0,3	Trapezoidal			
5	270	0,5	Trapezoidal			

Table 2: Operating modes of the WPR-B in Nice, France

2.4.2 Transmission duty cycle and signal processing characteristics

2.4.2.1 Definitions

- D_p dwell time; time to stay to point into one given direction to accomplish a measurement
- N_{CI} number of samples in the Coherent integration
- N_{FFT} number of points (discrete frequencies) in the Fourier's transform to present a spectrum
- N_{inch} number of spectra for incoherent integration
- T_L the processing time for the "low" mode
- T_H the processing time for the "high" mode
- T_G the global processing time including both "low" and "high" modes
- τ_L (τ_H) the pulse length (pulse width in time domain) for the "low" mode ("high" mode)
- T_{RL} (T_{RH}) the recurrence sample time for one sample (inter pulse period = $1/PRF$) for the "low" mode ("high" mode)
- τ_L (τ_H) the duty cycle for the "low" mode ("high" mode)
- k the system specific number of repeated measurement to perform a full profile in one mode typically $k = 1$ or 2)
- n the number of beam directions.

2.4.2.2 Duty Cycle

Duty cycle α is defined as the ratio between the effective emission time t and the recurrence period TR (multiplied by 100 to get the result as a percent).

$$\alpha(\%) = \frac{\tau}{T_R} \times 100$$

Table 3 provides the duty cycles and the corresponding operating modes.

Mode	τ (μ s)	T_R (μ s)	α (%)	Observations
1	0,5	25	$\square B = 2$	The maximum transmitter Duty Cycle is 5% ($\square \max = 5\%$)
3	2,5	65	$\alpha_H = 4,18$	

Table 3: Duty cycles for different modes of operation (WPR-B)

2.4.2.3 Processing time

Dwell period (D_p), is the time WPR measures in one given direction before pointing the beam to an other direction or changing the mode; e.g. high or low. The dwell period is a function of sample time (inter pulse period), the number samples used to coherent integration, multiplied by points required for Fourier transform to form one spectrum, and number of spectra needed to be averaged (incoherent integration).

$$D_p = T_R \cdot N_{Cl} \cdot N_{FFT} \cdot N_{inch}$$

The processing time is the time needed for one wind profile as a result of the measurements before the next measurement cycle can be started. Hence the processing time depends on the dwell period, number of beam directions (n), operating modes, usually two; low and high, and the system specific factor k .

- For the "low" mode, we have: $T_L = n \times k \times T_{RL} \times N_{Cl(L)} \times N_{FFT(L)} \times N_{inch(L)}$
- For the "high" mode, we have: $T_H = n \times k \times T_{RH} \times N_{Cl(H)} \times N_{FFT(H)} \times N_{inch(H)}$

The global processing time T_G is given by: $T_G = T_L + T_H$

The parameter settings in the Table 4 gives low mode processing time for a profile: $T_L = 104$ s, and for high mode: $T_H = 96$ s. Consequently the global processing time $T_G = 200$ s. If the requirement is to provide a consensus profile over a period of half an hour ($X(s) = 1800$ s) the WPR can use 9 spectra in the consensus calculations ($N_{Spectra} = 9$). The number of spectra used for consensus can be calculated by the formula:

$$N_{Spectra} = \text{Int} \left[\frac{X}{T_G} \right] \text{ with "Int" for integer part.}$$

The smaller $N_{Spectra}$ the worse the consensus for a data acquisition parameter.

Mode	T_R (μ s)	N_{Cl}	N_{FFT}	N_{inch}	n	k	$T_{B/H}$ (s)	T_G (s)	X (s)	$N_{Spectra}$
1	25	65	128	50	5	2	104	200	1800	9
3	60	25	128	50	5	2	96			

Table 4: Mode settings for the WPR-B type radar in Nice

For Nice (like Marseille), we have $k = 2$ because those radars are working with bi-phased mono-pulse ($0, \pi$) emission from one recurrence to the next. We add during the receiving of two successive recurrences which allows to get rid off or at least to reduce some parasitic echoes.

2.5 Wind Profiler Data Presentations

In typical wind profilers, the output data types of the radar processor include wind data and/or virtual temperature data, if the Radio Acoustic Sounding System (RASS) option is included, as text or database files, and spectral moments, spectra, and/or time-series as binary files.

The data can be displayed in many formats. In Figure 14 "wind barbs" are used to indicate the speed and direction for each height. Time is normally plotted from right to left as weather systems normally move from

west to east at mid-latitudes; this type of display thus approximates a vertical east-west slice through the atmosphere.

However, time is plotted from left to right in this example. Figure 14 shows clear change in wind direction just below 1000 m. The sudden change in wind direction and/or speed is known as a wind shear zone and is important for aviation applications.

The feathers and flags of "wind barbs" most often represent wind speed in knots, but sometimes other units are used; here, the winds are in m/s. A half feather corresponds to 2.5 m/s, a full feather to 5 m/s and a flag to 25 m/s. Traditionally, the feathers point in a clockwise direction for Northern Hemisphere observations and in a counter clockwise direction for Southern Hemisphere observations. The shaft of the "wind barb" points in the direction of wind flow. Other typical display modes are shown in Figure 15 as "Contour" plot and Figure 16 as "Stacked" plot, respectively. The contour plots are considered best when a qualitative conclusion is drawn for a given interference condition.

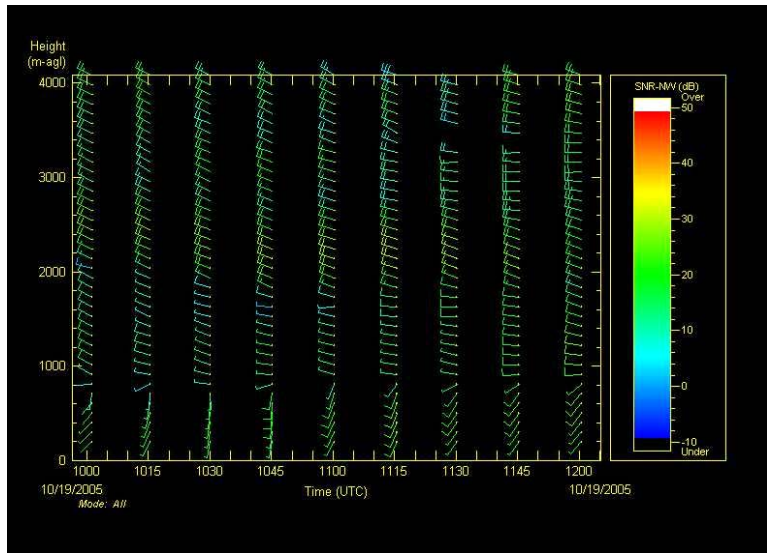


Figure 14 Wind data presentation taken from Helsinki WPR October 2005

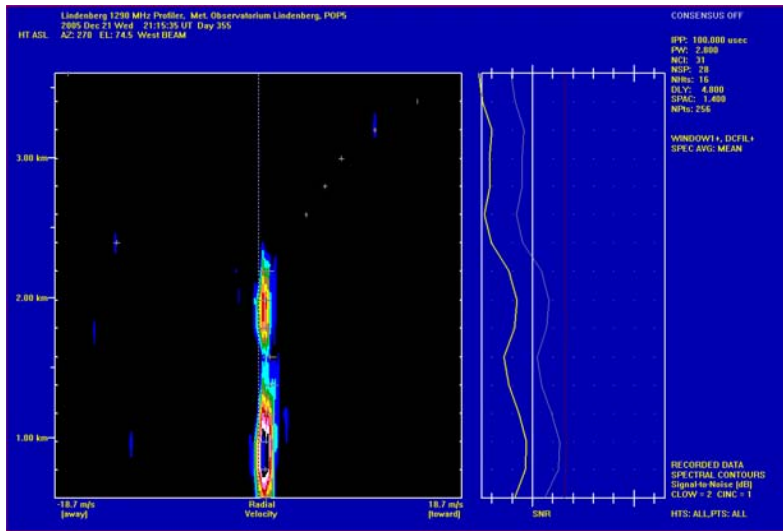


Figure 15: Example 2: Wind data as contour plot without interference (WPR-A)

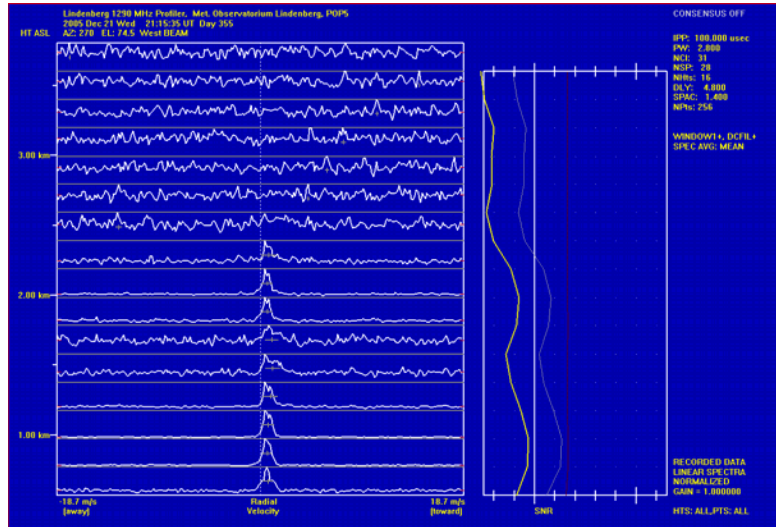


Figure 16: Example 3: Same wind data as before but as stacked plot (WPR-A)

2.6 Operating Techniques

There are two basic parameters to be set in a WPR:

- Pulse width (pw) and the
- Inter-pulse-period (IPP).

A narrow pulse width gives fine resolution and the ability to measure at close range, but does not have the energy to enable detection of the weak echoes from long range.

A short inter pulse period gives many echoes per unit time, and maximises the detection enhancement provided by averaging. But if the IPP is too short then a distant echo from pulse 1 may arrive at the same time as pulse 2 is transmitted, and be missed.

So compromises are involved, depending on the height range of interest.

There is a refinement to the system, which can improve its capability significantly. If the transmit pulse is made up of a number of sub-pulses of appropriate phases, then the receiver, with suitable decoding, can achieve precision and long range sensitivity at the same time. In addition, by changing the phases of the sub-pulses from one pulse to the next, it is possible to differentiate between a late echo from pulse one, and an early echo from pulse two.

2.7 Interference to WPR

Interference to profilers is caused by all electromagnetic emissions that are sufficiently strong to exceed the noise performance of the profiler receiver, mainly determined by the Low Noise Amplifier (LNA) and the processing system and algorithms. It is advantageous, to follow [33] and to discriminate between *coherent interference* and *incoherent interference* for profilers:

Coherent interference is any signal, that will be interpreted by the profiler as a valid signal in its Doppler spectrum. This is the most disruptive to profiler operation, because it may wrongly be interpreted as a valid atmospheric signal.

Incoherent interference in contrast is any signal, that is not detectable as a distinct peak in the Doppler spectrum but that raises the noise level of the system. This would not generate false estimates for atmospheric returns, but degrade the SNR and thus reduce the height coverage of the radar. Of course, this means that the interfering signal is sufficiently wide-band to the frequency response of the profiler and has a "white" spectral structure.

The effect of the additional noise contribution is a de-sensitization of the WPR which obviously leads to a decreased height coverage. However, this reduction in height coverage is very difficult to quantify. The reason

is the high dynamic range of volume reflectivity that accounts for the radar returns. The structure parameter of the refractive index may vary more than 20 dB daily and 20 dB annually, see [33].

Therefore, it makes only limited sense to ingest the Galileo E6-signal during a few hours of a particular day and then compare the determined wind profile with the measurements obtained in a undisturbed situation. While this has been made during the first phase of the Lindenberg experiment in November 2004, we focus here on a more systematic approach in the attempt to quantify the E6 effect. For doing that, one needs to know more about the frequency response of the profiler system.

The frequency response of the profiler system is determined by both, hardware such as filters, amplifiers, as well as digital signal processing. The following components have an influence on the frequency response of the system:

- 1 The frequency selectivity of the antenna (bandwidth).
- 2 Characteristics of the radar receiver front end (bandwidth and noise floor)
- 3 The characteristic of the pulse-matched filter (analogue or digital).
- 4 The filter characteristics emerging due to sampling and digital signal processing.

For ease of treatment, we will assume that the WPR frequency response is mainly determined by the receiver and the digital signal processing.

2.8 Interference Criteria

Based on WMO data requirements as given in ANNEX A, it can be assumed that aeronautical meteorology with measuring accuracy of 150 -600 m and observation cycle of 5 minutes are the tightest requirements for which availability and accuracy of the measured data is especially critical at airports. Compatibility studies for WPRs should therefore be based on aeronautical meteorology requirements.

Recommendations ITU-R M.1461 and ITU-R M.1463 set the formal criterion for the compatibility of Radiodetermination with other services. In case of continuous (non-pulsed) interference, an interfering signal power to radar receiver noise power level, an $I/N = -6$ dB is recommended as the protection criterion for the Radiodetermination radars, and that this level represents the net total protection level if multiple interference sources are present.

In addition, specific measurements have shown that generally a Signal to Noise Ratio (SNR) = -20 dB adequately suffices for the typical operational performance of a WPR. It can also be noted that, based on measurements, that apparently the instantaneous SNR is not only a sole function of altitude, because moist air at higher altitudes in the atmosphere might provide stronger power returns than the dry air below.

This fact also allows assuming that a SNR degradation of 1 to 1.5 dB could be acceptable that represents I/N ranging from -6dB to -4 dB. It has been demonstrated with representative RNSS signals of the European Galileo system that the signals can be assumed as (coloured) noise like signal, whereby an $I/N = -6$ dB can be adequate to protect WPR.

For noise like impact, and since the abovementioned $I/N = -6$ dB applies to one single beam, it can be considered that if the receiver I/N exceeds the value of -6 dB for a beam, the measured data of that beam does not meet the required accuracy.

For one spectra measurement, in the case of a three-beam radar the three beams need to be available to calculate the wind velocity vector. In the case of a five-beam radar, three beams including the vertical one or four beams are required to calculate the wind velocity vectors. The spectra availability can thus be defined for three-beam radars as the %-age of spectra with three-beams available and for five-beam radars as the %-age of spectra with three beams including the vertical one or four beams available.

3 RADIONAVIGATION SATELLITE SERVICE AND THE EUROPEAN GALILEO SYSTEM

3.1 The Galileo RNSS System

Among others, the radio navigation satellite service (RNSS) has also an allocation in the band 1215-1300MHz.

Due to propagation characteristics it is advantageous for RNSS systems to use this allocation for the provision of a second signal a few hundred MHz apart in addition to the transmissions in the band 1559-1610MHz to compensate ionospheric influence.

Dual-frequency reception increases significantly the availability of high position accuracy. The US-GPS and the RF-GLONASS system currently transmit their second signal in the 1215-1260MHz band while the European Galileo system transmits its E6-signal in the band 1260-1300MHz.

All satellites of the Galileo constellation will transmit signals in three separate RNSS allocated frequency bands as shown in Figure 17. The first satellite of the system was already launched in December 2005 and transmits the signals since early January 2006.

3.2 Constellation information

The full operational Galileo constellation eventually comprises 30 satellites controlled by a worldwide network of ground control stations. Each of the three circular orbit planes is inclined by 56° against the Earth's equatorial plane. Each orbital plane is situated around the globe by 120° separation (Right-ascension of ascending nodes). Nine operational satellites equidistantly travelling and one additional on-orbit spare populate each orbital plane.

The altitude above the Earth for all satellite is about 23600km.

3.3 Galileo signal characteristics

The baseline Galileo signal and frequency plan is shown in Figure 17.

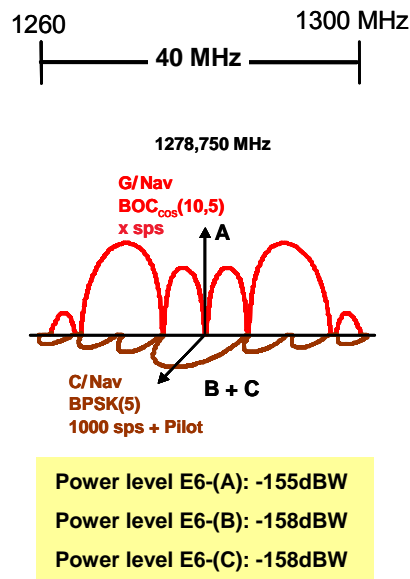


Figure 17: Galileo baseline signal and frequency plan

Galileo will permanently transmit three complex signals with in-phase and quadrature components as shown in the figure. The signal are so-far addressed as

- "E2-L1-E1" with a centre frequency of 1575.420 MHz
- "E6" with a centre frequency of 1278.750 MHz, and
- "E5" (E5a+E5b) with a centre frequency of 1191.795 MHz.

Each of the shown components is necessary and useful for the provision of positioning, navigation and time (PNT) services. Each component can be received and processed either independently or simultaneously in several reasonable combinations (dual or triple frequency high-end performance receivers), depending on the purpose of application.

The baseline characteristic of the E6 signal is given in Table 5:

Gal-E6 signal parameters	Values		
Carrier frequency (MHz)	1278.75		
Received signal power (dBW) ⁵	-152		
Nominal bandwidth (MHz)	40		
Antenna polarisation at satellite	Right hand circular		
Pulse shaping	Rectangular		
Multiplexing scheme	interplex		
Components	E6-A	E6-B	E6-C
Service/signal mapping (Galileo)	PRS (G/Nav)	CS (C/Nav)	Pilot
Modulation	BOC _{cos} (10,5)	BPSK	BPSK
Chip rate (Mc/s)	5.115	5.115	5.115
Code length (chips)	Very long (Non-periodic DS)	5115	511500
Power split	4/9	2/9	2/9
Data content	PRS data (CS)	CS data	No data
Encryption	Yes	Yes	
Symbol rate (sym/s)	100	1000	

Table 5: Galileo E6-signal parameter

3.4 Galileo E6-signal spectrum

Galileo plans to transmit three signals in the E6 band. This is part of the 1215-1300MHz RNSS allocation and is shared with the radiolocation service. The spectral shape of the Galileo E6-signal at a received power of -152 dBW is shown in Figure 18.

⁵ at minimum 10° elevation, received with a 0 dBi RHCP antenna

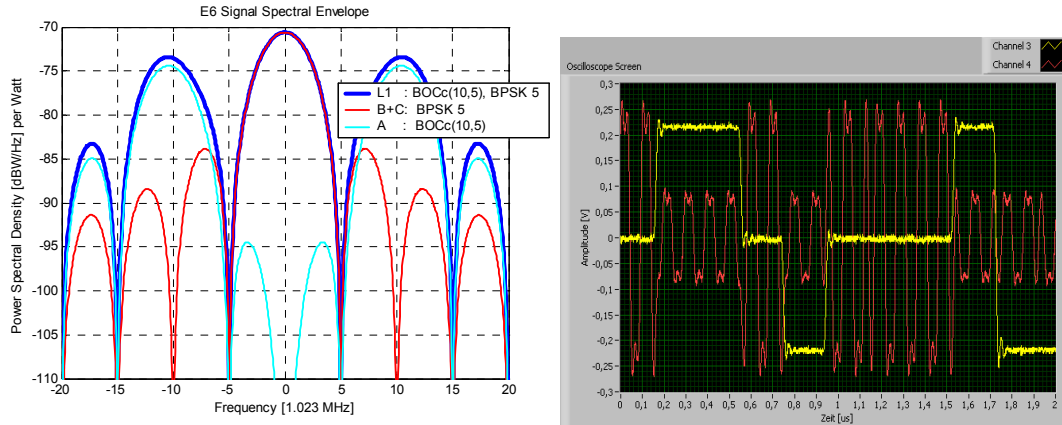


Figure 18: Power Spectral Density of the E6-signal components in frequency (l) and time (r) domain

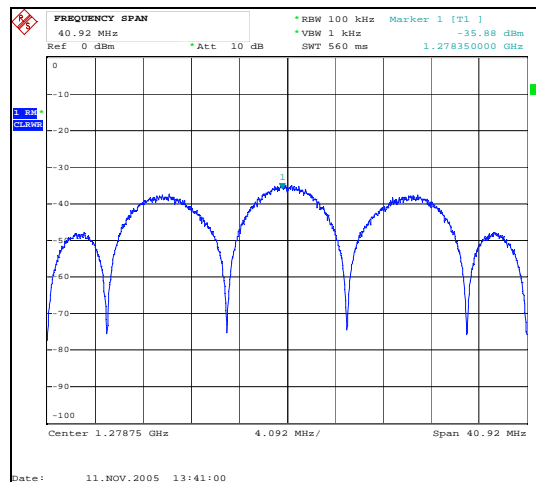


Figure 19: Resulting envelope of the transmitted E6-signal

Figure 18 shows the components transmitted as the composite E6-signal. It does not take into account satellite on-board filtering of the signal outside the RNSS allocation 1260-1300 MHz.

3.5 Galileo E6 Satellite PFD versus Elevation

Table 6: provides the Galileo E6 signal typical PFD versus elevation which can be used for simulations or measurements purposes to approximate a typical receive antenna characteristic. The values in the table have been derived from the typical received power level (with 0.5 dB margin) and the gain pattern of the satellite transmit antenna.

Moreover, the PFD is given at the most critical frequency (i.e. at the 1278.75 MHz frequency). If the WPR is operated with a frequency offset relative to the E6 central frequency the PFD levels hereafter should be adjusted with the corresponding attenuation in dB (corresponding to the difference between the PSD at this frequency with respect to the PSD at the central frequency).

Elevation Angle (°)	TYPICAL PFD (dBW/m ² /MHz)	Elevation Angle (°)	TYPICAL PFD (dBW/m ² /MHz)
0	-138.2	50	-136.4
5	-138.1	55	-136.5
10	-137.8	60	-136.7
15	-137.6	65	-136.9
20	-137.3	70	-137.2
25	-137.1	75	-137.5
30	-136.8	80	-137.8
35	-136.6	85	-137.8
40	-136.5	90	-137.8
45	-136.4		

Table 6: Typical Galileo pfd vs. elevation angle

Several RNSS systems have been notified to operate in the frequency range 1260-1300MHz. Galileo has already commenced operation of its first satellite. The Galileo E6 signal is considered to be typical and, thus, representative for further RNSS signals that could potentially interfere with WPR operations in the frequency range 1270-1295MHz.

4 SIMULATION STUDIES

4.1 Simulation objectives

Desktop simulations were conducted to assess the potential impact of Galileo transmissions on WPR. The simulation results provide both the I/N for each WPR beam as well as the corresponding overall WPR availability based on an availability algorithm.

In addition, an average WPR availability is also calculated over a representative WPR “averaging time” of 30 minutes to assess potential availability improvement that could be expected from time integration. In this case, in addition to the algorithm, the WPR is given as available if three over nine spectra are consistent over the averaging time. Therefore, the **average availability** can be defined as the % of consensus with at least 3 spectra available. It should be noted that this algorithm represents the best theoretical case for WPR.

4.2 Galileo System Parameters

Galileo system parameters used in the simulations are given in section 3.2. The satellites positions versus time were simulated and the total Galileo interfering power into WPR was computed during one day with a time step of four seconds.

4.3 WPR Characteristics

The following table provides the characteristics of the two main WPR types, as used in the simulations.

Wind profiler radar characteristics	WPR-A	WPR-B
Receiver noise figure	1.5 dB	3 dB
Receiver noise temperature	120 K	188.6 K
Antenna noise temperature	30 K	30 K
Cable loss	1dB	1dB
Cable temperature	290 K	290 K
Receiving system noise temperature	255.7 K	468.4 K
Maximum antenna gain $G_{wpr(0)}$	26.3 dBi	26 dBi
Antenna gain $G_{wpr(\varphi)}$ dB	$26.3 - 0.044 (1.1 + \varphi)^{2.83}$ $\varphi < 6.66^\circ$ $35 - 28.2 \log(\varphi)$ $6.66^\circ \leq \varphi < 80^\circ$ -18.7 $80^\circ \leq \varphi$	$26.05 - 0.05(1+\varphi)^{2.6}$ $0^\circ < \varphi < 8.6^\circ$ 8 $8.6^\circ \leq \varphi < 40^\circ$ 2 $40^\circ \leq \varphi < 55^\circ$ -20 $55^\circ \leq \varphi$
WPR antenna polarisation	Linear	Linear
Polarisation discrimination	-3 dB	-3dB
Receiving system noise power	-146.9 dB(W/MHz) (worst case, without any feeder loss) -144.5 dB(W/MHz) (taking into account 1 dB feeder loss)	-141.9 dB(W/MHz)

Table 7: WPR characteristics as used in the simulations

The simulations assumed a realistic 256 K system noise temperature (as well as a worst case system noise temperature of 150K) for WPR-A and 468 K for WPR-B. This corresponds to a system noise power density of -144.5 dBW/MHz (-146.9 dBW MHz for the worst case) for Vaisala and -141.9 dBW MHz for WPR-B respectively.

The antenna patterns for both WPR types are given in Figure 20.

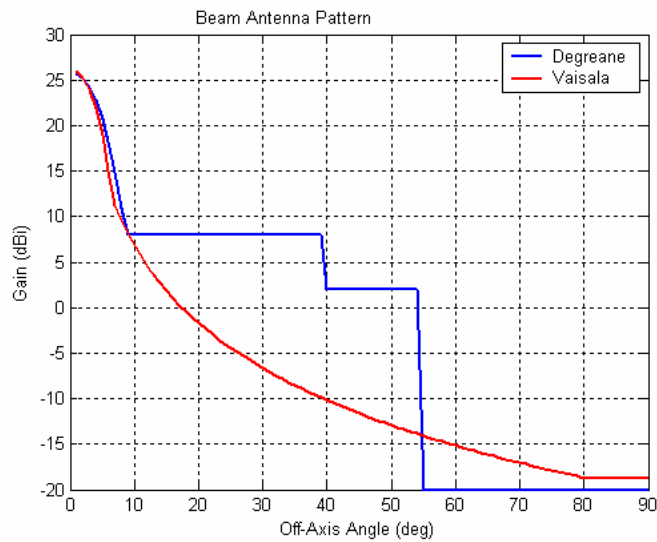


Figure 20: Antenna beam pattern used for simulation

4.4 Simulation Results

4.4.1 Assumptions

All simulations have been performed assuming a WPR central frequency of 1278.75 MHz. This corresponds to a worst case since it represents the frequency at which Galileo satellites transmit the maximum PFD level.

4.4.2 Simulation of WPR-A availabilities over location latitude

4.4.2.1 Calculated I/N and WPR Availability

Figure 21 shows the I/N for each WPR beam, respectively, and the corresponding spectra availability for 3-beam and five-beam WPR-A radars, with a system noise power density of -146.9 dBW/MHz, calculated for different latitudes (20° , 50° and 70°).

The beam elevation angle has been set to 78° for the 3-beam radar and 73° for the 5-beam radar.

In particular, it can be seen that the radar availability is 100% for 5-beam radar at 50° and 70° latitudes.

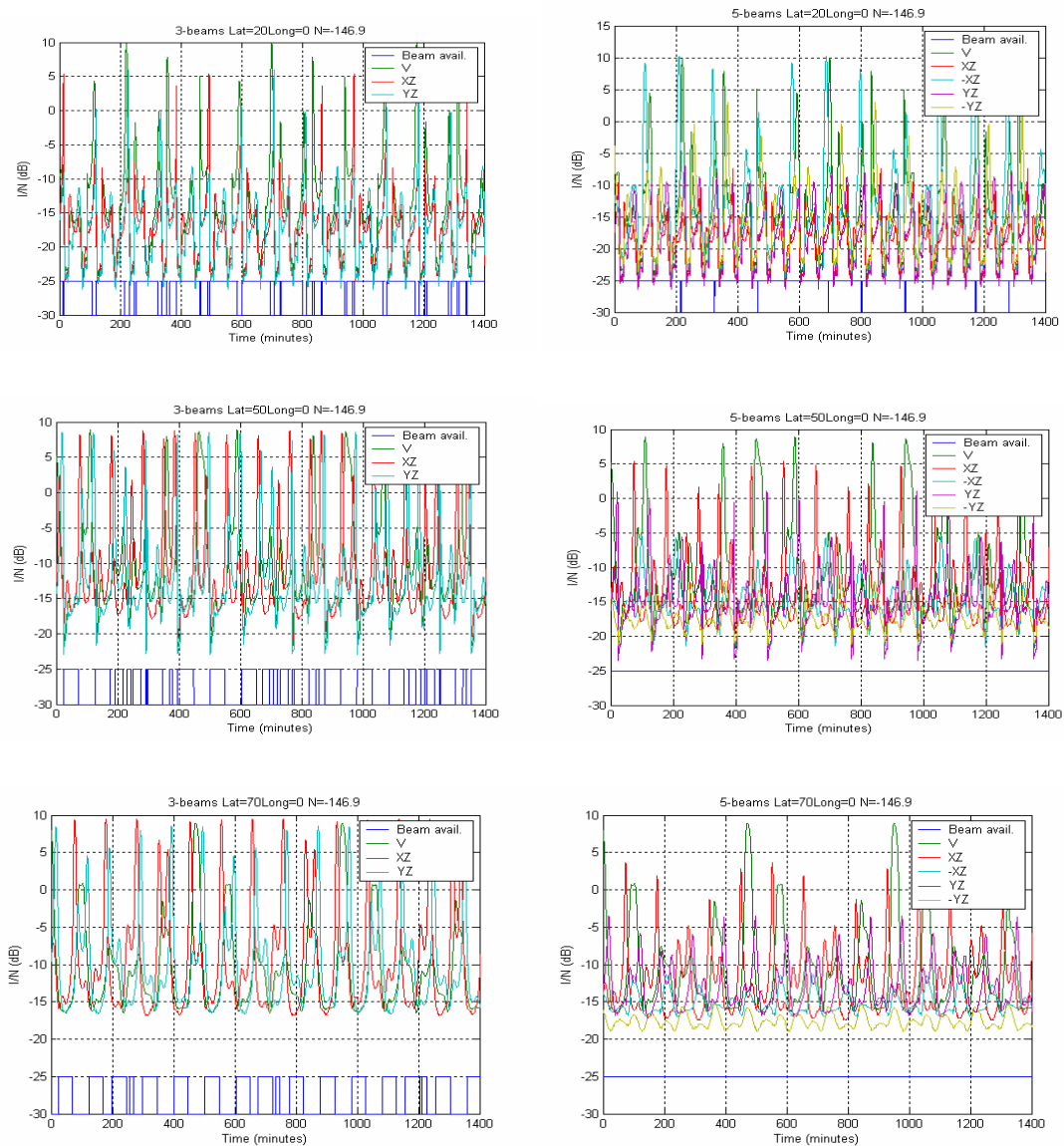


Figure 21: Simulation results for typical 3- and 5-beam WPRs at Latitudes 20° , 50° , and 70°

Additional simulations were performed for different beam elevation angles at different latitudes. The resulting radar availabilities corresponding to each type of radar is summarised in Table 8 and Table 9 for three- and five-beam WPRs, respectively.

Latitude	Elevation 65°	Elevation 73°	Elevation 75°	Elevation 78°	Elevation 85°
0°	92.31%	96.28%	96.28%	96,28%	96.06%
10°	91.88%	94.60%	94.60%	93,84%	93.47%
20°	91.91%	92.55%	92.25%	89,69%	89.29%
30°	91.11%	91,00%	88.86%	84,95%	85.48%
40°	87.23%	85.06%	80.40%	75,62%	78.19%
50°	87.38%	78.36%	71.25%	63,20%	72.38%
60°	84.80%	75.48%	67.26%	57,81%	68.71%
70°	86.86%	80.83%	69.99%	57,32%	66.56%

Table 8: WPR-A three-beam radars (-144.5 dBW/MHz noise power density)

Latitude	Elevation 65°	Elevation 70°	Elevation 73°	Elevation 75°	Elevation 80°
0°	100%	96.815%	96,96%	96.56%	94.92%
10°	100 %	100 %	98,14%	97.33%	91.11%
20°	100 %	100 %	99,06%	97.71%	88.87%
30°	100 %	100 %	100 %	97.91%	88.55%
40°	100 %	100 %	100 %	100%	84.57%
50°	100 %	100 %	100 %	100%	82.29%
60°	100 %	100 %	100 %	100%	97.83%
70°	100 %	100 %	100 %	100%	96.25%

Table 9: WPR-A five-beam radars (-146.9 dBW/MHz noise power density)

Even though these simulations results show occurrence of high levels of interference for three beam-WPR, it tends to demonstrate that the introduction of a higher number of beams largely improves the situation. This is the case at least for five-beam WPR, which, at European latitudes, are always available, at the exception of WPR with beams operating at 80° elevation angle.

The case of three-beam WPR is more critical since measurements on the 3 beams are needed and the availability ranges from about 57% to 87 %.

4.4.2.2 Average Availability

The tables below give a comparison of the WPR availability obtained with and without the application of the 3/9 “averaging time” integration algorithm.

Latitude	Spectra Availability without Averaging	Spectra Availability with 3/9 Averaging	Availability Gain
0°	95.46%	97.07%	1.61 %
5°	94.31%	96.01%	1.70%
10°	92.19%	94.98%	2.79%
15°	89.66%	93.63%	3.97%
20°	87.01%	91.12%	4.11%
25°	84.44%	88.85%	4.41%
30°	81.39%	86.01%	4.62%

Latitude	Spectra Availability without Averaging	Spectra Availability with 3/9 Averaging	Availability Gain
35°	75.44%	80.76%	5.32%
40°	71.02%	76.39%	5.37%
45°	66.12%	71.56%	5.44%
50°	56.96%	61.52%	4.56%
55°	54.62%	58.97%	4.35%
60°	53.4%	57.85%	4.45%
65°	51.83%	55.85%	4.02%
70°	51.71%	55.06%	3.35%

Table 10: WPR-A with three beams (Worst case N=-146.9 dBW) Elevation= 78°

Latitude	Spectra Availability without Averaging	Spectra Availability with 3/9 Averaging	Availability Gain
0°	96.96%	98.05%	1.09%
5°	97.27%	98.47%	1.20%
10°	98.14%	98.88%	0.74%
15°	98.41%	99.58%	1.17%
20°	99.06%	100%	
25°	99.18%	100%	
30°	100%	100%	
35°	100%	100%	
40°	100%	100%	
45°	100%	100%	
50°	100%	100%	
55°	100%	100%	
60°	100%	100%	
65°	100%	100%	
70°	100%	100%	

Table 11: WPR-A with five beams (N=-146.9 dBW, worst case) Typical Elevation=73°

It appears from the results that whereas, obviously, WPR “averaging time” integration improves the radar availability by several percents, this is valid for an algorithm that represent a best case for WPR and is likely not represent all possible cases.

For five-beam radars, the “averaging time” integration increases the availability to close to 100% at all latitudes and shows, at the end, that potential difficulties resulting from Galileo interference at European latitudes might only be limited to specific latitude/elevation sets.

On the other hand, for three-beam WPR whereas “averaging time” integration improve the situation, resulting un-availabilities are still quite high and the impact of Galileo emissions hence remain noticeable.

4.4.3 Simulation of WPR-B Wind Profiler Radar availabilities over location latitude

4.4.3.1 Calculation of I/N

Figure 22 show the I/N for each WPR beams and the corresponding spectra availability for three-beam and 5-beam WPR-A radars, with a system noise power density of -141.9 dBW/MHz, calculated for different latitudes (20° , 50° and 70°).

The beam elevation angle is 78° for the three-beam radar and 73° for the five-beam radar.

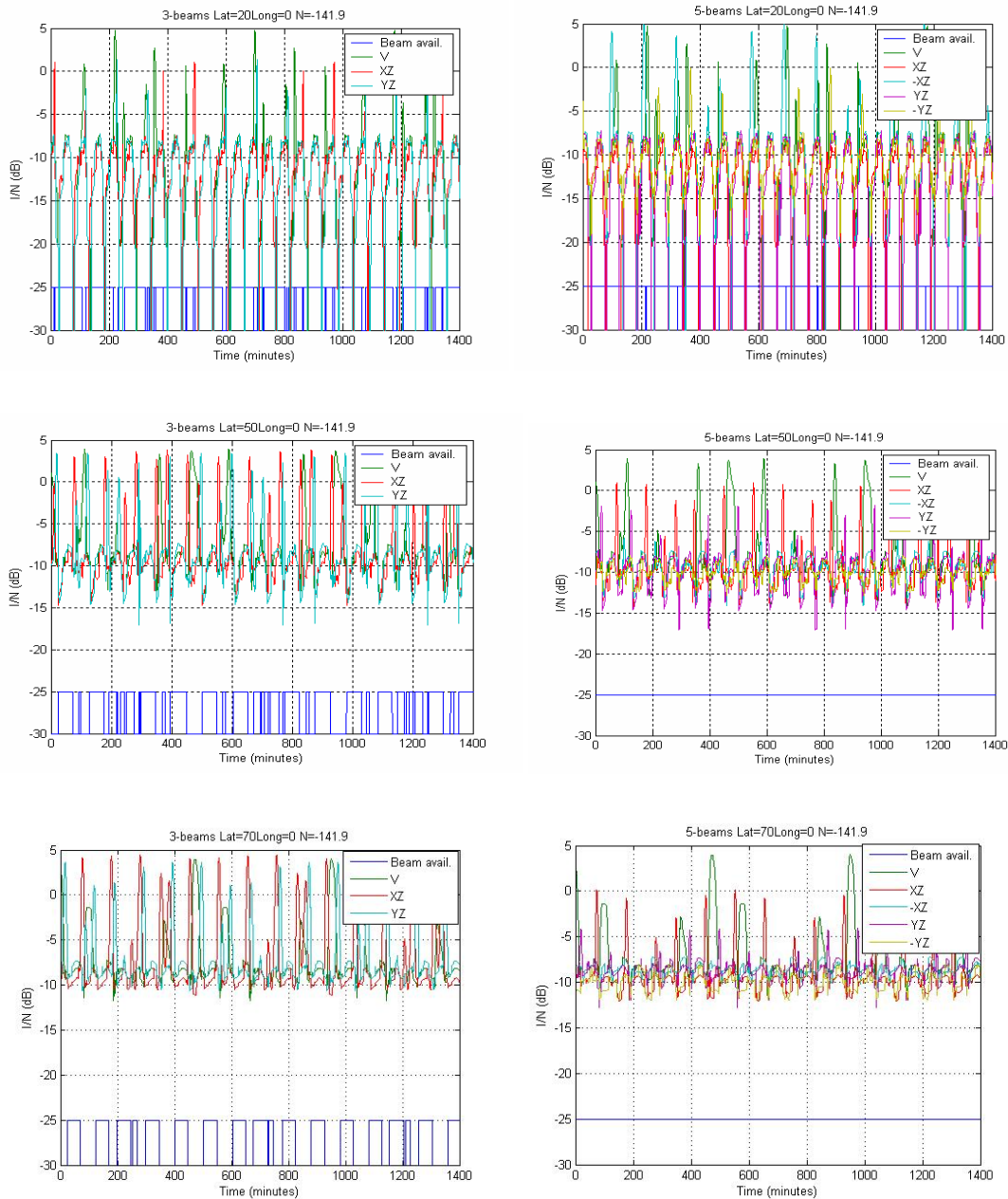


Figure 22: Simulation results for typical 3- and 5-beam WPRs at Latitudes 20° , 50° , and 70°

In particular, it can be seen that the radar availability is 100% for five-beam radar at 50° and 70° latitudes.

Additional simulations have been performed for different sets of latitude and beam elevation angles. Corresponding radar availabilities are summarised in the tables below.

Latitude	Elevation 65°	Elevation 73°	Elevation 75°	Elevation 78°	Elevation 85°
0°	90.97%	95.60%	95.60%	95.60%	95.47%
10°	89.92%	93.47%	93.47%	92.50%	92.25%
20°	88.37%	90.99%	90.31%	87.55%	88.00%
30°	89.64%	88.45%	86.26%	82.67%	83.07%
40°	84.03%	79.60%	75.76%	72.01%	76.17%
50°	83.93%	72.29%	64.35%	59.20%	68.02%
60°	83.25%	70.57%	60.40%	54.08%	64.42%
70°	83.25%	72.31%	61.33%	52.99%	63.75%

Table 12: WPR-B with three-beams (-141.9 dBW/MHz noise power density)

Latitude	Elevation 65°	Elevation 70°	Elevation 73°	Elevation 75°	Elevation 80°
0°	100%	97.45%	97.86%	98.44%	95.79%
10°	100%	100%	99.26%	98.88%	92.27%
20°	100%	100%	99.58%	98.79%	90.15%
30°	100%	100%	100%	98.59%	90.23%
40°	100%	100%	100%	100%	86.47%
50°	100%	100%	100%	100%	84.85%
60°	100%	100%	100%	100%	98.58%
70°	100%	100%	100%	100%	97.72%

Table 13: WPR-B with five-beams (-141.9 dBW/MHz noise power density)

Even though these simulations results show occurrence of high levels of interference for 3 beam-WPR, the introduction of a higher number of beams largely improves the situation. This is the case at least for 5-beam WPR at European latitudes that are always available, at the exception of WPR with beams operating at 80° elevation angle.

The case of three-beams WPR is more critical since measurements on the 3 beams are needed and availability range is from about 52 to 84 %.

It is interesting to note that, even though the reference noise level is different for both types of radars (WPR-B and WPR-A), availability results are similar and consistent. It seems actually that since unavailability events are mainly controlled by the WPR main beam coupling, the shape of the antenna main beam results in peak interference levels that increase and drop drastically by several dBs over very short period.

4.4.3.2 Average Availability

The tables below give a comparison of the WPR availability obtained with and without the application of the 3/9 “averaging time” integration algorithm.

Latitude	Spectra Availability without Averaging	Spectra Availability with 3/9 Averaging	Availability Gain
0°	95.60%	97.21%	1.61%
5°	94.55%	96.28%	1.73%
10°	92.50%	95.31%	2.81%
15°	90.03%	94.28%	4.25%
20°	87.55%	92.05%	4.50%

Latitude	Spectra Availability without Averaging	Spectra Availability with 3/9 Averaging	Availability Gain
25°	85.31%	90.01%	4.70%
30°	82.67%	87.13%	4.46%
35°	78.27%	84.11%	5.84%
40°	72.01%	78.30%	6.29%
45°	67.44%	73.05%	5.61%
50°	59.20%	64.68%	5.48%
55°	55.11%	59.43%	4.32%
60°	54.08%	58.74%	4.66%
65°	52.82%	56.46%	3.64%
70°	52.99%	56.69%	3.70%

Table 14: WPR-B with three beams (N=-141.9 dBW) Elevation= 78°

Latitude	Spectra Availability without Averaging	Spectra Availability with 3/9 Averaging	Availability Gain
0°	97.86%	99.58%	1.72%
5°	98.64%	100%	
10°	99.26%	100%	
15°	99.62%	100%	
20°	99.58%	100%	
25°	100%	100%	
30°	100%	100%	
35°	100%	100%	
40°	100%	100%	
45°	100%	100%	
50°	100%	100%	
55°	100%	100%	
60°	100%	100%	
65°	100%	100%	
70°	100%	100%	

Table 15: WPR-B with five-beams (N=-141.9 dBW) Typical Elevation= 73°

It appears from the results that whereas, obviously, WPR “averaging time” integration improves the radar availability by several percents, this is valid for an algorithm that represent a best case for WPR and is likely not represent all possible cases.

For five-beam radars, the “averaging time” integration increases the availability to close to 100% and shows, at the end, that potential difficulties resulting from Galileo interference at European latitudes might only be limited to specific latitude/elevation sets.

On the other hand, for three-beam WPR whereas “averaging time” integration improve the situation, resulting un-availabilities are still quite high and the impact of Galileo emissions hence remain noticeable.

4.5 Simulation Conclusions

These simulations, performed with the Galileo maximum transmitted power spectral density (i.e. at 1278.75 MHz) show that:

- Availability of five-beam WPR at European latitudes remains at 100% even without taking into account any possible “averaging time” integration, at the exception of specific cases for which WPR beams elevation is set to 80°. For this latter case (80° elevation), availability will always be higher than 82% (without “averaging time” integration) and higher than 90% when a 3/9 “averaging time” integration algorithm is introduced.
- Regarding three-beam WPR, in the worst case (N=-146.9 dBW/MHz), the spectra availability at European latitudes will be higher than 51% (without any “averaging time” integration algorithm) and higher than 55% when a 3/9 “averaging time” integration algorithm is introduced. For a more realistic Noise power (N=-144.5 dBW/MHz, taking into account 1 dB feeder loss), for a WPR elevation angle of 65° the spectra availability is higher than 84% (without the application of any consensus algorithm).

It must be pointed out that the results need to be considered at the light of detailed information concerning location and characteristics of WPR in Europe to be able to determine which specific existing or planned WPR might experience operational degradation and would hence need to apply specific mitigation techniques.

In conclusion, the simulations performed show that the provisioning of Galileo operation:

1. will not create harmful interference into five-beams WPR systems; No particular mitigation techniques is necessary which could become necessary for three-beams WPR. In these cases specific mitigation techniques would become necessary.
2. for future investments, it is strongly recommended that only five-beam WPR should be considered because their exposure rate to RNSS-satellites in boresight view can be minimised.

5 COMPATIBILITY TESTS

5.1 Introduction

Two different sets of tests were performed to assess or validate simulations conclusions, one performed by the UK, and a second by Germany of which details are given in the Annex D and E, respectively. Conclusions of these measurements are given below.

5.2 UK Measurement Campaign

5.2.1 Campaign objectives and performance

It should be noted that the Galileo power levels used in the UK measurement campaigns are higher than the values that will actually be transmitted by the satellites. Although these measurements give a good idea of the WPR behaviour when facing a RNSS-like type of interference, no conclusions about the impact of Galileo into WPR can be driven from these measurements.

5.2.2 WPR-B Test Conclusions

A complete set of measurements has been performed, which may be considered a representative ‘snapshot’ of events, given the variability of the natural environment. A great many measurements would be needed to fully characterise the impact of Galileo on WPR performance under all conditions.

The results that have been collected show the following.

- Re-tuning the WPR is a possible solution, but the following points must be borne in mind.
- Placing the WPR in the null E of the Galileo signal gives no discernable degradation even with a Galileo signal of 10dB above nominal. This necessitates retuning the WPR by 1%.
- Placing the WPR at least 20MHz away from the Galileo centre frequency will reduce the impact to below detectable, even at 10dB above the nominal interference level.
- If the WPR is retuned to be closer to any neighbouring service, the CW blocking figures provide a maximum acceptable adjacent channel power for close offsets. For an interferer with a known

modulation scheme, measurements similar to these should be performed, though if the level is below that of the minimum detectable CW interferer, any effect is unlikely to be worse than the CW case.

- If a WPR on 1290MHz can only be tuned by 0.5% then it may be possible to use null G (see Figure 30).

5.2.3 UK WPR Test Conclusions

A comprehensive set of measurements were performed, which may be considered a representative ‘snapshot’ of events, given the variability of the natural environment. A great many measurements would be needed to fully characterise the impact of Galileo on WPR performance under all conditions. The results that have been collected show the following. Reference frequencies for Nulls are provided in Table 16.

Re-tuning the WPR is a possible solution, but the following points must be borne in mind.

- If the WPR can only be tuned by 0.5% then it may be possible to use Null G or Null E. Null G provides satisfactory protection for the WPR-A ~18dB, and Null E, perhaps 5dB. In the light of the CW blocker results, it is possible that the closer out of band filtering in the WPR-A design affords a better protection against over sampled artefacts from nearby signals.
- Placing the WPR in the null H of the Galileo signal gives no discernable degradation even with the interferer 15dB above nominal. This necessitates retuning the WPR by 1%.
- Placing the WPR at least 20MHz away from the Galileo centre frequency will also reduce the impact to below detectable, even at ~20dB above the nominal interference level.
- If the WPR is retuned to be closer to any neighbouring service, the CW blocking figures provide a maximum acceptable adjacent channel power for close offsets. For an interferer with a known modulation scheme, measurements similar to these should be performed, though if the level is below that of the minimum detectable CW interferer, any effect is unlikely to be worse than the CW case.

FREQUENCY (MHz)	IDENT	Remarks
1258.290	Null A	beyond Res 217
1263.405	Null B (F7-F8)	beyond Res 217
1273.635	Null D (F1-F2)	Recommended as alternative
1283.865	Null E (F3-F4)	Recommended for mitigation
1294.095	Null G (F5-F6)	beyond Res 217
1299.210	Null H	beyond Res 217

Table 16: Nulls in the Galileo E6-signal transmission

5.3 German Measurement Campaign

5.3.1 Campaign objectives and performance

Another series of compatibility measurements to investigate the behaviour of an operational WPR under different levels of Galileo E6-signal interference concluded end of 2005. The main purpose of this experiment was to investigate the effects of an interfering E6 signal on the data output of an operational profiler radar. Three objectives were intended to be achieved with the campaign:

1. to investigate presumed coherent impacts of line spectra in the Galileo E6-signal potentially creating false alarms in the radar consensus process.
2. to investigate quantitatively and qualitatively the impact of an additional E6-signal raising the noise floor of the radar receiver, and
3. to verify potential mitigation strategies by shifting the radar transmission frequency into a spectral null of the E6-signal.

A variety of signal power level ranging from typical to excessive power were injected at point B of the test set-up as shown in Figure 23. Also the setting of radar parameter, particularly the pulse width was varied from 300ns to 2800ns to determine any potentially degrading impact on the operational radar.

Taking also into consideration that the radar normally takes a period of about 25 minutes after dwelling repeatedly in the five beam positions before a wind profile is determined as a result of the digital consensus process, the interference investigations concentrated on the more difficult case of instantaneous noise impact on the radar front-end. With even excessive power injected at point B, actually more than 20dB above nominal values the immediate perceivable appearance was studied.

The impact of a real constellation has also investigated. Details are provided in the report in Annex D.

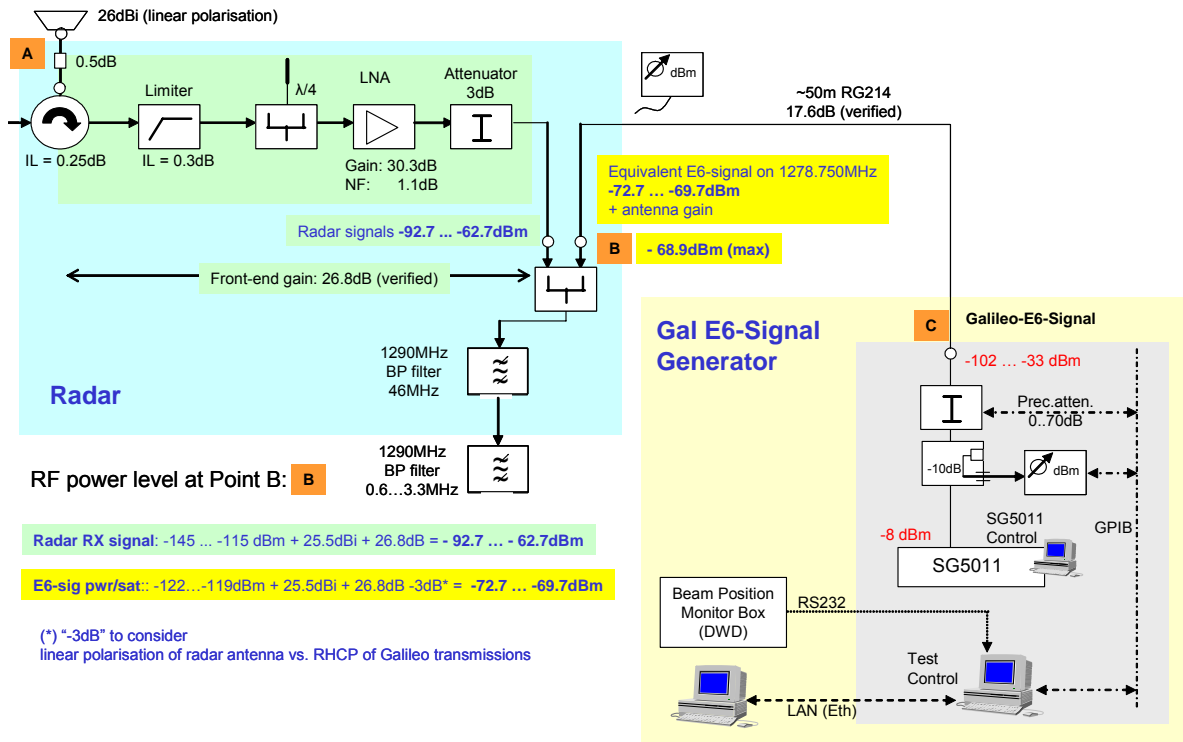


Figure 23: Test set-up and level diagram of WPR and injected Galileo E6-signal level

The nominal measurements were performed with a WPR at the centre frequency of 1290 MHz. Major frequency changes were only possible within the pass band of the given filter conditions as shown in Figure 23.

It was found that the effect at 1290 MHz of the E6 signal is twofold:

Results regarding the Coherent impact

The Galileo E6 signal has no coherent impact into the WPR radar receiver tested. This result can be assumed as representative since no spectral components that can fall into the low frequency Doppler processing is transmitted by the real E6-signal.

Earlier tests indicated a coherent impact due to a limitation that the hi-end standard signal generator could not produce a true representation of the Galileo E6-signal. This coherent impact was also observed in the UK tests.

Results regarding the Incoherent impact

The Galileo E6 signal can be assumed as a noise like signal increasing the overall system noise level and thus reducing the maximum height performance. If a mitigation technique achieves at least a 10 dB suppression of the profiler response to the E6 signal, the impact will be negligible.

In the case that mitigation is not possible only the use of the WPR for scientific and special purposes might be reduced for a short period of time. For other operational usage, this reduction is likely to be acceptable.

Finally, a few test measurements were made simulating a slightly shifted profiler carrier frequency (less than 1 percent), with the new carrier frequency moved into the spectral "Nulls" of the E6 signal.

Although this test needs to be repeated for various reasons, the preliminary results indicate that this mitigation technique is likely to give the required E6 signal suppression. It should also be noted that these measurements are based on the hypothesis that the Galileo signals are at the maximum PFD level during 100% of the time (i.e. when a satellite is in the WPR main beam) without taking into account the satellite motion.

Based on the measurements, limits where there is no impact at the receiver are:

- -140 dBW/MHz for degradations by coherent (false alarm) interference
- -150 dBW/MHz for degradations by incoherent (noise) interference.

5.3.2 German WPR Test Conclusions

Main objective of the measurement campaign was to determine the potential impact of the Galileo-E6 signal transmissions on the operational performance of Wind Profiler Radars. The tests were performed in a most representative manner because both, the WPR and the eventually applied signal generator for the Galileo signal have been determined to provide typical performance characteristics for compatibility analyses.

Taking earlier measurements as well as the results of the first phase of this campaign into consideration it can be stated that compability between Galileo and the European WPRs is ensured under normal operational conditions for weather observations. The radar used for the measurement campaign can be considered representative for the group of five-beam systems.

The mitigation option by shifting the radar carrier frequency into a Null of the Power Spectral Density of the E6-signal could be verified as an appropriate measure for special operation conditions when highest sensitivity is a mandatory pre-requisite, e.g. for scientific investigations.

Particularly under conditions of the very weak potential interference conditions imposed by an E6-signal, it remains difficult to quantify the exact loss of height performance as in a "non-interference" case. The instantaneous system noise of the receiver varies with external noise introduced by the up looking antenna and the sky noise captured. The nominal E6 signal can raise the noise level of the WPR receiver by 3 dB, if the satellite is at the boresight of the antenna.

The following conclusions can be drawn from the measurements:

1. Within the specified maximum power conditions provided by Galileo satellites there is no coherent influence on the consensus process, i.e. no creation of false alarm signals or changing values of wind profiles.
2. The noise floor increased in the presence of a satellite signal in antenna boresight view reduces marginally the operational height of the WPR.
3. In case of WPR-measurements for scientific purposes that the marginal noise increase creates problems in some special cases (e.g. scientific research), the shifting of the WPR carrier frequency into a Null of the transmitted Galileo signal spectrum would fully alleviate the problem other performance parameters of the WPR being equal.
4. The measurements also highlighted the sensitivity of the radar processor against low frequency discrete lines in interfering transmissions. The tests have shown that it is mandatory to transmit with variable bit patterns in the signal component provided for the data dissemination service (Galileo Commercial Service). Appropriate measure (e.g. channel coding) must be employed. This aspect has to be included in the Galileo system requirements.
5. One measurement investigated the compatibility conditions by replaying a typical fixed wind profile that was recorded during earlier measurements. Repeating this profile by means of a vector modulation generator (SMIQ) created a test environment that could be used for future representative lab-measurements to investigate in more detail varying signal conditions (Galileo or other RNSS transmissions).

6 INTERFERENCE MITIGATION - OPTIONS TO IMPROVE THE WPR-RNSS COMPATIBILITY

6.1 Interference analysis summary and options for interference mitigation

The analysis of simulations and measurements show that any in-band interference has the potential to degrade WPR performance, so the main question is how much degradation WPR users will accept. For noise like impact, mitigation techniques would be needed mainly for 3 beams WPR for which, a rough 10 dB suppression would be needed.

The Simulation Report concluded that the interference from the nominal Galileo emissions exceeds the WPR noise floor by about 6dB. Considering this, a suppression of about 12 dB is needed to comply with Rec ITU-R M.1461 and to maintain the WPR range performance at 95% of the no-interference value.

As a cross-check, the previous measurements on the WPR-A and WPR-B were reviewed. In the report, “nominal” Galileo was defined as the guaranteed minimum level, i.e -122dBm.

Measurements on the WPR-A

Subjective evaluation of the measurements has led to the conclusion that the theoretical and measured values are different because the effect of the interference is masked by atmospheric variations. It has therefore not been possible to come to a precise figure for the suppression needed, but a figure of 10 dB would not seem unreasonable.

Measurements on the WPR-B

Due to atmospheric variability, and processed results actually showed an increase in range when the interference was increased. But at Interference/Noise = +5dB, a clear degradation was seen. At Interference/Noise below -5dB, no interference was seen.

6.2 Possible Mitigation Techniques

6.2.1 Introduction

Measurements have shown that, other than for routine weather observations, a compatibility improvement might become necessary when scientific investigations are to be performed with a WPR. In these cases, the following mitigation measures are recommended. The techniques identified to mitigate the effect of Galileo signals on WPR operation involve changes to

- antenna subsystem and coverage
- signal processing algorithms
- WPR operating frequency

or combinations of the above.

6.2.2 Antenna Pointing

The normal arrangement for a three-beam WPR is shown in Figure 24.

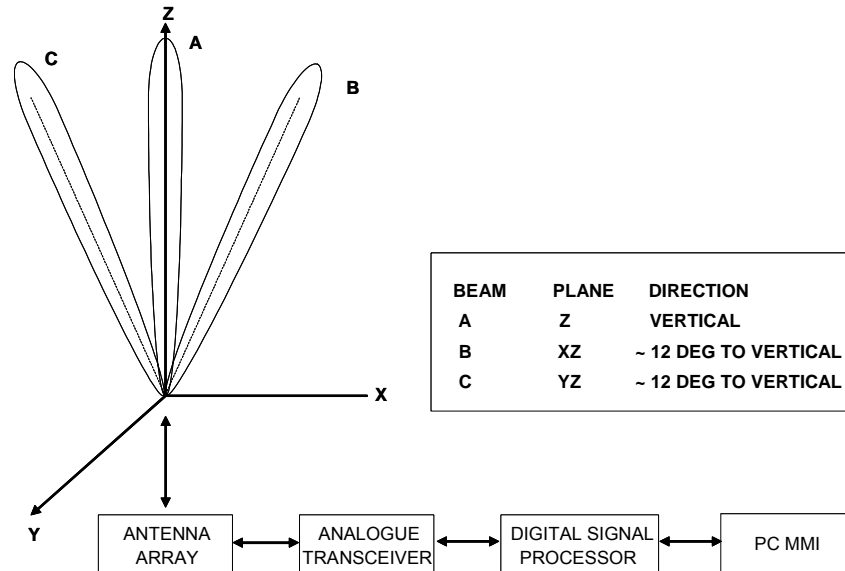


Figure 24: WPR Antenna pointing (3 beams)

The intersection of the beams with the Galileo constellation may be shown on a map similar to a Star Map. This is a polar plot in which the angle θ represents azimuth, and the radius r is proportional to the angle α from zenith to a particular point in the sky. Thus α varies from 0° to 90° . Such a map is shown in Figure 25.

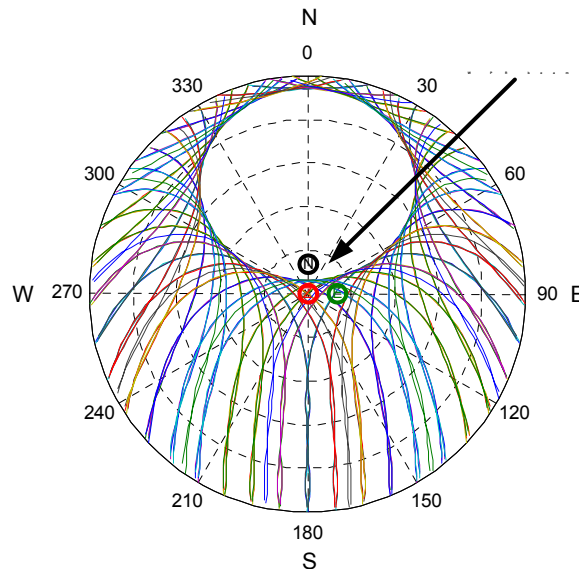


Figure 25 Galileo constellation as seen from the UK (Lat: 51°N)

Note the circles of constant r that occur at 18° intervals. This map has the southern UK (51°N) at its centre, and shows the paths of the Galileo satellites as coloured arcs. Note the near-circular area through which no satellites pass. The three-WPR beams are shown as circles near the centre of the plot.

The vertical WPR beam A is shown in red, and beams B and C are shown in the North (black) and East (green) positions respectively. The beam circle diameters represent the beam width, which we may define as the -18dB points in Figure 25, occurring at + 10°.

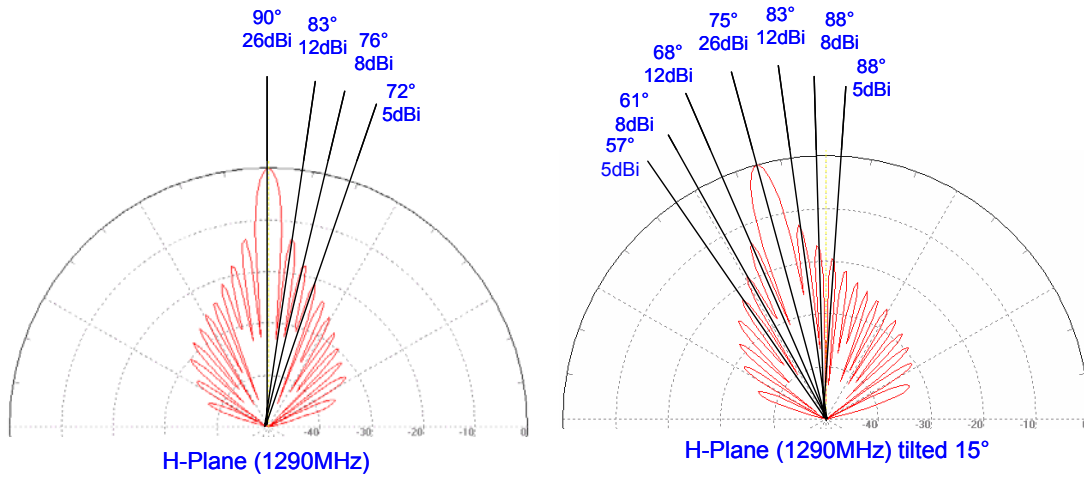


Figure 26: WPR Beam Patterns

If the whole antenna sub system is turned and tilted, so that the beam directions are modified as shown in Figure 27, the interference falls in the antenna sidelobes outside of the main beams.

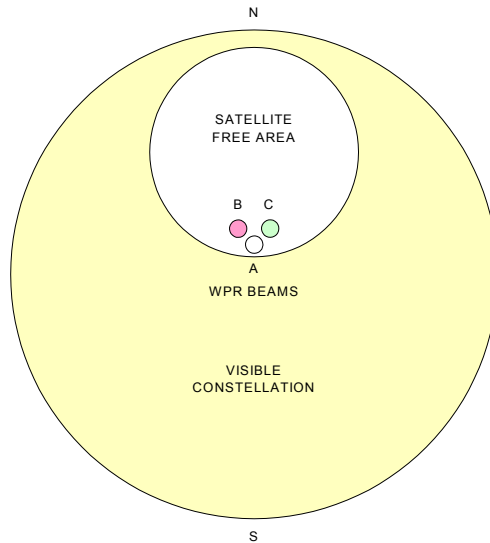


Figure 27: WPR beams, optimally positioned

The angle of tilt is equal to the sum of the angle from zenith to the highest point that the satellites reach, ϕ , and the WPR half-beamwidth. Calculation of ϕ is based on Figure 28, and gives a value of 6°.

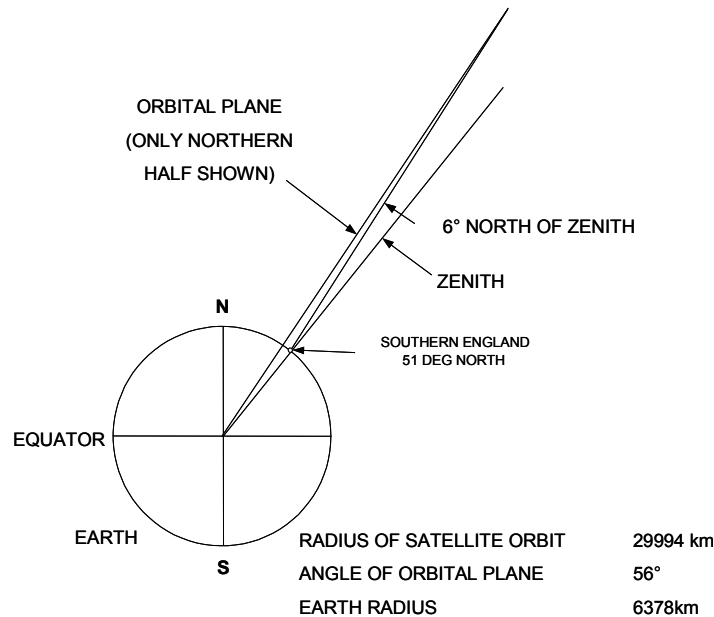


Figure 28: Orbit and WPR beam geometry

The WPR half-beamwidth to the 18dB down points is 10° , so the tilt angle is $6^\circ + 10^\circ = 16^\circ$. Rotation of the WPR beam-set should be as shown in Figure 27. This approach will give about 18dB suppression of the Galileo signals.

The height calibration software would need to be changed to allow for the tilt, since the WPR range to a given height would be increased. There will be a loss of sensitivity associated with the increased distance to the monitored region that is no longer directly overhead at the antenna location. Or put another way, the height for the same sensitivity is reduced by $\cos(16^\circ) = 0.96$

This is a simple, low cost approach as it requires no change to the WPR hardware or to the Internationally agreed operating frequency. However, this approach would not be applicable to more southerly locations such as Southern Europe and further study would be required to identify and verify optimum pointing angles for a given location.

Elevation pointing modification is not possible with existing systems. It might be possible for future systems, however there are physical constraints that need to be considered. For oblique beams, a zenith distance that is "too small" leads to bad error propagation (small errors in radial velocity will cause large errors in horizontal velocity).

Zenith distances that are "too large" will have a negative impact on the constraints of DBS (linear wind field with vanishing horizontal shear of the vertical wind). A zenith distance of approximately 15° has been found to be optimal under most conditions, it is therefore used in nearly all systems.

The antennas used in current European systems (and most systems throughout the worlds) are NOT fully steerable.

Systems using a phased array antenna use fixed time delay lines to generate (for 3 beams per axis, e.g. North-Vertical-South) three fixed linear phase progressions over the individual array elements. This allows three and only three fixed elevation angles in the same vertical plane (e.g. -15° , 0° , $+15^\circ$ zenith distance). The antennas also not steerable at all in azimuth, because the azimuth beam direction depends on the physical arrangement of the antenna.

Other systems use three or five separate fixed antennas to generate three or five separate beams. The individual antennas are not steerable at all. Of course it is possible to use fully steerable antennas, but this would cause much higher costs (such antennas do exist).

So a five-beam DBS wind profiler has exactly five fixed geometrical beam directions, which can be switched sequentially but there is no chance to continuously change elevation and azimuth.

6.2.3 Additional WPR Beam positions

A minimum WPR system has three beams. It may be seen from Figure 18 that the interference occurring in each beam varies with the time of observation and the geometrical relationship between the beams for given latitude of WPR location. It is likely that a fourth beam could be suitably positioned to virtually guarantee the availability of three non-coplanar beams without interference, for a given WPR location in the UK. Further analysis would be required to identify an optimal configuration. Changes to the design would include provision of an additional antenna, an extra port on the antenna selection switch, new antenna selection software, and modifications to the processing software to accept the angles associated with the three antennas finally selected.

An upgrade of a three-beam WPR-A system to five-beams would at least require a new beam steering unit (sometimes called phase-shifter unit). There might be more modifications necessary but this would need to be checked with the manufacturer.

For three beam WPR-B systems, additional antennas would at least be required and possible other necessary changes would also need to be checked with the manufacturer.

It should also be noted that some administrations operate three beams radars even though these radars are capable of using a higher number of beams. The rationale behind this is mainly that a lower number of beams would allow for a faster wind profile determination and could prevent clutters on some beams.

The possible application of this mitigation technique would hence likely provide improvement with regard to coexistence with Galileo but would have to be considered on a case-by-case basis.

6.2.4 Antenna beam polarisation

The Galileo signal is circularly polarised, but the WPR antennas are linearly polarised. This on its own gives ~3 dB suppression of the Galileo signal. If however the WPR is fitted with a circularly polarised antenna of the opposite hand to Galileo, then there is a potential for 20 to 30 dB rejection of the unwanted signal. This depends on the beam patterns of the Galileo and WPR antennas and the system geometry, since both beams would be imperfectly polarised off-axis. Further analysis is required.

Implementation of a circularly polarised solution would necessitate a complete mechanical and electrical redesign of the current WPR antenna configurations. In addition, it could also imply to use a circular polarisation for the WPR transmitter and the opposite polarisation for the WPR receiver. Finally, it should also require a general scientific and operational validation to assess the impact of such a technique on wind measurements.

Therefore, considering the potential hardware impact on WPR and the scientific and operational uncertainties, it is assumed that this solution, even though feasible on a theoretical basis, is not practicable.

6.2.5 Cancellation

Cancellation relies on being able to create a channel in which the interference level is much stronger than the wanted signal. For co-located interference sources it may be possible to obtain a sample of the unwanted signal for cancellation. This is clearly not applicable to the Galileo scenario. Where the interference source is remote, an auxiliary antenna is often used, pointed directly at the interferer, in order to generate the cancellation signal. However, in the situation of interest, the worst-case scenario occurs when the Galileo interferer is directly in line with the wanted signal, making it difficult to separate the two. To overcome this, the possibility of generating the interference signal locally was considered, using a Galileo space-time reference at the WPR. This was found to be possible however, as the PRS coded signal (E6A) has security issues which would prevent this.

A possible solution takes advantage of the fact that the Galileo E6 signal is symmetrical about the centre frequency, as shown in Figure 17. Using the lower side-band of the E6 spectrum it would be possible to create the upper side-band by digital means. This upper side-band would not contain the WPR signal, thus providing a sample of the interferer alone. This signal, together with a sample of the wanted-plus-interferer signal could then be processed in a canceller as shown in Figure 29.

It operates as follows. The interfering signal is split into two orthogonal components, and the quadrature component is correlated in mixer M1 with the sample of wanted-plus-interferer. One of the mixer outputs is a low frequency signal proportional to the amplitude of the interferer in the wanted-plus-interferer path.

This low frequency signal is then amplified and inverted in A1, selected by LPF1, and applied to multiplier M2. M2 then outputs an inverted sample of the quadrature interference, which when added to the wanted-plus-interferer signal tends to cancel out the quadrature component of the interferer in the wanted-plus-interferer

channel. The remaining quadrature interference goes round the loop until a high level of cancellation is obtained, as in a servo loop. Similarly, the lower half of the canceller attenuates the in-phase part of the interference.

Typically, 20 to 30 dB cancellation can be obtained by this technique but it is complex and unlikely to yield a cost-effective solution.

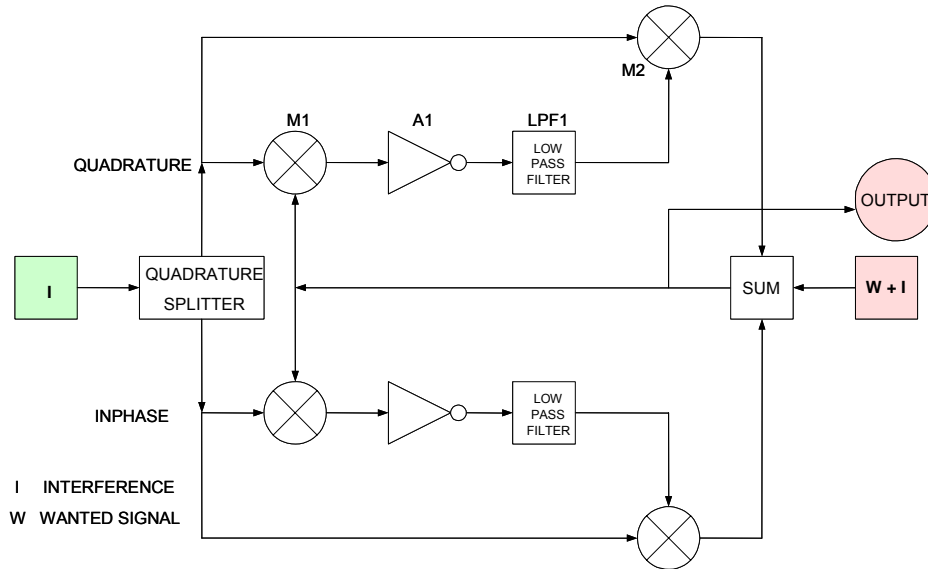


Figure 29: Basic Interference Canceller

6.2.6 WPR central frequency Shift within the 1270-1295 MHz

This solution proposes to shift the WPR central frequency to the frequency of a null in the Galileo E6 spectrum in order to ensure sufficient spectrum separation and hence power discrimination between WPR and Galileo. It is assumed that this mitigation method fully alleviates the interference problem, at least for WPR with comparable performance parameters as the ones used in this study.

The current definition of the Galileo spectrum is shown in Figure 17 and Table 17. On the WPR-B showed that Null E gave unacceptable results, but Null H gave no measurable degradation. Time restrictions prevented testing at null G. If change of WPR frequency becomes the preferred option, tests at null G should be carried out, as a change to null H is likely to involve many more design changes and consequent costs.

This mitigation technique would only be effective in case of the Galileo E6 signal since potential other RNSS systems that could operate in the same band may make use of the Galileo nulls.

It can be noted that there is currently one WPR operating, on a temporary basis, at 1238 MHz that is in a null of GPS. It appears that the most promising central frequencies that provide both sufficient interference suppression and that are not far away from existing operational central frequency are Nulls D and G at about 1274 and 1294 MHz.

FREQUENCY (MHz)	IDENT	Remarks
1258.290	Null A	beyond Res 217
1263.405	Null B (F7-F8)	beyond Res 217
1273.635	Null D (F1-F2)	Recommended as alternative
1283.865	Null E (F3-F4)	Recommended for mitigation
1294.095	Null G (F5-F6)	beyond Res 217
1299.210	Null H	beyond Res 217

Table 17: Nulls in the Galileo E6-signal transmission

6.2.7 *Spectral parasitic elimination*

In case of a CW effect, it seems that a software solution could reduce interference, assuming that Galileo response be spectral typical and taking into account that Galileo interference is accurately predictable.

However, the Galileo influence might not always manifest itself as a distinct peak in the Doppler spectrum (as a coherent effect). It is also unclear whether a software solution (a so-called multi-peak processing) would lead to improvement under all conditions. Indeed, in the last years several algorithms have been proposed that are multi-peak capable. However, there is no agreement in the scientific community on the universality of multi-peak signal processing techniques.

6.2.8 *Use of pulse compression coding*

Pulse compression coding could improve the SNR of the WPR and help to recover radar coverage at higher altitudes.

The principle idea is to use a pulse phase compression with a four moment coding that benefit is that we can increase the mean emission power without increasing the peak emission power. A longer pulse is transmitted keeping the same gate resolution (altitude).

A pulse, made up of x sub-pulses which width suits to the needed resolution, is transmitted. The average power is multiplied by factor x .

On receiving, specific algorithm allows to restore a pulse which width equals to the one corresponding to the needed resolution but which power level x times larger.

By mixing emission and receiving effects, we thus are able to win thus a factor x^2 on power.

A four-moment pulse coding which allows a factor 16 win (i.e. 12 dB). This factor must be slightly lower because of the filtering needed to get rid of parasitic bounds due to receiving processing. The win is rather of about 10 to 11 dB which suits to the suppression requirement.

On the other hand, this solution looks seductive at first but has several drawbacks:

- During the emission time receiver is locked and so, during a time equal to $4 \times 2.5 \mu\text{s} + 2\mu\text{s} + 1 \mu\text{s} = 12 \mu\text{s}$ ($2 \mu\text{s}$ represent climbing and descending times for one elementary pulse and $1 \mu\text{s}$ for receiver open) we receive no signal. This duration corresponds to an 1800-meter altitude! This does not mean that we cannot measure anything below but signal issued from those lower altitudes will be truncated and so will be of a lesser quality. Meanwhile, we can consider that for signal received up to 30%, quality will remain satisfactory the more as received signal issued from lower gates is the stronger. It results from this that the first measurement can be at a 700 meter-altitude if we use a processing algorithm, which allows an optimised data treatment quality.
- for a given recurrence period, the duty cycle will be multiplied by a factor four, which increases its value up to 16.7%, which may actually be incompatible with some system limit characteristics.

Some devices do not have the software allowing pulse coding; two for the “high” mode multiplies the acquisition time and raw treatment, thus the number of available Spectra would be reduced. It is known that pulse compression can suppress external RF interference to profilers. Recently, results have been published for two types of interference, namely noise-like interference and sinusoidal interference.

For example, in the case of noise interference an 8-bit bi-phase complementary code may give an interference suppression of 12 dB. Again, the results depend on the nature of the interference. Results on the achievable interference suppression for the E6-signal are yet unknown, in particular with regard to the CW impact. It should also be mentioned that pulse compression coding has an impact on the radar duty cycle and hence would have technical impacts and limits mainly on the transmitter and the power supplier of the radar.

6.2.9 *Combination of different modes*

WPR systems are in general able to run with different modes, even higher than 3. As such, it is not clear how this can help to suppress the effect of the E6 signal.

However, taking into account the use of pulse compression coding in different running modes, as described above, this could provide interference suppression advantage for the coded modes and in particular high altitude ones and, by associating different modes, could help recovering both range and data quality requirements.

This combination of different modes can take the form of

- running the WPR operations with three or more modes
- combining two same resolution modes (one coded and the other not)

6.3 Mitigation techniques summary

Considering 5MHz as the typical video bandwidth for a WPR as shown in Figure 30, about three potential frequency ranges can be identified where spectral Nulls of the Galileo E6-signal would provide best decoupling of both services.

The fourth options between F7 and F8 is outside the WPR allocation by Resolution 217 and even the range between F5 and F6 would not conform to the regulatory frame conditions. They are nevertheless mentioned here to indicate further potential for mitigation if needed.

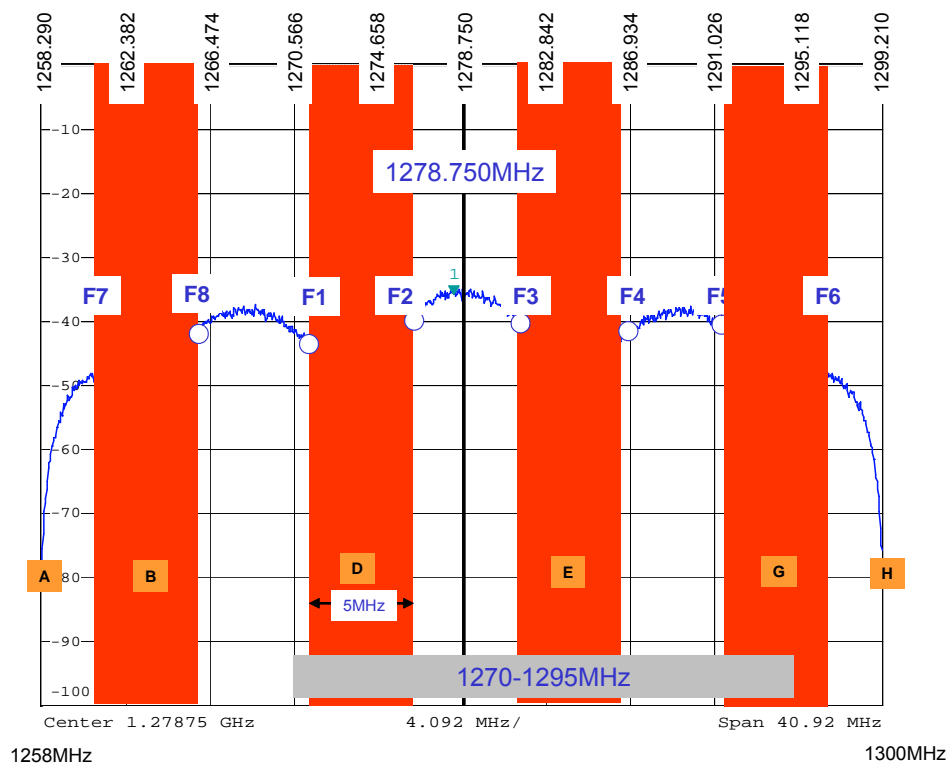


Figure 30: WPR video bandwidth at Nulls of the Galileo E6-signal spectrum

Mitigation technique		Applicability	Adv. and interference suppress. capability	Drawbacks/ Remarks
1	Antenna pointing	Northern Lat locations	About 18dB suppression of the Galileo E6-signal	Only for Northern latitude locations
2	Additional beams	3-beam WPRs	Reduces boresight visibility	Refurbishment of 3-beam WPR
3	LHC-Polarisation of WPR antenna	New WPR antennas	Adds 20..30dB cross-polarisation de-coupling	Requires modification of WPR antenna
4	Interference cancellation	For specific interference cases	Typically 20 to 30dB cancellation can be obtained	Requires additional hardware
5	Null-1 (F1-F2)	For scientific measurements	Rejects incoherent E6 impact by 10dB	Shifting of WPR transmit frequency; filter affected
6	Null-2 (F3-F4)	For scientific measurements	Rejects incoherent E6 impact by 10dB	Shifting of WPR transmit frequency; filter affected
7	Spectral parasitic elimination	For scientific measurements	In case of residual coherent interference	Limited effectiveness, further study required
8	Pulse compression	Applicable only for higher altitudes	In the case of noise interference an 8bit-Bi-phase complementary code may give an interference suppression of 12dB	signal issued from those lower altitudes will be truncated and so will be of a lesser quality. Increase the radar duty cycle. (Technical impacts and limits on the transmitter and the power supply) For next generation of WPR installations

Table 18: Summary and evaluation of mitigation options

7 CONCLUSIONS AND RECOMMENDATIONS

7.1 General conclusions related to RNSS in the 1270-1295 MHz band

This report has shown that the presently planned Galileo signals present a potential of interference and degradation to wind profiler operations at least for three-beam WPRs.

As far as noise like impact is concerned, it appears that mitigation techniques would be necessary for three-beam WPR whereas five-beam WPRs would be able to operate with minor degradation without applying any mitigation.

There are some processing features that could provide interference suppression capabilities. These techniques would however require software and possibly hardware modifications and could hence result in technical and costs consequences that are quite difficult to assess.

Finally, it should be noted that the interference analysis were performed using the maximum Galileo power, i.e. representing cases where the WPR central frequency would be close to the maximum of the Galileo spectrum.

Measurements have shown that shifting the WPR central frequency close to a Null of the Galileo spectrum would provide, at least for most types of WPR, sufficient interference suppression to ensure coexistence. However, it should be noted that this solution is Galileo system dependent and might not be possible for future RNSS systems.

Two frequencies are currently seen as good candidates for WPR operations: 1274 MHz and 1294 MHz. It should, however, be noted that this latter frequency is currently not in the frequency range as given in ITU-R Resolution 217 and could require, if needed, a specific regulatory work prior its implementation.

It is also recommended that the WPR manufacturers and operators should liaise with RNSS operators or system developers to establish the most appropriate mitigation technique to apply to WPR perhaps on an individual basis.

7.2 Specific conclusions related to Galileo and current European WPR in the 1270-1295 MHz band

All WPRs presently used for weather observations and scientific applications in CEPT-countries have been investigated and individual recommendations developed. These recommendations are provided in Table 19.

WPR location	Central Frequency (MHz)	Latitude N (°)	Possible beams	Beams used	Beam elevation (°)	Comments
Vienna (Austria)	1280	48.1	3, 4 or 5	3, 4 or 5	74.5	5 beams Recommended. Use of mitigation technique should be considered for 3 beams or specific applications requiring 1 beam.
Innsbruck (Austria)	1280	47.2	3, 4 or 5	3, 4 or 5	74.5	
Salzburg (Austria)	1280	47.5	3, 4 or 5	3, 4 or 5	74.5	
Faroe Island (Denmark)	1290	62	3	3	73	Use of mitigation technique should be considered
Marignane (France)	1274	43	3, 4 or 5	5	73	No compatibility problems
Nice (France)	1274 (during 06)	43.5	3, 4 or 5	5	73	No compatibility problems
Toulouse (France)	1274	Mobile system	3, 4 or 5	3, 4 or 5	73	No compatibility problems
Meteo-France	1274	Mobile systems	3, 4 or 5	3, 4 or 5	73	No compatibility problems
Lindenberg (Germany)	1290	52.2	3, 4 or 5	5	74.5	No compatibility problems for operational applications. Use of mitigation technique for scientific applications requiring 1 beam should be considered.
Germany	1290	Mobile systems	3, 4 or 5	3, 4 or 5	74.5	5 beams Recommended. Use of mitigation technique should be considered for 3 beams or specific applications requiring 1 beam.
Budapest (Hungary)	1290	47.7	3	3	73	Use of mitigation technique should be considered for 3 beams or specific applications requiring 1 beam.
Szeged (Hungary)	1290	46.4	3, 4 or 5	3, 4 or 5	74.5	5 beams Recommended. Use of mitigation technique should be considered for 3 beams or specific applications requiring 1 beam.
L'Aquila (Italy)	1290	42.5	3, 4 or 5	3, 4 or 5	74.5	
Torino (Italy)	1290	45.5	3, 4 or 5	3, 4 or 5	74.5	
Cabauw (Netherlands)	1290	51.9	3, 4 or 5	3	74.5	5 beams Recommended. Use of mitigation technique should be considered for 3 beams or specific applications requiring 1 beam.
Bilbao (Spain)	1290	43.4	3, 4 or 5	5	74.5	No compatibility problems for operational applications. Use of mitigation technique for specific applications requiring 1 beam should be considered.
Payerne (Switzerland)	1290	46.8	3, 4 or 5	3 or 4	74.5	5 beams Recommended. Use of mitigation technique should be considered for 3 beams or specific applications requiring 1 beam.
Meteo Swiss (Switzerland)	1290	Mobile system	3, 4 or 5	3	74.5	
Dunkeswell (UK)	1290	50.9	3, 4 or 5	4	74.5	
Wattisham (UK)	1290	52.1	3, 4 or 5	4	74.5	Use of mitigation technique should be considered for 3 beams or specific applications requiring 1 beam.
Aberystwyth (UK)	1290	52.5	3	3	73	
Helsinki (Finland)	1290	60.1	5	5	74.5	

Table 19: Recommendations for operational WPR in the CEPT countries

8 GLOSSARY AND LIST OF ACRONYMS

BOC	BOC type signals are usually expressed in the form $BOC(f_{\text{shift}}, f_{\text{chip}})$ where frequencies are indicated as integer multiples of the GPS C/A Code chip rate of 1.023 Mcps. For example, a BOC(10,5) signal has actually a sub-carrier frequency of $10 \times 1.023 \text{ MHz} = 10.230 \text{ MHz}$ and a code chip rate of $5 \times 1.023 \text{ MHz} = 5.115 \text{ MHz}$.
Nowcasting	Forecasting weather, for the next few minutes to a couple of hours, using all immediately available weather data
Observation cycle	impacts on the requirement of data availability and thence defines WPR system tolerance for short-term interruptions in case of interference.
Pilot	The pilot signal transmitted as third component is to improve the signal power for position determination by about 3dB. It bears no data channel, thus improves the acquisition and ranging performance significantly.
Vertical Resolution	requirement defining the altitude increment, and thus the usable pulse length and bandwidth of the WPR.

BOC	Binary Offset Carrier
CS	Commercial Service (Galileo data dissemination service)
DRP	Doppler Radar Profiler (see WPR)
DWD	Deutscher Wetterdienst (German Weather Service)
MOL	Meteorological Observatory Lindenberg of the DWD near Berlin, Germany
PRS	Public Regulated Service, accessible for closed Governmental user groups (Galileo)
WMO	World Meteorological Organisation
WPR	Wind profiler radar (usually called Doppler Profiler Radar)

9 REFERENCES

[1] Margot Ackley, Russ Chadwick, James Cogan, Christy Crosiar, Frank Eaton, Ken Gage, Earl Gossard, Rick Lucci, Francis Merceret, William Neff, Martin Ralph, Richard Strauch, Douglas van de Kamp, and Bob Weber and Allen White. U.S. Wind Profilers: A Review. Technical Report FCM-R14-1998, U.S. DoC/NOAA/OFCM, Washington, DC., March 1998.

[2] Donald Burgess and Peter S. Ray. *Mesoscale Meteorology and Forecasting*, chapter Principles of radar, pages 85–117. AMS, 1986.

[3] D.A. Carter, K.S.Gage, W.L.Ecklund, W.M.Angevine, P.E.Johnston, A.C.Riddle, J.Wilson, and C.R.Williams. Developments in UHF lower tropospheric wind profiling at NOAA’s Aeronomy Laboratory. *Radio Sci.*, 30(4):977–1001, July-August 1995.

[4] P.B. Chilson, A.Muschinski, and G.Schmidt. First observations of Kelvin-Helmholtz billows in an upper-level jet stream using VHF frequency domain interferometry. *Radio Sci.*, 32:1149–1160, 1997.

[5] Philippe B. Chilson, Tian-You Yu, Richard G. Strauch, Andreas Muschinski, and Robert D. Palmer. Implementation and validation of range imaging on a UHF radar wind profiler. *J. Atmos. Oceanic Technol.*, 20:987–996, 2003.

[6] Phillip B. Chilson. The retrieval and validation of Doppler velocity estimates from range imaging. *J. Atmos Oceanic Technol.*, 21:1033–1043, 2004.

[7] Larry B. Cornman, Robert K. Goodrich, Corinne S. Morse, and Warner L. Ecklund. A fuzzy logic method for improved moment estimation from Doppler spectra. *J. Atmos. Oceanic Technol.*, 15(6):1287–1305, December 1998.

[8] Richard J. Doviak and Dusan S. Zrnica. *Doppler Radar and Weather Observations*. Academic Press, 1993.

[9] R.J. Doviak, R.J. Latatis, and C.L. Holloway. Cross correlations and cross spectra for spaced antenna wind profilers - 1. theoretical analysis. *Radio Sci.*, 31:157–180, 1996.

[10] Warner L. Ecklund, David A. Carter, and Ben B. Balsley. A UHF wind profiler for the boundary layer: Brief description and initial results. *Journal of Atmospheric and Oceanic Technology*, 5:432–441, June 1988.

- [11] Dirk Engelbart, Hans Steinhagen, Ulrich Görsdorf, Jens Lippmann, and Joachim Neisser. A 1290 MHz profiler with RASS for monitoring wind and temperature in the Boundary Layer. *Beitr. Phys. Atmos.*, 69(1):63–80, February 1996.
- [12] D.T. Farley. On-line data processing techniques for MST radars. *Radio Sci.*, 20(6):1177–1184, November-December 1985.
- [13] S. Ferrat and M. Crochet. Methods of detection and estimation errors in ST radar studies. *Ann. Geophysicae*, 12:489–496, 1994.
- [14] Martin A. Fischler and Robert C. Bolles. Random sample consensus: A paradigm for model fitting with applications to image analysis and automated cartography. *Commun. Assoc. Comput. Mach.*, 24:381–395, 1981.
- [15] R.G. Frehlich and M.J. Yadlowsky. Performance of mean-frequency estimators for doppler radar and lidar. *J. Atmos. Oceanic Technol.*, 11:1217–1230, October 1994.
- [16] A.S. Frisch, B.L. Weber, R.G. Strauch, D.A. Merritt, and K.P. Moran. The altitude coverage of the Colorado wind profilers at 50, 405 and 915 MHz. *J. Atmos. Oceanic Technol.*, 3:680–692, December 1986.
- [17] Uriel Frisch. *Turbulence. The Legacy of A.N. Kolmogorov*. Cambridge University Press, 1996.
- [18] O. Ghebrehbrhan and M. Crochet. On full decoding of truncated ranges for ST/MST radar applications. *IEEE Trans. Geosci. Remote Sensing*, 30(1):38–45, January 1992.
- [19] Ogubazghi Ghebrehbrhan. Sidelobe properties of complementary codes. *Meteorologische Rundschau*, 42:109–114, Juni 1990.
- [20] Ulrich Görsdorf and Volker Lehmann. Enhanced accuracy of RASS measured temperatures due to an improved range correction. *J. Atmos. Oceanic Technol.*, 17:406–416, April 2000.
- [21] Earl E. Gossard and Richard G. Strauch. *Radar Observations of Clear Air and Clouds*. Elsevier, 1983.
- [22] Thomas Griesser. *Multipeakanalyse von Dopplerspektren aus Windprofiler-Radar-Messungen*. PhD thesis, Eidgenössische Technische Hochschule Zürich, 1998.
- [23] Kenneth R. Hardy and Kenneth S. Gage. The history of radar studies of the clear atmosphere. In *Radar in Meteorology*, chapter 17, pages 130–142. American Meteorological Society, Boston, 1990.
- [24] D. Helal, M. Crochet, H. Luce, and E. Spano. Radar imaging and high-resolution array processing applied to a classical VHF-ST profiler. *J. Atmos. Sol. Terr. Phys.*, 63:263–274, 2001.
- [25] Peter H. Hildebrand and R.S. Sekhon. Objective determination of the noise level in Doppler spectra. *J. Appl. Meteorol.*, 13:808–811, October 1974.
- [26] Lutz Hirsch, Vladislav Klaus, Henk Klein Baltink, Volker Lehmann, and Gerhard Peters. Fundamentals of wind profiler operations. In *COST Action 76 - Final report: Development of VHF/UHF Wind Profilers and Vertical Sounders for use in European Observing Systems*. EUROPEAN COMMISSION Directorate-General for Research, European Commission, Rue de la Loi/Wetstraat 200 (SDME 1/53), B - 1049 Brussels, 2003.
- [27] Akira Ishimaru. *Wave Propagation and Scattering in Random Media*. Academic Press, 1978.
- [28] Steven M. Kay and JR. Stanley Lawrence Marple. Spectrum analysis - a modern perspective. *Proc. IEEE*, 69(11):1380–1491, November 1981.
- [29] R. Jeffrey Keeler and Richard E. Passarelli. Signal processing for atmospheric radars. In D. Atlas, editor, *Radar in Meteorology*, chapter 20a, pages 199–229. American Meteorological Society, Boston, 1990.
- [30] E. Kudeki and G. Stitt. Frequency domain interferometry: A high resolution technique for studies of atmospheric turbulence. *Geophys. Res. Lett.*, 14:198–201, 1987.
- [31] R. J. Lataitis. Theory of a radio-acoustic sounding system (RASS). Technical Report NOAA Technical Memorandum ERL WPL-230, NOAA, 1993.
- [32] R.J. Lataitis, S.F. Clifford, and C.L. Holloway. An alternative method of inferring winds from spaced-antenna radar measurements. *Radio Sci.*, 30:463–474, 1995.
- [33] Daniel Law, Frank Sanders, Gary Patrick, and Michael Richmond. Measurements of wind profiler EMC characteristics. Technical Report NTIA Report TR-93-301, NTIA, 1993.

- [34] D.C. Law, S.A. McLaughlin, M.J. Post, B.L. Weber, D.C. Welsh, D.E. Wolfe, and D.A. Merritt. An electronically stabilized phased array system for shipborn atmospheric wind profiling. *J. Atmos. Oceanic Technol.*, 19:924–933, June 2002.
- [35] H. Luce, M. Yamamoto, S. Fukao, D. Helal, and M. Crochet. A frequency domain radar interferometric imaging (fii) technique based on high resolution methods. *J. Atmos. Solar. Terr. Phys.*, 63:201–214, 2001.
- [36] Peter T. May and Richard G. Strauch. An examination of wind profiler signal processing algorithms. *J. Atmos. Oceanic Technol.*, 6:731–735, August 1989.
- [37] James B. Mead, Geoffrey Hopcraft, Stephen J. Frasier, Brian D. Pollard, Christopher D. Cherry, Daniel H. Schaubert, and Robert E. McIntosh. A volume-imaging radar wind profiler for atmospheric boundary layer turbulence studies. *J. Atmos. Oceanic Technol.*, 15:849–859, 1998.
- [38] Wim A. Monna and Russell B. Chadwick. Remote-sensing of upper-air winds for weather forecasting: Wind-profiler radar. *Bull. WMO*, 47(2):124–132, April 1998.
- [39] Corinne S. Morse, Robert K. Goodrich, and Larry B. Cornman. The NIMA method for improved moment estimation from Doppler spectra. *J. Atmos. Oceanic Technol.*, 19:274–295, March 2002.
- [40] Andreas Muschinski. The first moments of the variance- and cross-spectra of standard and interferometric clear-air-doppler-radar signals. Technical Report NCAR/TN-441+STR, National Center for Atmospheric Research Boulder, Colorado, May 1998.
- [41] Andreas Muschinski. Local and global statistics of clear-air Doppler radar signals. *Radio Sci.*, 39(RS1008):doi:10.1029/2003RS002908, 2004.
- [42] Andreas Muschinski, Volker Lehmann, Lutz Justen, and Gerd Teschke. Advanced radar wind profiling. *Meteorol. Z.*, xx(xx):1–46, 2005.
- [43] Andreas Muschinski and Donald H. Lenschow. Future directions for research on meter- and submeter-scale atmospheric turbulence. *Bull. Amer. Meteorol. Soc.*, 82(12):2831–2843, December 2001.
- [44] Tomohiro Oguchi. Electromagnetic wave propagation and scattering in rain and other hydrometeors. *Proc. IEEE*, 71(9):1029–1078, September 1983.
- [45] Robert D. Palmer, Tian-You Yu, and Phillip B. Chilson. Range imaging using frequency diversity. *Radi Sci.*, 34(6):1485–1496, 1999.
- [46] G. Peters, H. Timmermann, and H. Hinzpeter. Temperature sounding in the Planetary Boundary Layer by RASS-system. *Int. J. Remote Sens.*, 4:49–63, 1993.
- [47] Brian D. Pollard, Samir Khanna, Stephen J. Frasier, John C. Wyngaard, and Dennis W. Thomson. Local structure of the convective boundary layer from a volume-imaging radar. *J. Atmos. Sci.*, 57:2281–2296, 2000.
- [48] A.C. Riddle and W.M. Angevine. Ground clutter removal from profiler spectra. In B. Edwards, editor, *Proceedings of the Fifth Workshop on Technical and Scientific Aspects of MST Radar*, pages 418–420, 1406 W. Green Street, Urbana, IL 61801, USA, 1991. Scientific Committee on Solar Terrestrial Physics (SCOSTEP), SCOSTEP Secretariat, University of Illinois.
- [49] J. Röttger and M.F. Larsen. UHF/VHF radar techniques for atmospheric research and wind profiler applications. In *Radar in Meteorology*, chapter 21a, pages 235–281. American Meteorological Society, Boston, 1990.
- [50] Gerhard Schmidt, Rüdiger Ruster, and Peter Czechowsky. Complementary code and digital filtering for detection of weak VHF radar signals from the Mesosphere. *IEEE Trans. Geosci. Electron.*, GE-17(4):154–161, October 1979.
- [51] Merrill I. Skolnik. *Introduction to Radar Systems*. McGraw-Hill, 2001.
- [52] Lydi Sma’ini, Hubert Luce, Michel Crochet, and Shoichiro Fukao. An improved high-resolution processing method for a frequency domain interferometric imaging (fii) technique. *J. Atmos. Oceanic Technol.*, 19:954–966, 2002.
- [53] Igor Smalikho. Techniques of wind vector estimation from data measured with a scanning coherent Doppler lidar. *J. Atmos. Oceanic Technol.*, 20:276–291, February 2003.

- [54] Eric Spano and Ogubazghi Ghebrebrhan. Complementary sequences with high sidelobe suppression factors for ST/MST radar applications. *IEEE Transactions on Geoscience and Remote Sensing*, 34(2):317–329, March 1996.
- [55] Eric Spano and Ogubazghi Ghebrebrhan. Pulse coding techniques for ST/MST radar systems: A general approach based on a matrix formulation. *IEEE Transactions on Geoscience and Remote Sensing*, 34(2):304–316, March 1996.
- [56] Eric Spano and Ogubazghi Ghebrebrhan. Sequences of complementary codes for the optimum decoding of truncated ranges and high sidelobe suppression factors for ST/MST radar systems. *IEEE Transactions on Geoscience and Remote Sensing*, 34(2):330–345, March 1996.
- [57] Hans Steinhagen, Jochen Dibbern, Dirk Engelbart, Ulrich Görsdorf, Volker Lehmann, Joachim Neisser, and John W. Neuschaefer. Performance of the first European 482 MHz wind profiler radar with RASS under operational conditions. *Meteorologische Zeitschrift*, N.F.7:248–261, October 1998.
- [58] R. G. Strauch, D. A. Merritt, K. P. Moran, K. B. Earnshaw, and D. van de Kamp. The Colorado wind profiling network. *J. Atmos. Ocean. Technol.*, 1:37–49, March 1984.
- [59] M.P. Sulzer and R.F. Woodman. Quasi-complementary codes: A new technique for MST radar sounding. *Radio Science*, 19(1):337–344, January-February 1984.
- [60] V. I. Tatarskii. *Wave propagation in a turbulent medium*. McGraw-Hill, 1961.
- [61] Keith Tomkinson, Zoran Dobrosavljevic, and Mike Page-Jones. WPR-Galileo Interference Study. Technical report, Roke Manor Research Ltd. Roke Manor, Romsey Hampshire, SO51 0ZN, UK, 2004.
- [62] Toshitaka Tsuda. *Middle Atmosphere Program - Handbook for MAP*, volume 30, chapter Data Acquisition and Processing, pages 151–183. ICSU Scientific Committee on Solar-Terrestrial Physics (SCOSTEP), 1989. ISAR 24.-28. November 1988, Kyoto.
- [63] Koichiru Wakasugi and Shoichiro Fukao. Sidelobe properties of a complementary code used in MST radar observations. *IEEE Transactions on Geoscience and Remote Sensing*, GE-23(1):57–59, January 1985.
- [64] Timothy L. Wilfong, David A. Merritt, Richard J. Latatis, Bob L. Weber, David B. Wuertz, and Richard G. Strauch. Optimal generation of radar wind profiler spectra. *J. Atmos. Oceanic Technol.*, 16:723–733, June 1999.
- [65] Timothy L. Wilfong, David A. Merritt, Bob L. Weber, and David B. Wuertz. Multiple signal detection and moment estimation in radar wind profiler spectral data. unpublished manuscript, 1999.
- [66] R. F. Woodman. Spectral moment estimation in MST radars. *Radio Sci.*, 20:1185–1195, 1985.
- [67] Ronald F. Woodman and Alberto Guillen. Radar observation of winds and turbulence in the stratosphere and mesosphere. *J. Atmos. Sci.*, pages 493–505, 1974.
- [68] Dusan S. Zrnica. Simulation of weatherlike Doppler spectra and signals. *J. Appl. Meteorol.*, 14:619–620, June 1975.

ANNEX A: WMO DATA QUALITY REQUIREMENTS

The World Meteorological Organization (WMO) has carried out a thorough analysis of data requirements covering the main applications. The study was made in close cooperation with National Meteorological Services, as well as the international organizations such as ICAO and UNEP. The requirements state how firm the requirement is on a four-step scale (firm, reasonable, tentative, and speculative).

Requirement	Vertical resolution	Accuracy	Observation Cycle	Confidence
Lower troposphere	150 - 600 m	2 - 5 m/s	5 - 10 min	Firm
Higher troposphere	150 - 600 m	2 - 5 m/s	5 - 10 min	Firm
Lower stratosphere	150 - 600 m	2 - 5 m/s	5 - 10 min	Firm

Table 20: Aeronautical Meteorology

Requirement	Vertical resolution	Accuracy	Obs Cycle	Confidence
Lower troposphere	500 - 1000 m	1 - 5 m/s	0.25 - 6 h	Firm
Higher troposphere	500 - 1000 m	1 - 8 m/s	0.25 - 4 h	Firm
Lower stratosphere	500 - 1000 m	1 - 5 m/s	0.25 - 6 h	Firm

Table 21: Nowcasting Meteorology (Nowcasting meteorology serves immediate weather analysis, with a short term outlook.)

Requirement	Vertical resolution	Accuracy	Obs Cycle	Confidence
Lower troposphere	0.4 - 5 km	1 - 5 m/s	0.5 - 12 h	Firm
Higher troposphere	1 - 10 km	1 - 8 m/s	0.5 - 12 h	Firm
Lower stratosphere	1 - 10 km	1 - 5 m/s	0.5 - 12 h	Firm

Table 22: Regional Meteorology (Regional meteorology covers typically continental scale analysis and predictions out to about 2 days.)

Requirement	Vertical resolution	Accuracy	Obs Cycle	Confidence
Lower troposphere	0.1 - 2 km	2 - 5 m/s	3 - 12 h	Firm
Higher troposphere	0.1 - 2 km	2 - 8 m/s	3 - 12 h	Firm
Lower stratosphere	0.1 - 2 km	2 - 5 m/s	3 - 12 h	Firm

Table 23: Synoptic Meteorology (Synoptic scale meteorology applications cover hemispheric scale, and provides weather forecasts for approximately 4 days.)

Requirement	Vertical resolution	Accuracy	Obs Cycle	Confidence
Lower troposphere	0.4 - 5 km	1 - 5 m/s	1 - 12 h	Firm
Higher troposphere	1 - 10 km	1 - 8 m/s	1 - 12 h	Firm
Lower stratosphere	1 - 10 km	1 - 5 m/s	1 - 12 h	Firm

Table 24: Global Meteorology (The global scale numerical forecasting provides predictions to 10 days ahead.)

ANNEX B: WIND PROFILER RADAR SITES IN CEPT COUNTRIES

	Vienna	Innsbruck	Salzburg
WMO Station No.	11036	11120	11150
Latitude / Longitude	48.13(N) / 16.55(E)	47.16(N) / 11.23(E)	47.47(N) / 13.00 (E)
Station Height	227m	614m	430m
Type of System	LAP3000 (9 panel) Vaisala	LAP3000 (9 panel) Vaisala	LAP3000 (9 panel) Vaisala
Antenna	1x Electrically steerable micropatch phased array formed by nine 0.87m x 0.87m antenna panels	1x Electrically steerable micropatch phased array formed by nine 0.87m x 0.87m antenna panels	1x Electrically steerable micropatch phased array formed by nine 0.87m x 0.87m antenna panels
Aperture	7.3m ²	7.3m ²	7.3m ²
Az./Elev. Scan rate	Not scanning	Not scanning	Not scanning
RF Power (dBW)	Mean 19dBW (72W)	Mean 19dBW (72W)	Mean 19dBW (72W)
Transmitted	Peak 28dPW(600W)	Peak 28dPW(600W)	Peak 28dPW(600W)
RF Power (dB)	Mean 45dB	Mean 45dB	Mean 45dB
Radiated (eirp)	Peak 54dP	Peak 54dP	Peak 54dP
Frequency	1280MHz	1280MHz	1280MHz
Possible beams	3, 4 or 5 (15.5°)	3, 4 or 5 (15.5°)	3, 4 or 5 (15.5°)
No of beams used.	?	?	?
Beam width	6 degrees (approx)	6 degrees (approx)	6 degrees (approx)
Relative Gain (dBi)	+ 29dBi	+ 29dBi	+ 29dBi
Averaging Period	30 minutes	30 minutes	30 minutes
Pulse repetition freq	3000 per second	3000 per second	3000 per second
Pulse Width	0.7 µsec	0.7 µsec	0.7 µsec
IPP	?	?	?
System Status	Operational Airport Operations NWP Assimilation + Nowcasting	Operational Airport Operations NWP Assimilation + Nowcasting	Operational Airport Operations NWP Assimilation + Nowcasting

Table 25: Austria (Austro Control) - Wind Profiler System Technical Information

	Greenland	Faroe Islands
WMO Station No.	n/a	n/a
Latitude / Longitude	67.08(N) / 50.50(W)	62.00(N) / 7.00(W)
Station Height	unknown	unknown
Type of System	LAP3000 (9 panel) Vaisala	Degreane
Antenna	1x Electrically steerable micropatch phased array formed by nine 0.87m x 0.87m antenna panels	3 separate panels of 64 dipoles
Aperture	4m ²	4m ²
Az./Elev. Scan rate	Not scanning	Not scanning
RF Power (dBW)	Mean 19dBW (72W)	Mean 0.35kW
Transmitted	Peak 28dPW(600W)	Peak 3.5kW
RF Power (dB)	Mean 45dB	
Radiated (eirp)	Peak 54dP	
Frequency	1215MHz	1290MHz
Possible beams	3, 4 or 5	3
No of beams used.	?	3
Beam width	8 degrees (approx)	6 degrees (approx)

	Greenland	Faroe Islands
Relative Gain (dBi)	?	+ 29dBi
Averaging Period	?	?
Pulse repetition freq		
Pulse Width		
IPP		
System Status	Research	Airport Operations (u/s at present)

Table 26: Denmark - Wind Profiler System Technical Information

	Le Ferte Vidame	Marignane	Nice	Clermont-Ferrand	Lannemezan
WMO Station No.	07112	07650	07690	07453	07626
Latitude / Longitude	48.62(N) / 0.92(E)	43.43(N) / 5.23(E)	43.66(N) / 7.19 (E)	45.70(N) / 3.10 (E)	43.08(N) / 0.22 (-W)
Station Height	245m	7m	4m	660m	4m
Type of System	Degreane & Meteo France	Degreane	Degreane	LAMP-OPGC	CRA
Antenna	Array of 156 YAGI antennas each 4.5m high	5 separate panels of 64 dipoles	5 separate panels of 64 dipoles	Array of YAGI antennas	Array of YAGI antennas
Aperture (metres)	4185m ²	5m ²	5m ²	4096m ²	4096m ²
Az./Elev. Scan rate	Not scanning	Not scanning	Not scanning	Not scanning	Not scanning
RF Power (dBW)	Mean 3.6kW	Mean 0.35kW	Mean 0.35kW	Mean 0.80kW	Mean 0.80kW
Transmitted	Peak 18kW	Peak 3.5kW	Peak 3.5kW	Peak 5.0kW	Peak 5.0kW
RF Power (dB)					
Radiated (eirp)					
Frequency	52.05MHz	1238MHz (will change to 1274)	1274MHz	45MHz	45MHz
Possible beams	?	3, 4 or 5 (17°)	3, 4 or 5 (17°)	?	?
No of beams used.	?	5	5	?	?
Beam width	6.5 degrees (approx)	9 degrees (approx)	9 degrees (approx)	5.6 degrees (approx)	5.6 degrees (approx)
Relative Gain (dBi)	+ 78.5dBi	+ 29dBi	+ 29dBi	+ 30dBi	+ 30dBi
Averaging Period	30 minutes	27 minutes	27 minutes	60 minutes	60 minutes
Pulse repetition freq					
Pulse Width					
IPP					
System Status	Operational NWP Assimilation	Operational Airport Operations NWP Assimilation + Nowcasting	Operational NWP Assimilation + Nowcasting	Research system. Regular data to WINPROF for NWP Assimilation	Research system. Regular data to WINPROF for NWP Assimilation
	Lannemezan	Toulouse	Toulon		
WMO Station No.	n/a	n/a	n/a		
Latitude / Longitude	Mobile System	Mobile System	Mobile System		
Station Height					
Type of System	Degreane	Degreane	Degreane		
Antenna	5 separate panels of 64 dipoles	5 separate panels of 64 dipoles	3 separate panels of 64 dipoles		
Aperture (metres)	5m ²	5m ²	5m ²		
Az./Elev. Scan rate	Not scanning	Not scanning	Not scanning		

	Lannemezan	Toulouse	Toulon
RF Power (dBW)	Mean 0.35kW	Mean 0.35kW	Mean 0.35kW
Transmitted	Peak 3.5kW	Peak 3.5kW	Peak 3.5kW
RF Power (dB)/ Rad (eirp)			
Frequency	1238MHz	1274MHz	1238MHz
Possible beams	3, 4 or 5	3, 4 or 5	3
No of beams used.	3, 4 or 5	3, 4 or 5	3
Beam width	9 degrees (approx)	9 degrees (approx)	9 degrees (approx)
Relative Gain (dBi)	+ 29dBi	+ 29dBi	+ 29dBi
Averaging Period			
Pulse repetition freq			
Pulse Width			
IPP			
System Status	Research System Mobile for measurement campaigns	Research System Mobile for measurement campaigns	Research System Mobile for measurement campaigns

Table 27: France - Wind Profiler System Technical Information

	Bayreuth	Lindenberg	Lindenberg	Nordholz	Ziegendorf
WMO Station No.		10394	10394	10135	10266
Latitude / Longitude		52.21(N) / 14.13 (E)	52.21(N) / 14.13 (E)	53.78(N) / 8.67 (E)	53.31(N) / 11.84 (E)
Station Height		103m	103m	18m	57m
Type of System	LAP 16000 Vaisala	LAP 16000 Vaisala	LAP 3000 Vaisala	LAP 16000 Vaisala	LAP 16000 Vaisala
Antenna	Phased array (CoCo) 180 antenna elements (14 dipoles each)	Phased array (CoCo) 120 antenna elements (20 dipoles each)	Phase array (microstrip) Nine 0.87m x 0.87m antenna panels	Phased array (CoCo) 180 antenna elements (14 dipoles each)	Phased array (CoCo) 180 antenna elements (14 dipoles each)
Aperture	142 m ²	169m ²	7.3m ²	142 m ²	142 m ²
Az./Elev. Scan rate	Not scanning	Not scanning	Not scanning	Not scanning	Not scanning
RF Power (kW)	Mean 2.4 kW	Mean 1.6kW	Mean 0.06kW	Mean 2.4 kW	Mean 2.4 kW
Transmitted	Peak 16.0 kW	Peak 16.0kW	Peak 0.8kW	Peak 16.0 kW	Peak 16.0 kW
RF Power (dB) Radiated (eirp)					
Frequency	482MHz	482MHz	1290MHz	482MHz	482MHz
Possible beams	3, 4 or 5	3, 4 or 5	3, 4 or 5 (15°)	3, 4 or 5	3, 4 or 5
No of beams used.	4	5	5	4	4
Beam width	3 degrees (approx)	3 degrees (approx)	6 degrees (approx)	3 degrees (approx)	3 degrees (approx)
Relative Gain (dBi)	34dBi	34dBi	26 dBi	34dBi	34dBi
Averaging Period	30 minutes	30 minutes	30 minutes	30 minutes	30 minutes
Pulse repetition freq		66 / 269 µs	35 µs	82 / 141 µs	66 / 183 µs
Pulse Width		1.7 / 8 x 3.3 µs	0.7 µs	4 x 1.7 / 4 x 3.3 µs	1.7 / 8 x 3.3 µs
IPP					
System Status	Installation planned in Summer 2005	Operational and Research NWP Assimilation + Nowcasting	Research.	Operational NWP Assimilation + Nowcasting	Operational NWP Assimilation + Nowcasting

ECC REPORT 90

Page 64

	Andenes	Karlsruhe	Hungriger Wolf
WMO Station No.	01012	Mobile	Mobile
Latitude / Longitude	69.28(N) / 16.03 (E)		
Station Height	0m		
Type of System	ALWIN Radar	IMKWTR	MPI-WTR
Antenna			
Aperture (metres)	2704m ²	10m ²	2.5m ²
Az./Elev. Scan rate	Not scanning	Not scanning	Not scanning
RF Power (dBW)	Mean 6.0kW	Mean 3.0kW	Mean 0.5kW
Transmitted	Peak 150kW	Peak 3.0kW	Peak 0.5kW
RF Power (dB)			
Radiated (eirp)			
Frequency	53.3MHz	1235MHz	1235MHz
Possible beams	?	?	?
No of beams used.	?	?	?
Beam width	6.5 degrees (approx)	4 degrees (approx)	8 degrees (approx)
Relative Gain (dBi)	+ 29dBi	+ 30dBi	+ 24dBi
Averaging Period			
Pulse repetition freq			
Pulse Width			
IPP			
System Status	Research	Research.	Research.

Table 28: Germany - Wind Profiler System Technical Information

	Budapest	Szeged
WMO Station No.	12843	12982
Latitude / Longitude	47.7(N) / 19.2 (E)	46.40(N) / 20.20 (E)
Station Height	139m	83m
Type of System	Degreane	LAP3000 (9 panel) Vaisala
Antenna	3 separate panels of 64 dipoles	1x Electrically steerable micropatch phased array formed by nine 0.87m x 0.87m antenna panels
Aperture	4m ²	7.3m ²
Az./Elev. Scan rate	Not scanning	Not scanning
RF Power (dBW)	Mean 0.35kW	Mean 19dBW (72W)
Transmitted	Peak 3.5kW	Peak 28dPW(600W)
RF Power (dB)/ Rad (eirp)		Mean 45dB/ Peak 54dP
Frequency	1290MHz	1290MHz
Possible beams	3	3, 4 or 5 (6°)
No of beams used.	3	?
Beam width	8.5 degrees (approx)	8 degrees (approx)
Relative Gain (dBi)	+ 25dBi	+ 29dBi
Averaging Period	30 minutes	30 minutes
Pulse repetition freq		
Pulse Width		
IPP		
System Status	System used for Forecasting	System used for Forecasting

Budapest**Szeged**

Regular data to WINPROF for NWP Assimilation

Regular data to WINPROF for NWP Assimilation

Table 29: Hungary - Wind Profiler System Technical Information

	L'Aquila	Rome	Torino
WMO Station No.	16228	16239	16300
Latitude / Longitude	42.42(N) / 13.65 (E)	41.83(N) / 12.64 (E)	45.40(N) / 7.40 (E)
Station Height	1000m	121m	277m
Type of System	LAP3000 (9 panel) Vaisala	Degreane VHF Radar	LAP3000 (4 panel) Vaisala
Antenna	1x Electrically steerable micropatch phased array formed by nine 0.87m x 0.87m antenna panels	Array of YAGI antennas	1x Electrically steerable micropatch phased array formed by four 0.87m x 0.87m antenna panels
Aperture (metres)	7.3m ²		4m ²
Az./Elev. Scan rate	Not scanning	Not scanning	Not scanning
RF Power (dBW)	Mean 19dBW (72W)		Mean 19dBW (72W)
Transmitted	Peak 28dPW(600W)		Peak 28dPW(600W)
RF Power (dB)	Mean 45dB		Mean 45dB
Radiated (eirp)	Peak 54dP		Peak 54dP
Frequency	1290MHz	65MHz	1290MHz
Possible beams	3, 4 or 5		3, 4 or 5 (15.5°)
No of beams used.	?		?
Beam width	8 degrees (approx)		8 degrees (approx)
Relative Gain (dBi)	+ 29dBi		+ 29dBi
Averaging Period			30 minutes
Pulse repetition freq			
Pulse Width			
IPP			
System Status	Research System Data to WINPROF for NWP Assimilation when operating	System for airport operations. Very little data received operationally	System used for pollution forecasting Data to WINPROF for NWP Assimilation when operating

Table 30: Italy - Wind Profiler System Technical Information**Cabauw**

WMO Station No.	06348
Latitude / Longitude	51.95(N) / 4.88 (E)
Station Height	0m
Type of System	LAP3000 (9 panel) Vaisala
Antenna	1x Electrically steerable micropatch phased array formed by nine 0.87m x 0.87m antenna panels
Aperture (metres)	7.3m ²
Az./Elev. Scan rate	Not scanning
RF Power (dBW)	Mean 19dBW (72W)
Transmitted	Peak 28dPW(600W)
RF Power (dB)	Mean 45dB
Radiated (eirp)	Peak 54dP
Frequency	1290MHz
Possible beams	3, 4 or 5 (15.5°)
No of beams used.	?

Cabauw

Beam width	8 degrees (approx)
Relative Gain (dBi)	+ 29dBi
Averaging Period	
Pulse repetition freq	
Pulse Width	
IPP	
System Status	Research System Data to WINPROF for NWP Assimilation when operating

Table 31: The Netherlands - Wind Profiler System Technical Information

Bilbao

WMO Station No.	n/a
Latitude / Longitude	43.37(N) / 3.03 (W)
Station Height	100m
Type of System	LAP3000 (9 panel) Vaisala
Antenna	1x Electrically steerable micropatch phased array formed by nine 0.87m x 0.87m antenna panels
Aperture (metres)	7.3m ²
Az./Elev. Scan rate	Not scanning
RF Power (dBW)	Mean 19dBW (72W)
Transmitted	Peak 28dPW(600W)
RF Power (dB)	Mean 45dB
Radiated (eirp)	Peak 54dP
Frequency	1290MHz
Possible beams	3, 4 or 5
No of beams used.	?
Beam width	8 degrees (approx)
Relative Gain (dBi)	+ 29dBi
Averaging Period	
Pulse repetition freq	
Pulse Width	
IPP	
System Status	Research System

Table 32: Spain - Wind Profiler System Technical Information

Kiruna

WMO Station No.	02043
Latitude / Longitude	67.88(N) / 21.10 (W)
Station Height	295m
Type of System	ATRAD VHF Radar
Antenna	Array of 144 YAGI antennas each 4m high
Aperture (metres)	2500m ²
Az./Elev. Scan rate	Not scanning
RF Power (dBW) / Transmitted	Mean 72kW
RF Power (dB) / Radiated (eirp)	
Frequency	52MHz
Possible beams	Various
No of beams used.	?
Beam width	8 degrees (approx)

Kiruna

Relative Gain (dBi)	+ 29dBi
Averaging Period	60 min
Pulse repetition freq	
Pulse Width	
IPP	
System Status	Research System Data to WINPROF for NWP Assimilation when operating

Table 33: Sweden - Wind Profiler System Technical Information

	Payerne	Zurich
WMO Station No.	06610	06670 (Temporary)
Latitude / Longitude	46.82(N) / 6.95 (E)	47.48(N) / 8.53 (E)
Station Height	491m	425m
Type of System	LAP3000 (9 panel)	LAP3000 (4 panel)
Antenna	Vaisala 1x Electrically steerable micropatch phased array formed by nine 0.87m x 0.87m antenna panels	Vaisala 1x Electrically steerable micropatch phased array formed by four 0.87m x 0.87m antenna panels
Aperture (metres)	6.8m ²	3.0m ²
Az./Elev. Scan rate	Not scanning	Not scanning
RF Power (dBW)	Mean 72W	Mean 50W
Transmitted	Peak 600W	Peak 450W
RF Power (dB)	Mean 45dB	43dB
Radiated (eirp)	Peak 54dP	52dP
Frequency	1290MHz	1290MHz
Possible beams	5 (15.5°)	5 (6°)
No of beams used.	3	3
Beam width	6 degrees	10 degrees (approx)
Relative Gain (dBi)	+ 29dBi	+ 26dBi
Averaging Period	30 minutes	30 minutes
Pulse repetition freq	25us typical	25us typical
Pulse Width	Low 291ns / high 1416ns	Adjustable 300 to 2800 ns
IPP	Low 23000ns / high 45000ns	Adjustable
System Status	Operational System Data to WINPROF for NWP Assimilation	Mobile System; Data to WINPROF for NWP Assimilation when operating

Table 34: Switzerland - Wind Profiler System Technical Information

	Camborne	Dunkeswell	Wattisham	Isle of Man	South Uist
WMO Station No.	03808	03840	03591	03203 (proposed from May05)	03023
Latitude / Longitude	50.22(N) / -5.32(-W)	50.87(N) / -3.23(-W)	52.7(N) / 0.058 (-W)	54.10(N) / -4.62 (-W)	57.21(N) / -7.22 (-W)
Station Height	88m	253m	87m	50m	4m
Type of System	LAP3000 (9 panel) Vaisala	LAP3000 (9 panel) Vaisala	LAP3000 (9 panel) Vaisala	LAP3000 (4 panel) Vaisala	LAP12000 Vaisala
Antenna	1x Electrically steerable micropatch phased array formed by nine	1x Electrically steerable micropatch phased array formed by nine 0.87m x 0.87m antenna	1x Electrically steerable micropatch phased array formed by nine 0.87m x 0.87m antenna	1x Electrically steerable micropatch phased array formed by four 0.87m x 0.87m	Array of 144 YAGI antennas each 2m high

ECC REPORT 90

Page 68

	Camborne	Dunkeswell	Wattisham	Isle of Man	South Uist
	0.87m x 0.87m antenna panels	panels	panels	antenna panels	
Aperture	7.3m ²	7.3m ²	7.3m ²	4m ²	1225m ²
Az./Elev. Scan rate	Not scanning	Not scanning	Not scanning	Not scanning	Not scanning
RF Power (dBW) Transmitted	Mean 19dBW (72W)	Mean 19dBW (72W)	Mean 19dBW (72W)	Mean 19dBW (72W)	Mean 37dBW
	Peak 28dPW(600W)	Peak 28dPW(600W)	Peak 28dPW(600W)	Peak 28dPW(600W)	Peak 50dPW
RF Power (dB)	Mean 45dB	Mean 45dB	Mean 45dB	Mean 45dB	Mean 65dB
Radiated (eirp)	Peak 54dP	Peak 54dP	Peak 54dP	Peak 54dP	Peak 78dP
Frequency	915MHz	1290MHz	1290MHz	915MHz	64MHz
Possible beams	3, 4 or 5	3, 4 or 5 (15.5°)	3, 4 or 5 (15.5°)	3, 4 or 5	3, 4 or 5
No of beams used.	3	3	3	3	4
Beam width	8 degrees (approx)	8 degrees (approx)	8 degrees (approx)	8 degrees (approx)	6.7 degrees (approx)
Relative Gain (dBi)	+ 29dBi	+ 29dBi	+ 29dBi	+ 29dBi	+ 30dBi
Averaging Period	30 minutes	30 minutes	30 minutes	30 minutes	30 & 15 minutes
Pulse repetition freq	3000 per second	3000 per second	3000 per second	3000 per second	2-10kHz
Pulse Width	0.7 µsec	0.7 µsec	0.7 µsec	0.7 µsec	1-4 µsec
IPP	23000ns low / 67000ns high	29000ns low / 97000ns high	23000ns low / 67000ns high	23000ns low / 67000ns high	193000ns low / 283000ns high
System Status	Operational	Operational	Operational	Planned to be operational June 05	Operational
	NWP Assimilation + Nowcasting	NWP Assimilation + Nowcasting	NWP Assimilation + Nowcasting		NWP Assimilation + Nowcasting
Aberystwyth					
WMO Station No.	03501			N/A	
Latitude / Longitude	52.42(N) / -4.00(-W)			52.42(N) / -4.00(-W)	
Station Height	50m			50m	
Type of System	MST Wind Profiler			Degreane	
Antenna	Array of 400 YAGI antennas			3 separate panels of 64 dipoles	
Aperture	12100m ²			4m ²	
Az./Elev. Scan rate	Not scanning			Not scanning	
RF Power (dBW) / Transmitted	Mean 0.06kW / Peak 160kW			Mean 0.35kW / Peak 3.5kW	
RF Power (dB) / Radiated (eirp)					
Frequency	45.5MHz			1290MHz	
Possible beams	12			3 (6°)	
No of beams used.	Various			3	
Beam width	3.3 degrees			8.5 degrees (approx)	
Relative Gain (dBi)	+ 36dBi			+ 25dBi	
Averaging Period	12 minutes			30 minutes	
Pulse repetition freq					
Pulse Width					
IPP					
System Status	Operational			Research	
	NWP Assimilation + Nowcasting			Based at Aberystwyth but mobile system	

Table 35: UK (Met Office) - Wind Profiler System Technical Information

ANNEX C: TEST CAMPAIGN UK (SUMMARY)

COMPATIBILITY & SHARING OF WIND PROFILER RADARS WITH THE RADIONAVIGATION SATELLITE SERVICE IN THE BAND 1270-1295MHZ MEASUREMENT – UK STUDY

1 TEST OUTLINE

To verify results of simulations, the both sets of measurements were first made with the WPR and Galileo frequencies and signal levels set to nominal.

To determine the effect of Galileo E6 signals on the WPR, the power level of the Galileo signal was varied from slightly above the nominal level, and reduced to the point where no impact on the recorded spectra could be seen. As part of this process the “interference off” condition was also measured for reference. Typical displays of the measurements were recorded, in both spectrum and contour format.

To determine the rejection of Galileo E6 signals needed to maintain WPR performance, the above results were analysed and summarised.

The next tests were aimed at evaluating the minimum shift in WPR frequency which would allow un-degraded WPR operation. As the WPR frequency is fixed by the manufacturers, the effect of moving the frequency of the WPR was simulated by altering the frequency of the Galileo interference and keeping the WPR frequency fixed instead. The WPR spectrum and the planned Galileo spectrum are shown below.

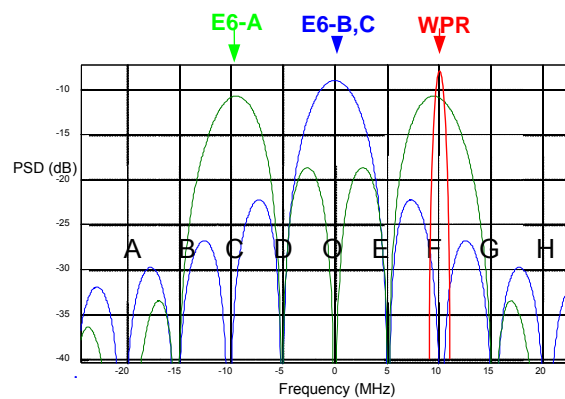


Figure 31: Galileo E6 and WPR Spectra

There are two components to the Galileo E6 spectrum, the PRS signal E6A (green) and the Commercial signal E6B,C (blue). These two components are in phase-quadrature, the PRS signal being I and the Commercial Q. Absolute Galileo frequencies are given in. Note the identification of the nulls, particularly E, G and H, which were chosen for tests as they represent attenuations between about 15dB and 30dB with respect to nominal interference, and cover tuning the WPR down as well as up in frequency.

FREQUENCY MHz	IDENT
1258.29	Null A
1263.405	Null B
1268.52	Null C (Commercial only)
1273.635	Null D
1278.75	Origin Centre frequency (Null in PRS)
1283.865	Null E
1288.98	Null F (Commercial only)
1294.095	Null G
1299.21	Null H

Table 36: Exact Galileo frequencies (no Doppler)

IDENT	WPR Offset from Galileo Centre (MHz)	Interference freq equivalent for 1290WPR (MHz)
No re-tune	+11.25	1278.75
Null E	5.115	1284.885
Null G	15.345	1274.655
Null H	20.460	1269.540

Table 37: Frequencies at which to inject re-tuned interference to simulate re-tuned WPR

The last test set measured rejection of nearby CW signals needed to maintain WPR performance. This was aimed at quantifying the effect of shifting the WPR frequency towards a non-Galileo interferer. The levels of “just visible” interference were measured at 1,2,3,5 and 10 MHz offset.

Throughout the measurement campaign the interferer was periodically switched off to allow the WPR to sample background, thus helping us to separate natural events from the effects of the Galileo signals.

WPR settings were adjusted according to the weather conditions so that the echoes were measurable.

It must be stressed that measurements made “in the real world” are not as deterministic and repeatable as those carried out under carefully controlled conditions in the laboratory.

2 DEGREANE WPR

2.1 The Degreane 1300 WPR

The WPR was sited in an open area with all three antennas having a clear view of the sky. The WPR was then levelled using the built-in spirit levels, and the side antennas were deployed with bore-sight at 12° from zenith, as shown in Figure 32.



Figure 32: WPR deployed

The geometry of the Galileo constellation is such that only one WPR beam can contain a satellite.

2.2 Interpreting the WPR Outputs

The WPR output can vary substantially from moment to moment, both due to transient weather phenomena, and external disturbances such as birds. In normal operation the outputs of many sweeps of the WPR are combined to make averages of 15 or 30 minute blocks of data, and a consensus algorithm rejects results that are too different from the rest of the samples taken.

2.3 The Simulated Galileo signal

The test system consists of an RF signal generator with provision for high speed vector modulation (Rhode Und Schwarz SMIQ), the phase and amplitude of which are modulated by a pre-calculated waveform stored in a large buffer arbitrary waveform generator (Rhode Und Schwarz AMIQ). This is pre-loaded with a Galileo-like signal which can be switched on or off at will. Because the final Galileo signal format was still not finalised at the time of tests, and contains some components that do not repeat for many hours, a ‘cut-down’ version of the signal was produced, containing those components that are known, and with the sequence “11111...” multiplied by the correct spreading sequences, for those data components yet to be defined. This pre-calculated data is simply produced as an endless loop, and the repetition rate is ~10Hz. During the test the power of the Galileo signal was increased in 5dB steps, from 10dB below to 10dB above the nominal service level, incrementing at 15 minute intervals. The nominal level of Galileo signal used during the UK tests was approximately +2dB on the currently defined Galileo signal levels. This change was due to an update in Galileo characteristics by the European Commission.

2.4 Measurement results

2.4.1 Presentations

By adjusting the software settings this data can be re-presented using colours to indicate signal to noise ratio instead of wind speed. When plotted this way the deterioration of signal to noise ratio with increasing Galileo level can be illustrated. This is shown in Figure 33 and Figure 34 below, where the rise in noise from around 16:00 onwards is quite marked, more so in the short pulse data.

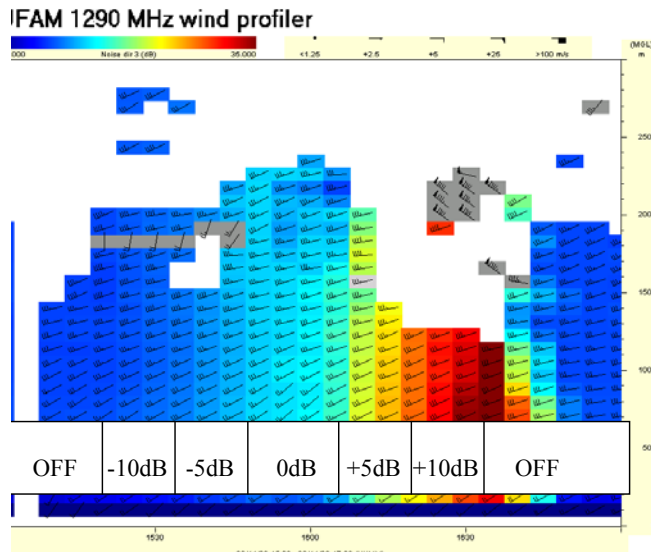


Figure 33: Noise levels, short pulse setting

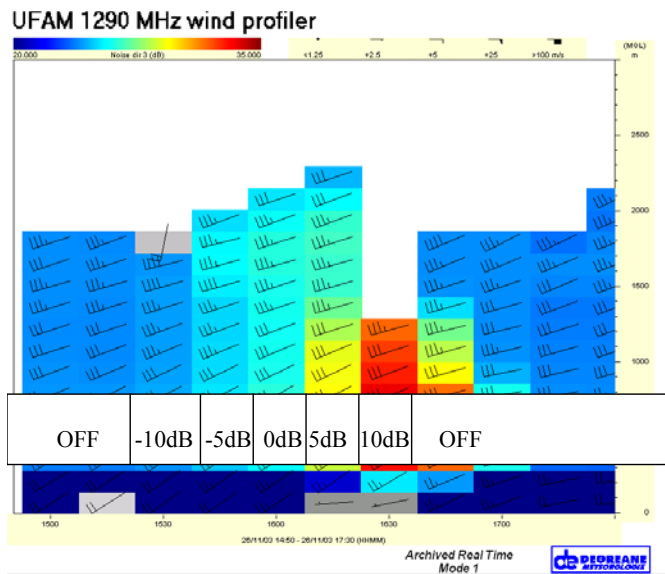


Figure 34: Noise levels, long pulse setting

This confirms that on average the noise floor is noticeably increased, and recovers its original values once the interference is switched off.

2.4.2 WPR at Null E

To mimic the effect of re-tuning the WPR, the simulated Galileo signal was re-tuned, so that the WPR signal fell into null E. In a final system this would be equivalent to re-tuning the WPR to a frequency of 1283.865MHz. As before, the signal level was ramped in 5dB steps from 10dB below to 10db above nominal level, see below.

The spectral plots of the WPR and Interferer for this test are shown below.

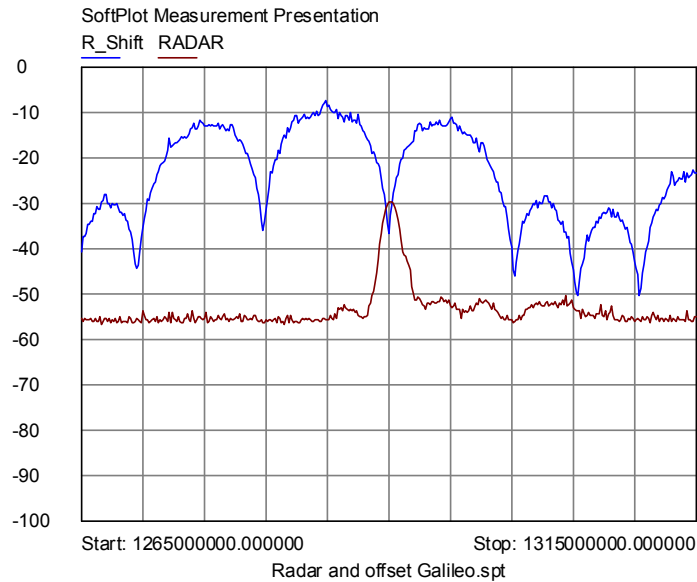


Figure 35: Spectrum of WPR and interferer tuned to Null E

2.4.3 Degreane WPR Test Conclusions

A complete set of measurements has been performed, which may be considered a representative ‘snapshot’ of events, given the variability of the natural environment. A great many measurements would be needed to fully characterise the impact of Galileo on WPR performance under all conditions. The results that have been collected show the following.

- If no action is taken WPR useful range will be reduced – although the impact varies with the beam chosen and the detail of software settings.
- Re-tuning the WPR is a possible solution, but the following points must be borne in mind.
- Placing the WPR in null G between the Commercial and PRS components of the Galileo signal gives no discernable degradation even with the interferer 10dB above nominal. This necessitates retuning the WPR.
- Placing the WPR at least 20MHz away from the Galileo centre frequency will reduce the impact to below detectable, even at 10dB above the nominal interference level.

During the tests some coherent signal were noticed due to the limitations of Galileo Pseudorandom code repetition and caused an artificial artefact during WPR analysis of its received data; the artefact in the raw data was sufficiently wind-like to cause the software to mark it as good data even when the WPR was placed in null E between the Commercial and PRS components of the Galileo signal. With purely incoherent interference, this effect did not appear.

3 VAISALA WPR

3.1 The Vaisala LAP3000 WPR

The large square skip-like structure is an absorptive clutter screen, which surrounds the flat panel array antenna. The multiple beam directions are synthesized by phase shifting the corporate feed network of a rectangular antenna array.



Figure 36: Vaisala WPR and instrument compound at Dunkeswell

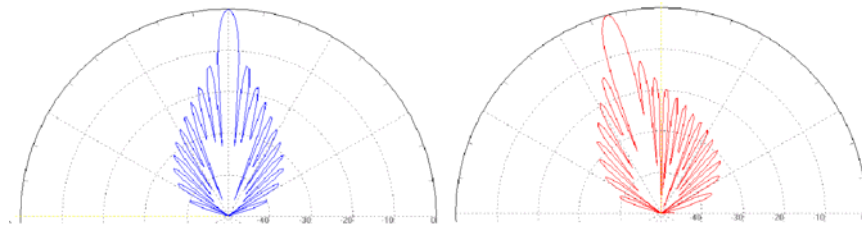


Figure 37: Vaisala modelled WPR antenna patterns at 1290 MHz

3.2 Interpreting the WPR Outputs

The output of WPR's can vary substantially from moment to moment, both due to transient weather phenomena, and external disturbances such as birds. In normal operation the outputs of many sweeps of the WPR are combined to make averages of typically 30 minute blocks of data, and a consensus algorithm rejects results that are too different from the rest of the samples taken.

3.3 Measurement Results

3.3.1 Nominal conditions

During the test the power of the Galileo signal was generated at nominal level. In the following figures, the blue lines are the Doppler spectra of each altitude measured, with the centre representing no Doppler shift, and the right representing an echo from an object approaching the WPR, and the left representing a receding echo. The x-axis is then velocity towards or away from the antenna array in m/s, and the Y axis is altitude in metres above sea level. The amplitudes of the spectra themselves is normalised by an internal algorithm, so the traces become noisier at high altitudes when the echoes are weaker.

The strong central signal for the first few hundred metres may be ground clutter within a short distance of the WPR, although the deviation to the left may mean the air has a small velocity. The red marks indicate that the software has identified these features and is tracking them as peaks. The vertical traces at the right of the plots are the noise floor, and signal itself. The second type of output available from the Vaisala software is the "contour" data. A typical plot is shown below. Once again the X axis represents wind speed, while the Y axis is altitude.

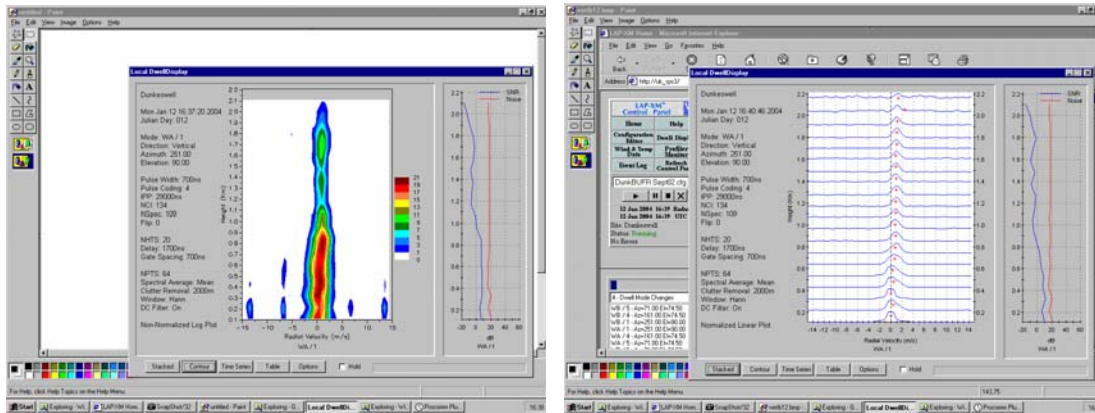


Figure 38: Echo spectra without interference

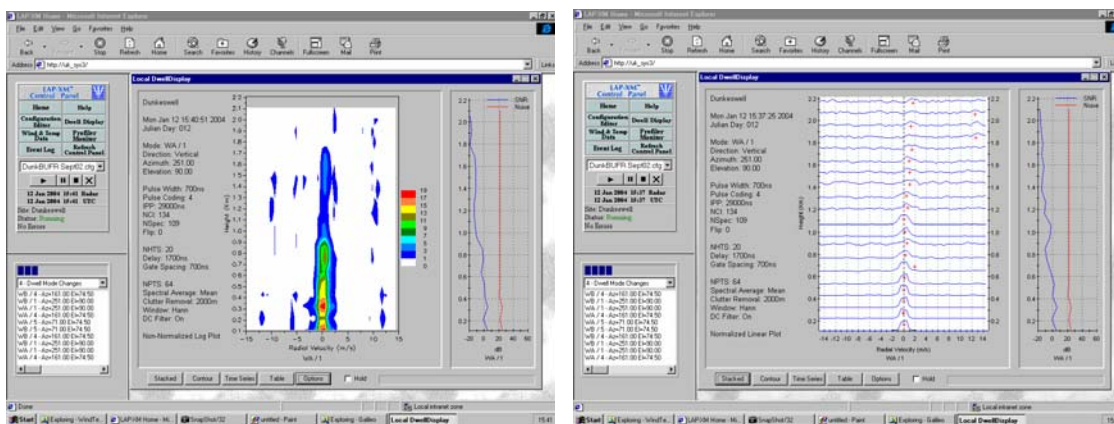


Figure 39: Echo spectra with nominal level Galileo interference

These show results when short pulse settings were used. The increased ‘streaking’ of the averaged contour plot is evident, as is the noisier nature of the higher altitude traces. Comparing the contour displays, we see that the effective range is reduced from 2.1km to 1.75km, about 17%.

On average the noise floor is noticeably increased, and recovers its original values once the interference is switched off. The overall effect of the interference will be most marked in those conditions when the WPR would have been working near the limit of its sensitivity, less so when the echoes are clear and strong. It is for meteorologists to indicate if such degradation is likely to be acceptable or not.

As an additional test, data was captured as the interfering signal was ramped down in 2dB steps until the ‘streaking’ effect on the contour traces was un-noticeable. This required a reduction of 10 to 12dB from the nominal level. On the last day, this experiment was repeated, with an additional refinement, that the data content of the signal was varied, to compare the effect of a repetitive transmission with a more scrambled one. Unsurprisingly the repeated data version is more troublesome than the random, although only by ~2dB. In real operation the signal is likely to be somewhere between these extremes.

3.3.2 WPR at Null E

To mimic the effect of re-tuning the WPR, the simulated Galileo signal was re-tuned, so that the WPR signal fell into null E. In a final system this would be equivalent to re-tuning the WPR down to a frequency of 1283.865 MHz. Although previous measurements with the Degreane WPR in this null had been unsatisfactory, the results with the Vaisala were relatively good. Placing the WPR in this notch with the Galileo signal at nominal levels produced a practically interference free signal from the WPR, with no evidence of the type of artefacts seen with the other WPR.



Figure 40: Spectrum of WPR and interferer, WPR at null E

The contour short pulse data, without interference and with interference, is shown in Figure 41 and Figure 42.

The level of interference was increased until interference effects on the traces were just seen, and this occurred at about 5dB above the nominal level for the short pulse mode, although the long pulse mode remained unaffected until the level was raised a further 3 or 4 dB. This may be due to the greater spectral width of the short pulse mode, causing more of the adjacent signals to be folded in with the wanted signal, although this assumes the receiver bandwidth is altered in sympathy with the pulse length.

In summary, to re-tune the WPR to this notch would give at least 5dB of protection with respect to the nominal Galileo level, or the signal from the satellites would have to be 5dB higher than nominal for interference artefacts in the lowest contour level (dark blue in this example) to be seen.

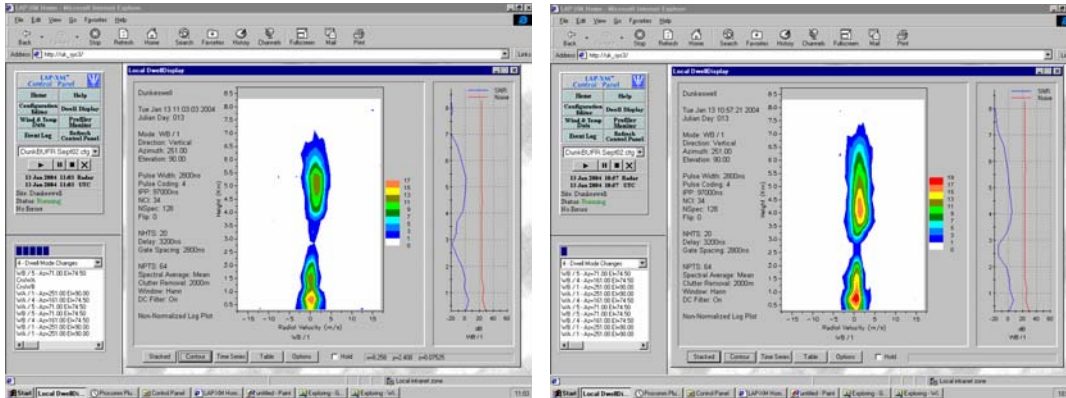


Figure 41: Contour Plots, WPR at null E, short pulse, interferer off and at nominal level

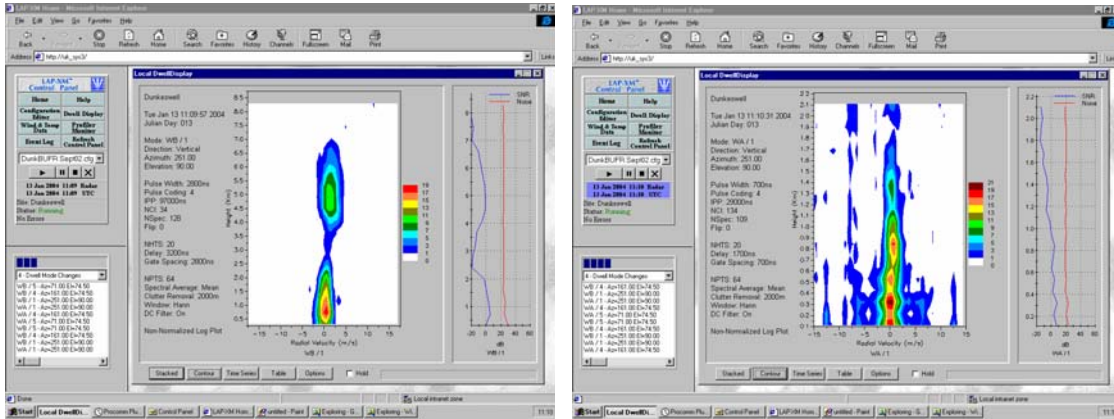


Figure 42: Contour Plots, WPR at null E, long pulse, interferer off and 5dB over nominal level

3.3.3 WPR at Null G

Null G was investigated as an alternative frequency nearby, although one that would require tuning the WPR up in frequency, as opposed to down. Results are shown in Figure 43 and Figure 44. Once again at nominal levels, or even a few dB higher, no interference could be detected.

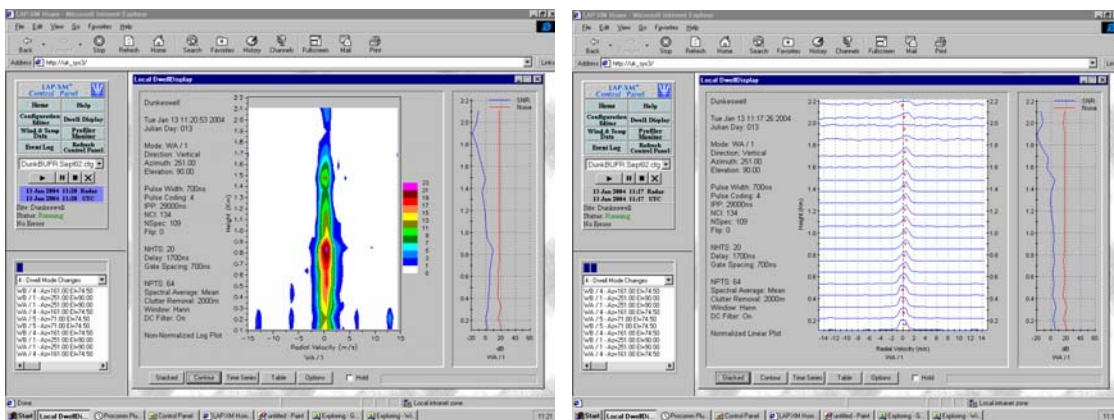


Figure 43: Interference at nominal level, WPR in null G, short pulse, vertical beam

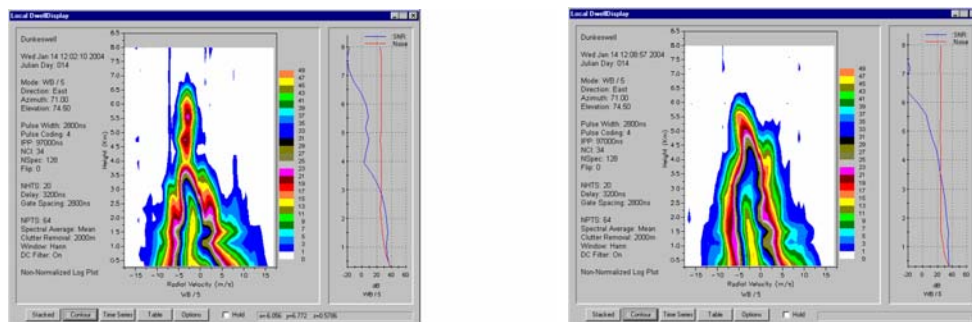


Figure 44: WPR at null G, data at nom+18dB, and pseudo-random data at nom+20 dB

In summary, null G offers at least 18dB of protection against signals at the expected Galileo level, before signals are even noticeable. This null would be a safe frequency to which to re-tune the WPR, and be confident of no further disruption when Galileo is activated.

3.3.4 WPR at Null H

Null H was investigated because it was significantly deeper than the others and has less energy in adjacent spectral lobes. As with null G with the Galileo signal at or slightly above nominal level, no interference could be detected at all, despite repeated measurements. A similar process suggests that the protection offered by this null is at least 15dB, but these measurements have an uncertainty of a few dB caused by changeable weather on the day of measurement.

3.3.5 Tests with Other Pulse Lengths at Nominal Frequencies

The WPR pulse length settings described in the above tests were the ones used by the Met office. Other settings are available, so tests to see how much the interference needs to be reduced to fall below detection were repeated for different pulse lengths. These are summarised in Table 5 below.

Pulse duration	Range gate length	Reduction from nominal to eliminate (dry)	Reduction from nominal to eliminate (wet)
500nS	60m	12 to 14 dB	Not measured
700nS	100m	9 to 10dB	10 to 12dB
1400nS	200m	~12dB	Not measured
2800ns	400m	10dB to 12dB	12dB to 14dB

Table 38: Interference attenuation required for various WPR pulse lengths

Generally, it seems reasonable to assume that changing the pulse length setting has no more effect than the variation caused by fluctuations in the weather conditions, and there is little to be gained by changing pulse lengths.

3.4 Vaisala WPR Test Conclusions

A comprehensive set of measurements has been performed, which may be considered a representative ‘snapshot’ of events, given the variability of the natural environment. A great many measurements would be needed to fully characterise the impact of Galileo on WPR performance under all conditions. The results that have been collected show the following.

- If no action is taken WPR useful range will be marginally reduced – although the impact varies with the beam chosen and the detail of software settings.
- Re-tuning the WPR is a possible solution, but the following points must be borne in mind. If the WPR can only be tuned by ½% then it may be possible to use null G or null E. Null G provides satisfactory protection for the Vaisala WPR ~18dB, and Null E, perhaps 5dB. Placing the WPR in the third null (H) between the Commercial and PRS components of the Galileo signal gives no discernable degradation even with the interferer 15dB above nominal. This necessitates retuning the WPR by 1%.
- Placing the WPR at least 20MHz away from the Galileo centre frequency will also reduce the impact to below detectable, even at ~20dB above the nominal interference level.

4 SUMMARY

This report comprises the results of investigations into the effect of proposed Galileo satellite emissions on Wind Profiling Radars (WPR’s). Its primary focus was on the UK, but European issues were also considered. The investigation was in the form of a simulation study, measurements on two WPR’s from different manufacturers, and a study of mitigation techniques. The main conclusions are as follows.

At latitudes above about 60 deg N, mitigation may not be needed, but within the UK some interference effects will be seen. These may be mitigated by re-pointing the antenna and modifying the software, but will involve a small reduction in range. If this is not tolerable, a higher cost solution involving re-tuning the WPR by 0.5 to 1.0% should be considered.

Changing the pulse length of the WPR output had little mitigation effect. There is little to be gained by changing pulse lengths.

The Mitigation showed that above 60N no mitigation will be necessary. From 60N to 60S about 12dB some interference suppression or mitigation will be needed. For the UK, this may be achieved by re-pointing the antenna subassembly, and minor software changes. South of the UK, other alternatives such as additional antenna beams, polarisation changes, new operating frequencies or interference cancellers should be used.

ANNEX D: TEST CAMPAIGN GERMANY (SUMMARY)

WPR-GALILEO E6 (RNSS) COMPATIBILITY MEASUREMENT REPORT -D STUDY

1 OBJECTIVES OF THE GERMAN COMPATIBILITY TESTS

Changes in the definition of the Galileo E6-signal in the frequency band 1260-1300MHz made it necessary to revisit measurements that were performed in the UK-campaign. To achieve generic results on the compatibility it was important to apply the latest baseline version of the Galileo-signal as well as to ensure that the generated E6-signal was not degraded by performance constraints of the used signal generator.

In addition, the German Weather Service as the owner of the operational radar enabled to inject the signal directly into the radar receiver, thus avoiding ambiguities of an RF-coupled signal through a separate test antenna. The used test architecture shown in Figure 45 allowed injecting equivalent RF power level to precisely simulate various potential interference conditions. The system as well as the corresponding power level shown were verified prior the measurements.

The tests performed comprised investigations of potential coherent and incoherent (noise) impacts on the WPR under normal operating conditions and the investigation of interference mitigation options to be applied when higher protection is required e.g. in case of scientific investigations.

2 TEST SET-UP

2.1 Test system architecture and level diagram

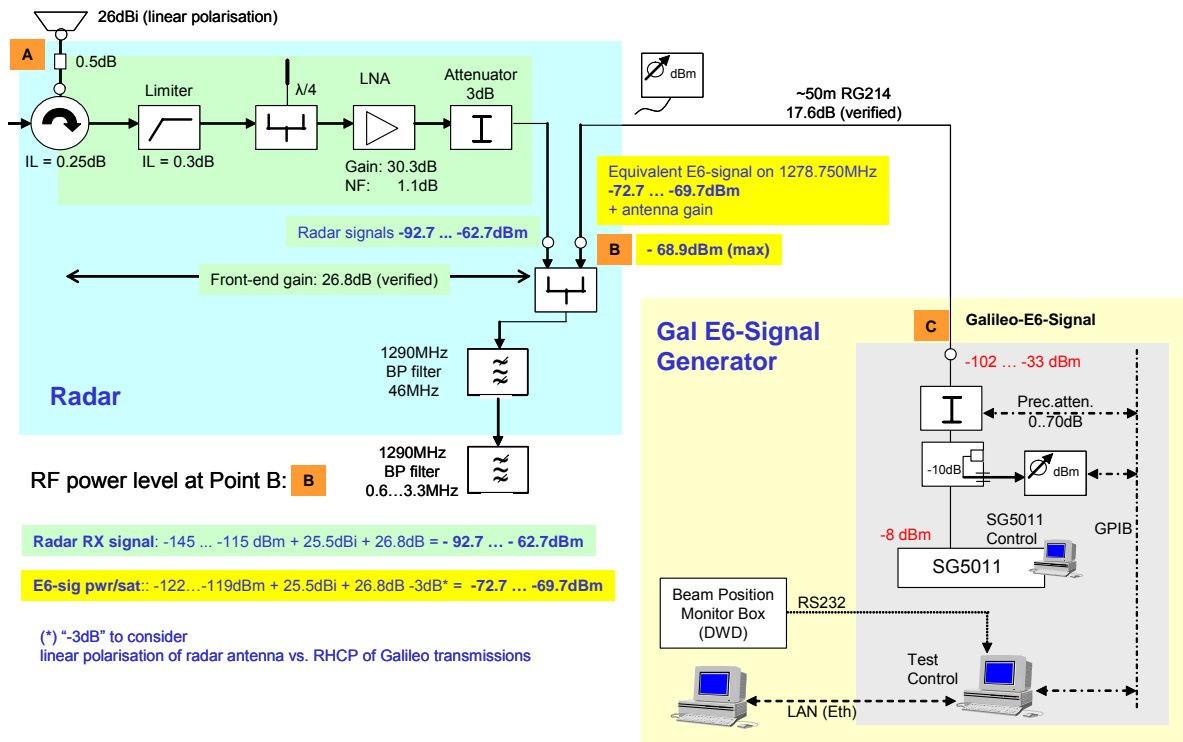


Figure 45: Test architecture and representative power level

2.2 The new baseline Galileo E6-signal

The latest baseline definition of the Galileo E6-signal requires a different implementation of the Binary Offset Coded signal scheme for the transmission of the PRS-component (BOC(10,5)). This can be implemented in two options: sin and cos. The mathematical expression for the BOC_{\sin} is:

$$G_{BOC(f_s, f_c)}(f) = f_c \cdot \left[\frac{\sin\left(\frac{\pi \cdot f}{2 \cdot f_s}\right) \cdot \sin\left(\frac{\pi \cdot f}{f_c}\right)}{\cos\left(\frac{\pi \cdot f}{2 \cdot f_s}\right) \cdot (\pi \cdot f)} \right]^2$$

with

- f = Carrier frequency
- f_s = sub-carrier frequency
- R_c = Chip rate

This signal characteristic was used in the first series of tests performed by the UK. The new Galileo baseline, however, specifies the "cosine"-alternative for the PRS-component of the E6-signal which is described by

$$G_{BOC_{\cos}(f_s, f_c)}(f) = \frac{1}{f_c} \left(\frac{1 - \cos\left(\frac{\pi \cdot f}{2f_s}\right)}{\pi \cdot f \cdot \cos\left(\frac{\pi \cdot f}{2f_s}\right)} \cdot \sin\left(\frac{\pi \cdot f}{f_c}\right) \right)^2, \frac{2f_s}{f_c} \text{ even}$$

$$G_{BOC_{\cos}(f_s, f_c)}(f) = \frac{1}{f_c} \left(\frac{1 - \cos\left(\frac{\pi \cdot f}{2f_s}\right)}{\pi \cdot f \cdot \cos\left(\frac{\pi \cdot f}{2f_s}\right)} \cdot \cos\left(\frac{\pi \cdot f}{f_c}\right) \right)^2, \frac{2f_s}{f_c} \text{ odd}$$

The $BOC_{\cos}(10,5)$ -signal is multiplexed with a BPSK(5) signal for the Galileo Open Service (OS) signal as defined by:

$$G_{BPSK(R_c)}(f) = \frac{1}{R_c} \cdot \sin^2\left(\frac{f}{R_c}\right)$$

All components of the multiplex are permanently transmitted simultaneously. The consideration of using spectral nulls in the E6-signal for alternative WPR carrier frequencies has to keep this in mind.

A direct comparison of the distribution in spectral power density between a BOCcos and a BOCsin is shown in Figure 46.

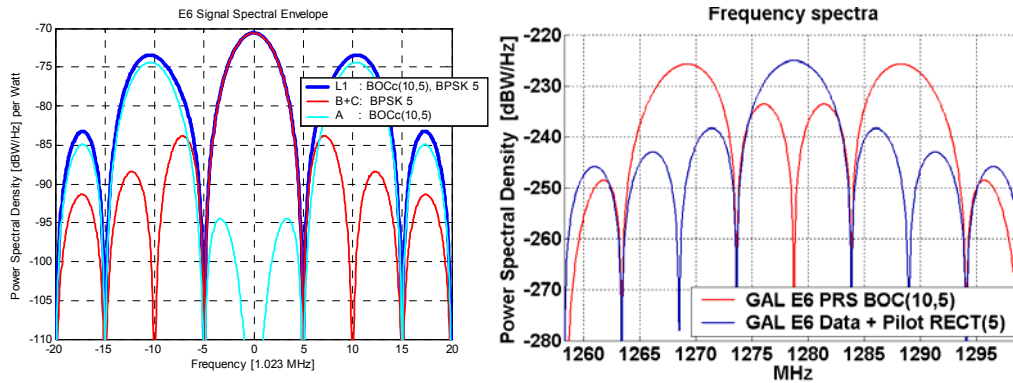


Figure 46: Comparison of BOCcos vs. BOCsin

2.3 E6-signal generator

A newly designed and manufactured Galileo signal generator (NSG5011) provides an authentic Galileo E6 signal. The design allows a maximum flexibility regarding modulation schemes, code types and code length as well as data rates for the dissemination of the navigation message. The primary and secondary PRN-codes are stored in buffers. They can be loaded and configured in a second cycle process. The maximum code lengths are 32768 chips for the primary and 200 chips for the secondary code. The real codes are adjustable to any integer value between 1 and the maximum code length.

The modulation of the E6 data channels will be done by look-up tables. These tables are memory based and user reconfigurable, the modulation schemes can therefore be changed if necessary.

3 TEST RESULTS

3.1 Test schedule

All measurement results together with test conditions were recorded with time tags as scenes (Take), similar to a movie production as listed in Table 39.

Measurement	Time/ UT	Date	File	TX	E6-pwr @ B	Remarks
Take #1	10:00-11:15	14.12.05	1.3MB	OFF	-56,5dBm	Impact of coherent interference
Take #2	11:18-13:54	14.12.05	5.3MB	OFF	-46,5dBm	coherent
Take #3	14:02-15:29	14.12.05	3.3MB	OFF	-64,5dBm	coherent
Take #4	15:34-23:59	14.12.05	19.6MB	ON	No E6 injected	coherent
Take #5	00:00-12:45	15.12.05	29.9MB	ON	-68,9dBm (max E6 pwr)	coherent and nav data "on-off" test
Take #6	12:54-13:05	15.12.05	0.4MB	OFF	No E6 injected	
Take #7	13:36-14:46	15.12.05	2.9MB	OFF	-32.65 to -102.65dBm	Impact of <u>in</u> coherent interference with automated level setting
Take #8	14:53-15:11	15.12.05	0.7MB	OFF	-82,65 to 93,65dBm	
Take #9	15:14-16:00	15.12.05	1.8MB	ON	-68,9dBm (max E6 pwr)	coherent
Take #10	16:03-23:59	15.12.05	19.4MB	OFF	-32.65 to -102.65dBm	<u>In</u> coherent with long-term wind profiling
Take #11	00:00-09:48	16.12.05	23.6MB	OFF		
Take #12	10:11-10:31	16.12.05	0.8MB	OFF	-62,65 to -83,65dBm	<u>in</u> coherent with automated Level setting and pw = 2800ns
Take #13	10:45-13:36	16.12.05	22.3MB	OFF	-32.65 to -102.65dBm	<u>in</u> coherent with automated Level setting and pw = 300ns
Take #14	13:47-14:59	16.12.05	2.9MB	OFF	-32.65 to -102.65dBm	<u>in</u> coherent with automated Level setting and pw = 1400ns
Take #15	13:44-15:43	20.12.05	4.9MB	ON	-32.65 to -102.65dBm	TX off from 10:05h - impact of mitigation at Null 1 (fo+5MHz)
Take #16	16:07-23:59	20.12.05	19.2MB	OFF	-78.65 to -102.65dBm	<u>in</u> coherent with automated Level

Measurement	Time/ UT	Date	File	TX	E6-pwr @ B	Remarks
Take #17	00:00-08:23	21.12.05	20.4MB	OFF		setting and pw = 300ns
Take #18	09:06-10:19	21.12.05	2.9MB	OFF	-32.65 to -102.65dBm	incoherent with automated Level setting and pw = 2800ns
Take #19	10:20-10:23	21.12.05	0.1MB	ON	-68,9dBm (max E6 pwr)	verify Null 1 and 2
Take #20	10:25-11:55	21.12.05	3.7MB	OFF	-32.65 to -102.65dBm	incoherent with pw = 300ns at Null 2 (fo+10MHz)
Take #21	12:24-12:33	21.12.05	0.4MB	ON	No E6 injection	Normal wind profiling
Take #22	12:46-13:04	21.12.05	0.8MB	OFF	-68,9dBm (max E6 pwr)	Injection of WPR SMIQ; new method for radar calibration
Take #23	13:15-23:59h	21.12.05	25.0MB	ON	-68,9dBm (max E6 pwr)	Normal wind profiling

Table 39: List of measured sequences (Takes)

3.2 Tests performed

3.2.1 Overview

TEST	Objective	Associated Takes #	Remarks
A	Verification of Test Set-up	None	
B	Impact of coherent noise interference onto radar	1, 2, 3, 4, 5, 9	Confirming no impact of coherent noise
C	Impact of incoherent noise interference (coloured noise)	7, 10, 11, 12, 13, 14	Showing impact of noise in contour plots
D	Variable radar parameter	13, 14, 17, 18, 21, 22, 23	Coherent and incoherent tests
E	Options for interference mitigation	15, 16, 17, 18, 20	

Table 40: List of Test Cases considered

3.2.2 Test A: Verification of test set-up

The total gain of radar receiver front-end was verified with the values in Table 41. This leads to the determination of the equivalent power level that the E6-signal would generate at the injection point B in Figure 45. Note that the y-axis in all following level diagrams provides "estimated noise level" in dB. This parameter reflects the varying system noise conditions of the radar front-end as well as the sky noise and the contributions of the added E6-signal power.

Element	Gain and Losses	Remarks
Antenna gain	26.0 dBi	Boresight gain. Side lobes are partially considered (only the first three, otherwise gain < -96dBm).
Antenna cable	- 0.50 dB	Feed to circulator
Circulator	- 0.25 dB	
Limiter	- 0.30 dB	
$\lambda/4$ - Stub	0.00 dB	LNA overload protection
LNA	30.30 dB	slightly different value to the first phase because the former LNA had to be replaced after a lightning strike in summer 05
Attenuator	- 3.00 dB	
Total gain (RF front-end)	26.8 dB	Verified over a bandwidth of 40MHz
Total gain including antenna gain	52.8 dB	

Table 41: Determination of the WPR front-end gain performance

The overall gain of the first receiver stage including the antenna is thus +52.3 dB, which is in good agreement with theoretical values. An E6 power level at the antenna input of - 122 dBm would thus translate to an input level at point B (the two-way combiner) of - 69.7 dBm. Similarly, the contributions of all relevant elements of the E6-signal injection path were determined.

3.2.3 Test B: Impact of coherent noise interference onto radar

With this test, the potential impact is measured that coherent signal interference might create (false alarm probability). This test analyses a potential signal interference of the Galileo signal with the radar consensus calculations.

Take #	E6 Pwr @ B [dBm]	Time	Remarks
1	-56.5dBm (1) -65.5dBm (2) -46.5 dBm (3) -36.5 dBm (4)	10:00 – 11:05	Heavy overload condition; in comparison: the nominal level of the E6 at point B is -72.9dBm
2	-46.5dBm	10:35 – 11:04	E6 level constant but changes in radar setting; testing of different test conditions. Results are to be taken with care.
3	-64.5 dBm (1) -56.5 dBm (2)	14:02 - 15:29	
4	No E6	15:34 - 23:59	
5	-68.9dBm		Nominal E6 after 09:00h showing impact of data on signal
9	-68.9 dBm	15:15 - 15:30	Determining impact of coherent noise

Table 42: Test conditions for "coherent" noise investigations

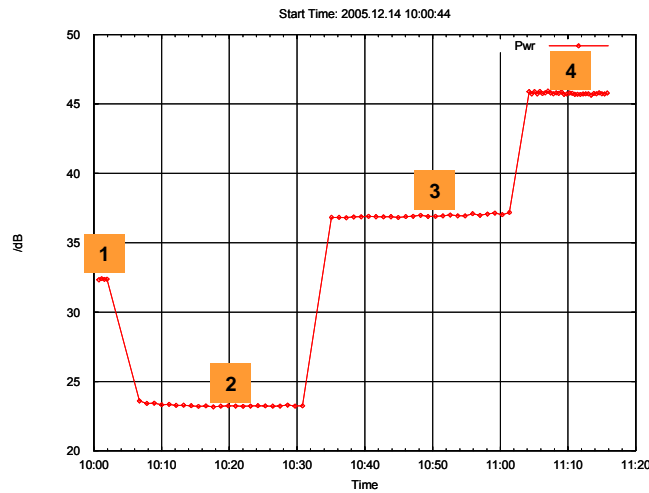


Figure 47: Take #1 - radar noise level including E6 over time

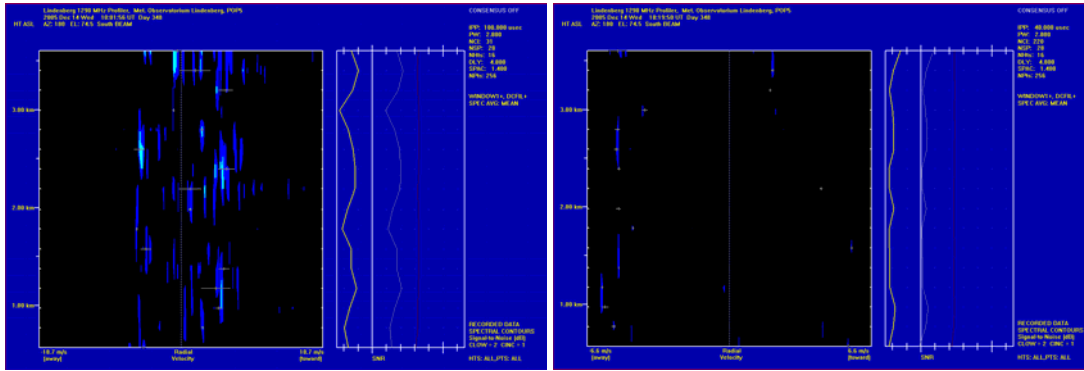


Figure 48: Take#1: -56dBm @ 10:01h (1) and -65dBm @ 10:20h (2)

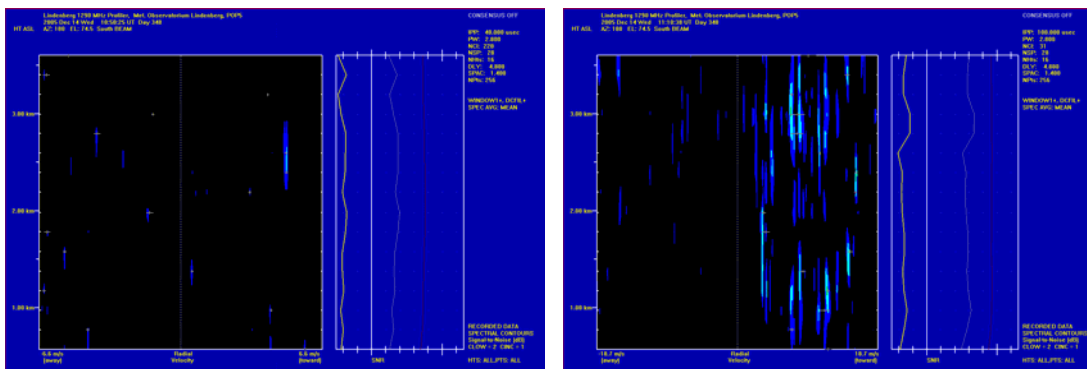


Figure 49: Take #1: -46dBm @ 10:50h (3) and -36dBm @ 11:10h (4)

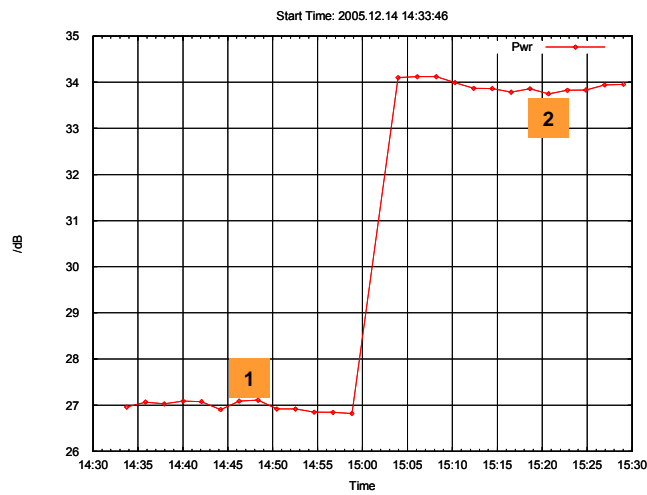


Figure 50: Take #3 - radar noise level including E6 over time

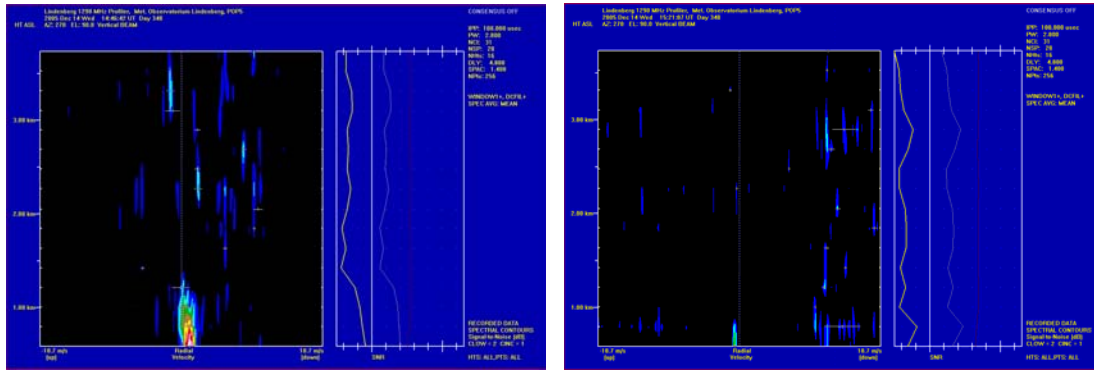


Figure 51: Take #3: -64dBm @ 14:46h (1) and -56dBm @ 15:21h (2)

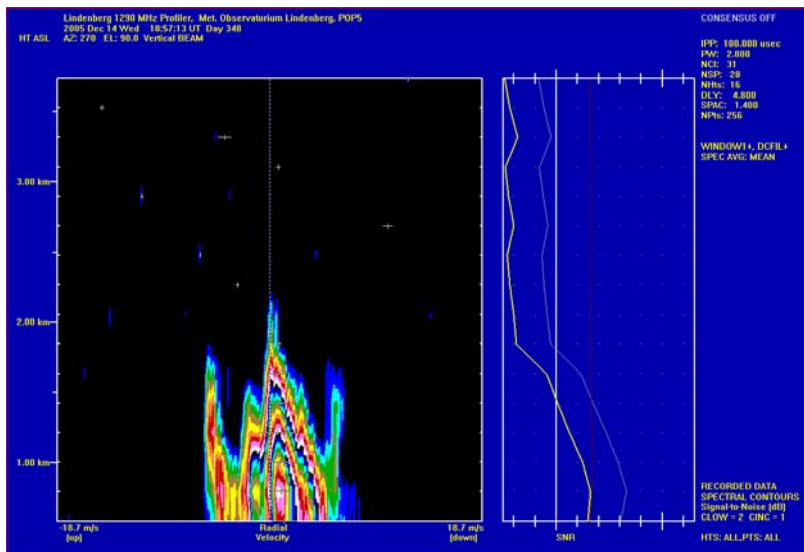


Figure 52: Take #4: Vertical beam with no E6-signal @ 18:57h

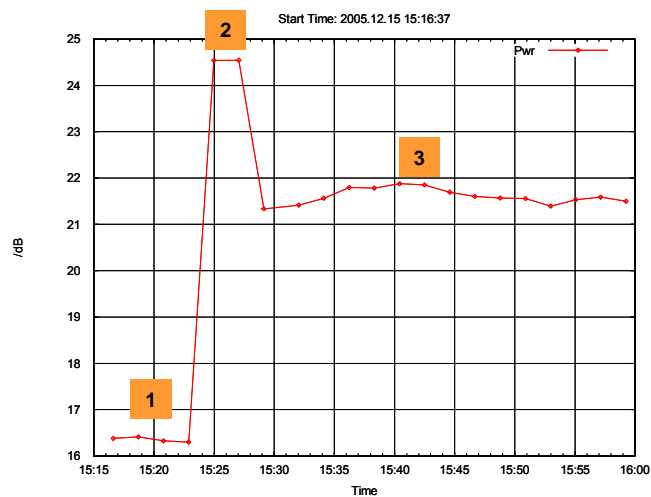


Figure 53: Take #9 - radar noise level including E6 over time

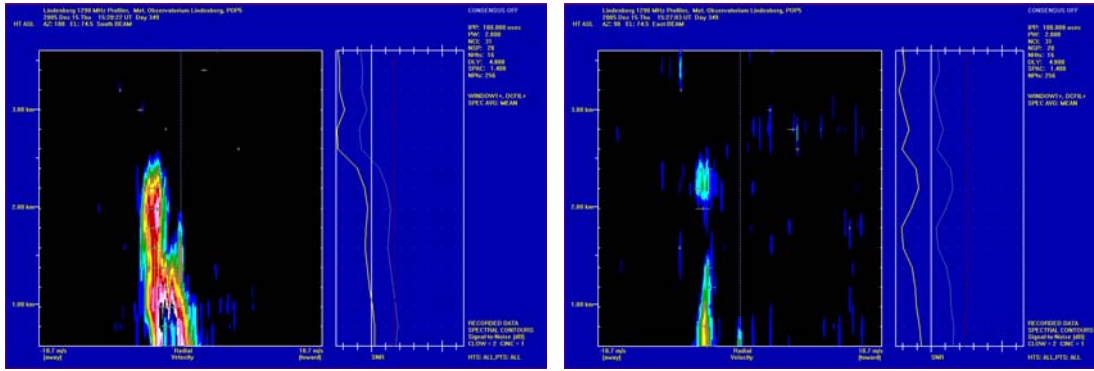


Figure 54: Take#9: -69dBm @ 15:20h (1) and -61dBm @ 15:27h (2)

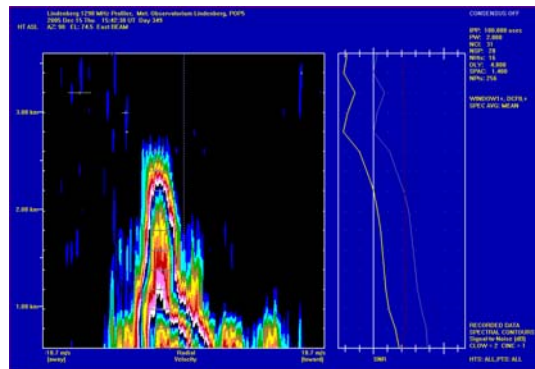


Figure 55: Take#9: -64dBm @ 15:42h (3)

Changes in radar noise performance can be observed even when E6-signal injection was kept at a constant level. This is due to changes in radar system noise and weather observations (sky noise contributions).

In conclusion it can be said, that the wind profiling process performs nominal and no detrimental observations are visible in the recordings. The signal shape of the Galileo transmissions has no degrading impact on the WPR consensus process.

The E6-signal comprises a BPSK(5)-component for Galileo's so-called "Commercial Service (CS)". It is important that the data messages disseminated through CS are at no time patterns with a strong DC-component. It must be ensured that at no time all zeros or all ones are transmitted. The resulting discrete lines in the signal spectrum can have a coherent impact on the consensus processor.

3.2.4 Test C: Impact of incoherent noise interference (coloured noise)

The test with excessively high power of the E6 signal was performed as shown in Table 43.

Take #	E6 Pwr @ B [dBm]	Time	Remarks
7	-32.7 dBm to -102.7dBm	13:30	-1dB and 9dB steps; transient at 13:46h caused by switching attenuator
10	-32.7 dBm to -102.7dBm	16:03	
11	-102.7dBm	00:00	Minimum E6-signal over time
12	-62.7 dBm to -83.7dBm	10:11	-1dB and 9dB steps;
13	-32.7 dBm to -102.7dBm		-1dB and 9dB steps; transient at 11:00h caused by switching attenuator
14	-32.7 dBm to -102.7dBm		

Table 43: Test conditions for "incoherent" noise investigations

No distinct coherent response (DCR) of the WPR was found with the used parameter settings. However, the noise level of the profiler was significantly raised compared to the undisturbed case, which clearly is a manifestation of the incoherent response (ICR) of the WPR to the E6 signal.

This result was expected and confirmed the results of the first phase. One major objective for the second phase was therefore to determine the limiting case, i.e. which is the maximum E6 power level that leads to virtually no increase in the profiler noise level. Below that power level, the E6 signal is invisible to the WPR.

Another test was made in the afternoon of the same day, to qualitatively estimate the effects of such excessively high signals on the wind measurements:

It can be seen that the increase in the noise level is accompanied by a decrease in height availability of the WPR. If the noise level exceeds a certain limit, no wind measurements are possible. Note that

- the used E6 power levels are excessively high (the expected maximal power level at point B in reality is ~ - 69 dBm , and thus at least 4.5 dB smaller)
- a quantitative estimation of the incoherent effect on profiler height availability would need to take the high variability of the atmospheric backscattering conditions into account. These can vary over several orders of magnitude within one hour

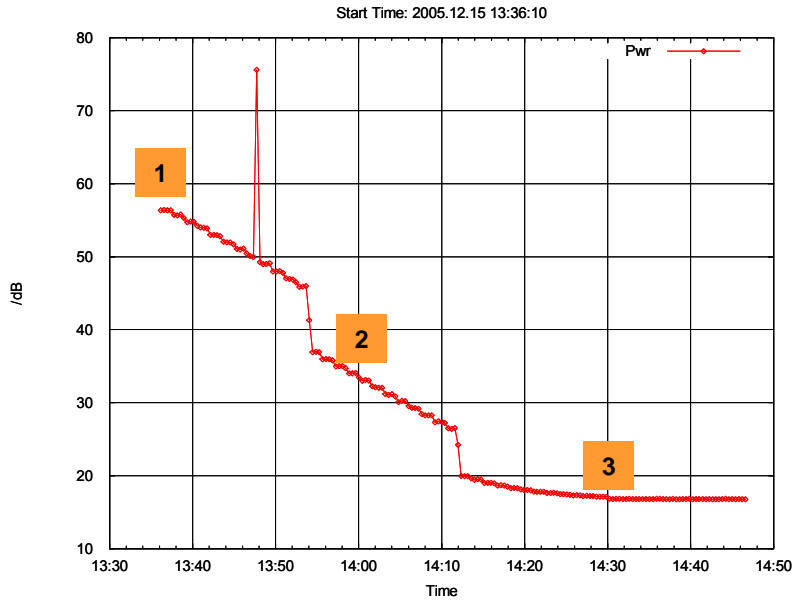


Figure 56: Take#7 - radar noise level including E6 over time

Note: The spike at 13:48h is caused by incorrect switching, therefore irrelevant for the purpose of measurement.

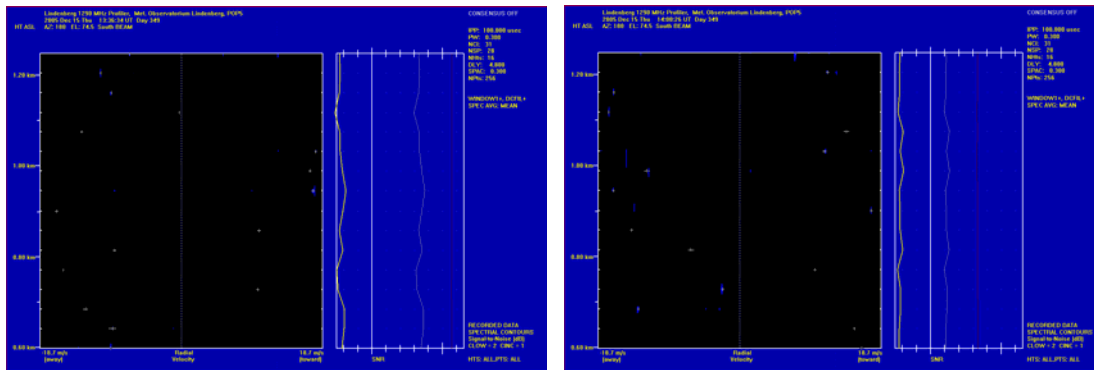


Figure 57: Take#7: -33dBm @ 13:36h (1) and -56dBm @ 14:00h (2)

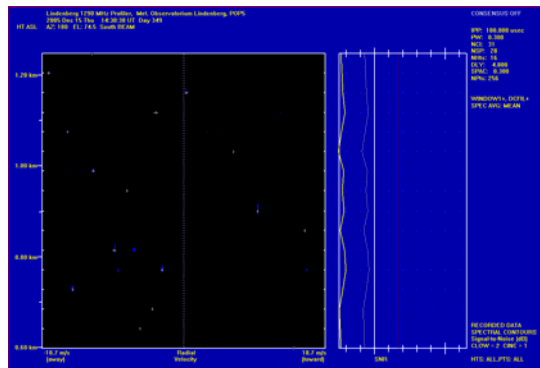


Figure 58: Take#7: -103dBm @ 14:00h (3)

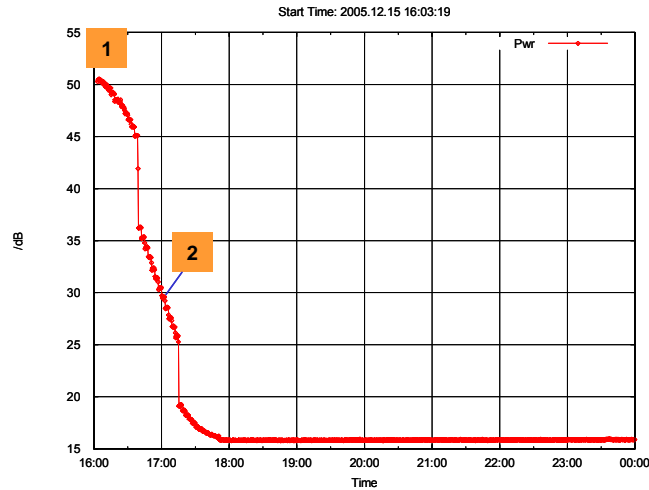


Figure 59: Take#10 - radar noise level including E6 over time

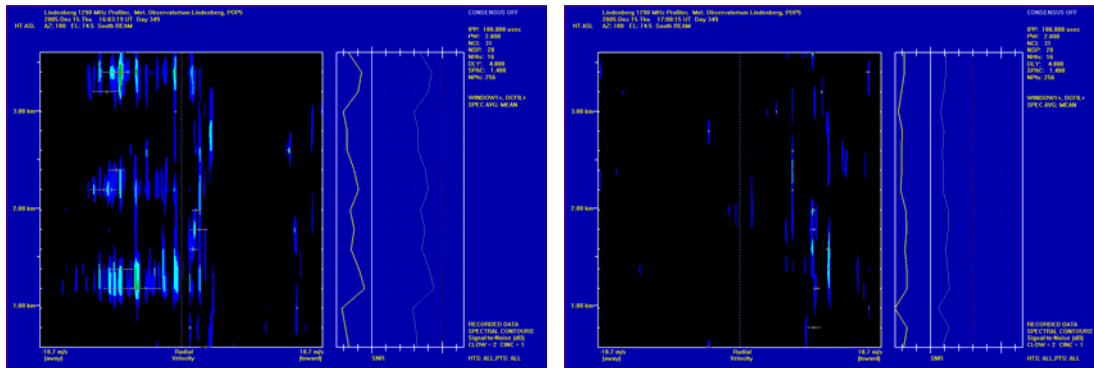


Figure 60: Take#10: -33dBm @ 16:03h (1) and -53dBm @ 17:00h (2)

In conclusion

- No distinct coherent response (DCR) even under excessive power condition.
- Raise of noise floor due to excessive power decreases radar height performance.

3.2.5 Test D: Variation of radar parameters

Beside regular wind observations, WPRs are also used for scientific weather research purposes. To investigate the interference conditions with a variation of main radar parameter settings the potential influence of Galileo is to be determined.

Different radar settings, particularly the impact of long (low resolution) and high (high resolution) pulses were investigated as shown in

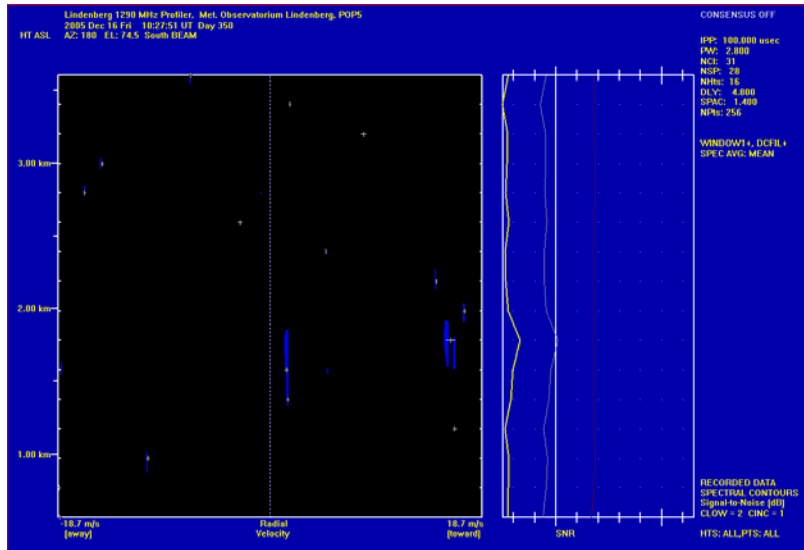


Figure 63: Take#12: -70dBm@ 10:27h (3) (pw=2800ns)

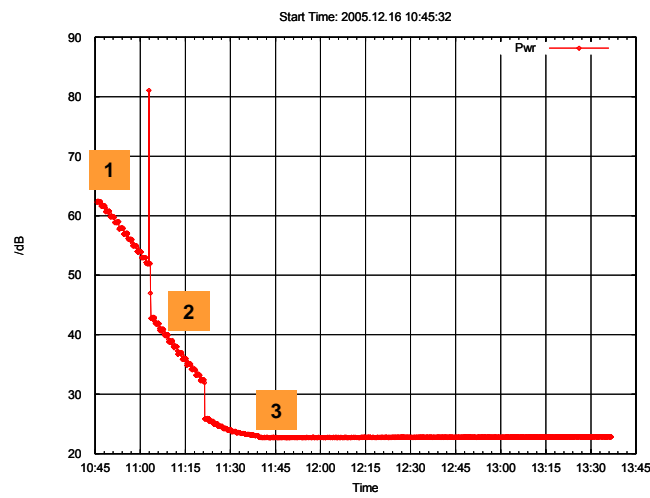


Figure 64: Take#13 Radar noise level including E6 over time (pw=300ns)

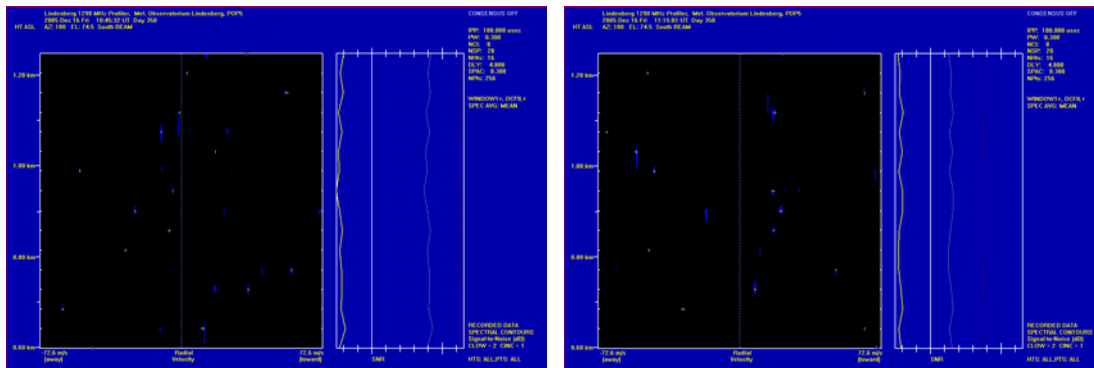


Figure 65: Take#13: -33dBm@ 10:45h (1) and -63dBm@ 11:15h (2) (pw=300ns)

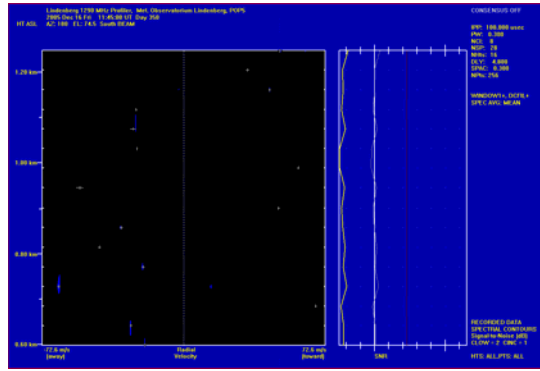


Figure 66: Take#13: -103dBm@11:45h (pw=300ns)

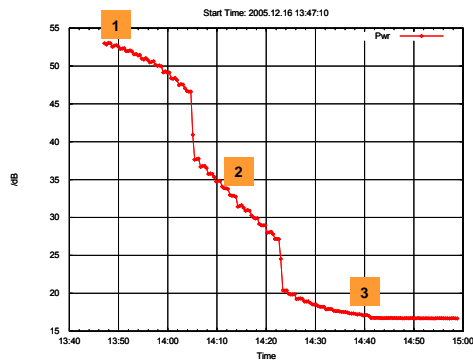


Figure 67: Take#14: Radar noise level including E6 over time (pw=1400ns)

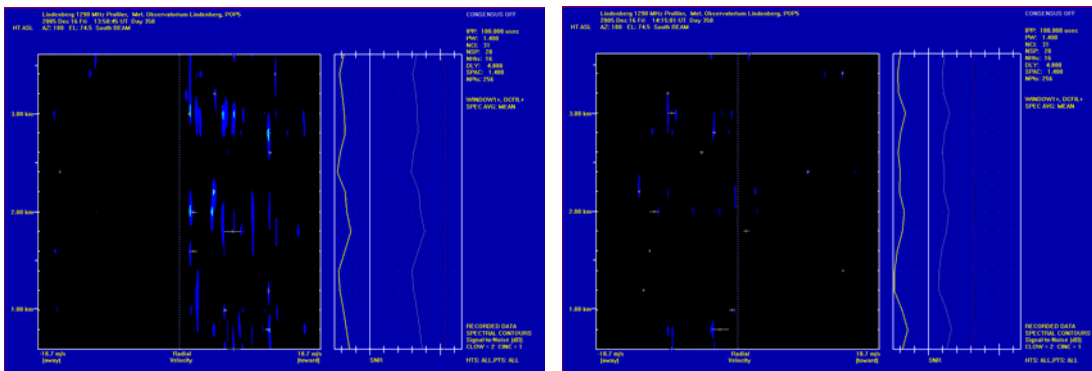


Figure 68: Take#14: -33dBm@ 13:50h (1) and -53dBm@14:15h (2) (pw=1400nsec)

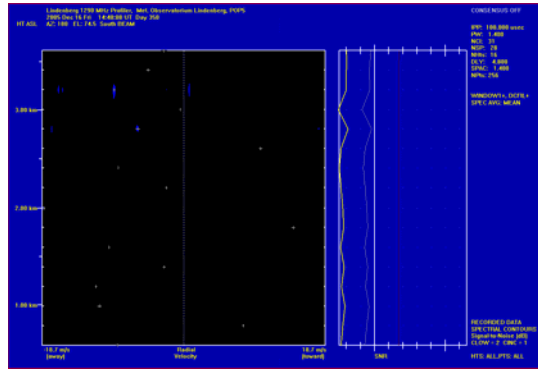


Figure 69: Take#14: -103dBm@14:40h (3) (pw=1400nsec) (3)

3.2.6 Test E: Options for interference mitigation

In case of weather research investigations the radar can be operated under various parameter settings which however could not be tested in full detail due to limited time available. Options exist to further reduce potential interference constraints by shifting the WPR carrier frequency into spectral nulls of the E6-transmissions. This test investigated the potential improvement of height performance when the radar is operated on one of two nulls offered by the E6-signal. For practical reasons (filter) the E6-signal was shifted to bring the E6-nulls in line with the radar transmissions.

Take #	E6 Pwr @ B	Time	Remarks
15	-32.6dBm to -102.6dBm	13:44	Changing E6 carrier frequency to $f_c + 5.115\text{MHz}$
16	-78.6dBm to -102.6 dBm	16:07	Investigating a higher resolution of E6-signal noise contribution
17	-78.6dBm to -102.6 dBm	00:00	
18	-32.6dBm to -102.6dBm	09:06	
20	-32.6dBm to -102.6dBm	10:25	

Table 45: Signal parameter for mitigation investigation

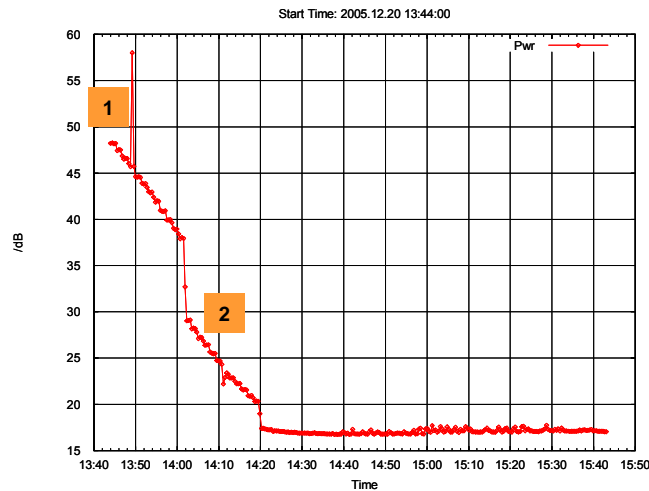


Figure 70: Take#15: Radar noise level including E6 over time

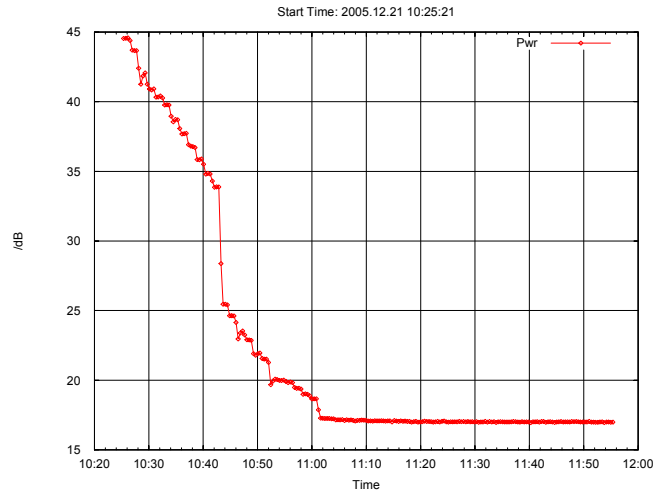


Figure 74: Take#20: Radar noise level including E6 over time (pw = 300ns)

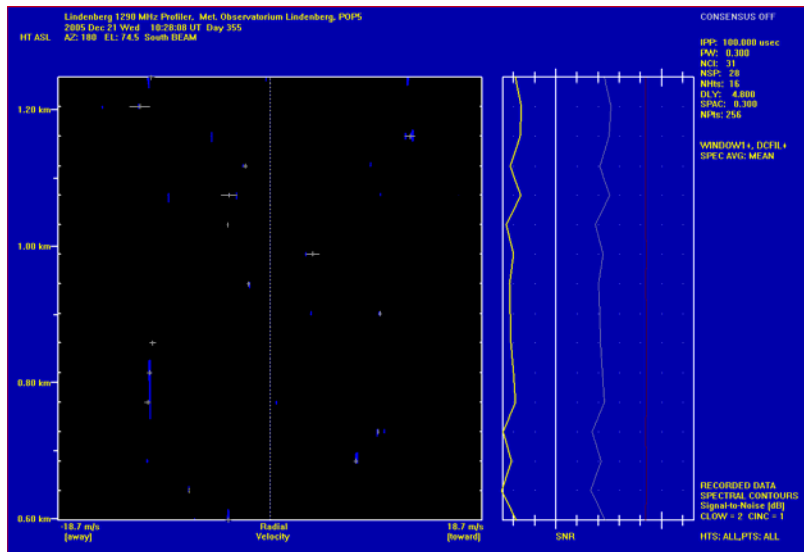


Figure 75: Take#20: -32dBm @10:28h - Null 2 - (pw=300nsec)

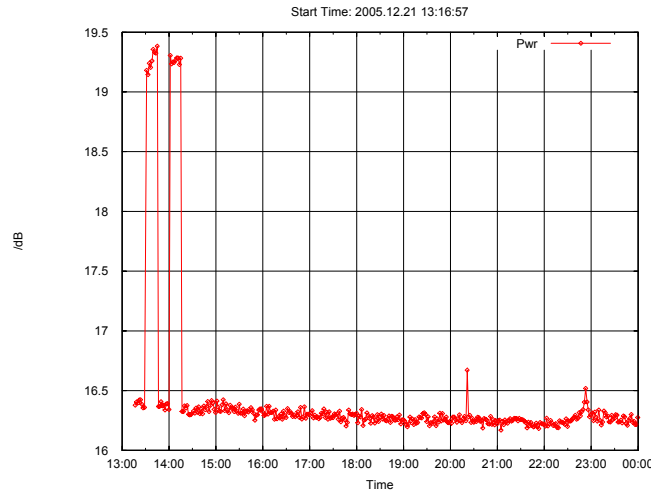


Figure 76: Take #23 - radar noise level including E6 over time (pw = 300ns)

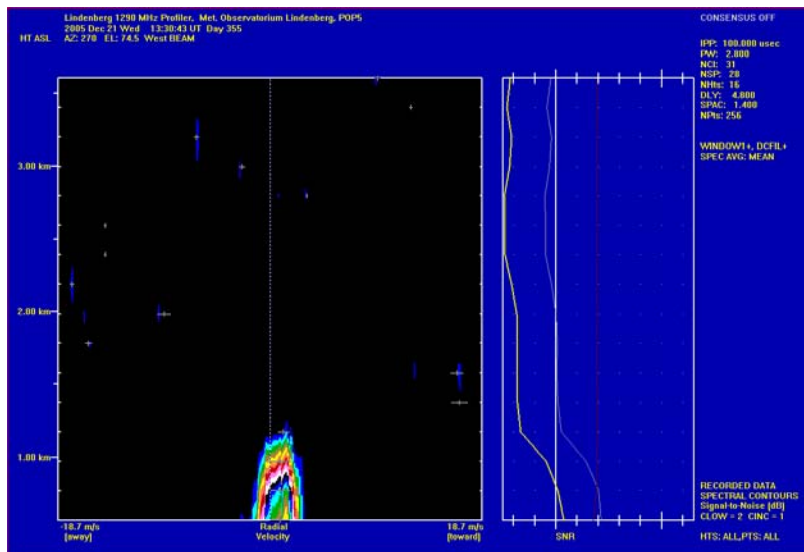


Figure 77: Take#23: -70dBm @13:30h

Further reduction of already marginal noise contribution from the E6-signal can be achieved when the WPR operates on a Null of the E6-spectrum.

4 CONCLUSIONS

The following conclusions can be drawn from the measurements:

- Within the specified maximum power conditions provided by Galileo satellites there is no coherent influence on the consensus process, i.e. no creation of false alarm signals or changing values of wind profiles.
- The noise floor increased in the presence of a satellite signal in antenna boresight view reduces marginally the operational height of the WPR.
- In case of WPR-measurements for scientific purposes that the marginal noise increase creates problems in some special cases (e.g. scientific research), the shifting of the WPR carrier frequency into a Null of the transmitted Galileo signal spectrum would fully alleviate the problem.

- The measurements also highlighted the sensitivity of the radar processor against low frequency discrete lines in interfering transmissions. The tests have shown that it is mandatory to transmit with variable bit patterns in the signal component provided for the so-called data dissemination service (Galileo Commercial Service). Appropriate measure (e.g. channel coding) must be employed. This aspect has to be included in the Galileo system requirements.
- Take#22 investigated measurements by replaying a typical fixed wind profile that was recorded during earlier measurements. Repeating this profile by means of a vector modulation generator (SMIQ) created a test environment that could be used for future representative lab-measurements to investigate in more detail varying signal conditions (Galileo or other RNSS transmissions).

In conclusion it can be said, that the interference conditions in all measurements performed can be concluded as insignificant, although, due to time and budget constraints, not all potential operating modes were tested.

However, actual weather conditions during test performance and the selected parameter settings of the WPR-system can be taken as particularly critical scenarios to determine the compatibility conditions for most of usage time.